Clinically Relevant Conventional Dose of Ionizing Radiation Enhances Tumour Cell Migration in Human Breast Cancer Cell Lines

by

Ada Young

B.Sc., The University of British Columbia, 2013

A THESIS SUBMITTED IN PARTIAL FULFILLMENT OF

THE REQUIREMENTS FOR THE DEGREE OF

MASTER OF SCIENCE

in

THE FACULTY OF GRADUATE AND POSTDOCTORAL STUDIES

(Pathology and Laboratory Medicine)

THE UNIVERSITY OF BRITISH COLUMBIA

(Vancouver)

April 2017

Abstract

It is estimated that >90% of cancer-related deaths are associated with the development and growth of tumour metastases. While tumour cell migration can be enhanced by high doses of ionizing radiation (IR) *in vitro*, the effect of lower, clinically relevant conventional IR doses on tumour cell migration and metastasis is unclear. **I hypothesize that tumour cells that survive radiation therapy have a higher propensity to migrate *in* vitro and extravasate into the lungs *in vivo*, independent from radiation-induced changes in the solid tumour microenvironment.**

Breast cancer cell lines treated with 2.3Gy IR were imaged in real-time over 72h to quantify changes in single cell migration. EMT statuses of cell lines were determined using Western blot and flow cytometry. We used conditioned medium from irradiated cells to determine whether cellular migration was influenced by secreted factors. TGF-β ELISAs were used to elucidate its role in enhancing cell migration after IR. Pre-irradiated and sham treated breast tumour cells were IV-injected into mice to examine changes in lung extravasation.

The mesenchymal MDA-MB-231 and LM2-4 cell lines treated with 2.3Gy of IR migrated a greater total distance and/or displaced further from the point of origin compared to untreated cells. No induction of EMT by 2.3Gy irradiation was observed, although MCF-7 cells migrated further from the point of origin after IR. Conditioned media from 2.3Gy treated tumour cells enhanced migration and displacement of untreated tumour cells. TGF-β ELISA analysis of supernatants from sham and 2.3Gy treated MDA-MB-231 cells revealed an almost two-fold increase in TGF-β1 72h post treatment. Chemokine antibody arrays revealed a number of up-regulated proteins after 2.3Gy treatment. 8 hours after IV injection, 2.3Gy pre-irradiated tumour cells was observed with enhanced lung colonization compared to sham controls.

IR dose of 2.3Gy are sufficient to enhance migration of both non-metastatic and metastatic breast cancer cell lines independent of EMT. By quantifying changes in the metastatic ability of tumour cells treated with a clinically relevant dose of radiation, my findings will help to determine whether there is a need for additional administration of targeted secondary therapy to minimize tumour cell dissemination.

Preface

The hypothesis, aims of this study and the experimental design were developed with guidance and mentorship from Dr. Kevin L. Bennewith. All *in vitro* experiments outlined in this study were conducted by me, with flow cytometry data collection assisted by Liz C. Halvorsen and analysis performed by me. All single cell tracking migration studies, clonogenic assays, ELISA, chemokine antibody array was conducted and analyzed by me. I performed the *in vivo* experiments (tumour implants and IV injections) with assistance from Nancy E. LePard and Dr. Kevin L. Bennewith. Subsequent analysis of collected tissue using flow cytometry and tissue sectioning was done by me. Tissue section immunofluorescence (staining and analysis) was completed with assistance from Brennan J. Wadsworth. A version of chapters 2 and 3 has been submitted to *Radiation Research*, titled "Ionizing radiation enhances breast tumour cell migration *in vitro*". The entirety of the experiments and writing of the manuscript and thesis was completed by me with guidance and editing by Dr. Kevin L. Bennewith.

All mouse work was completed with approval from the University of British Columbia's Committee on Animal Care Project Number A13-0223 (Protocol #B13-0046). I was funded by Dr. Kevin Bennewith's operating grant (CIHR; MOP-126138).

Table of Contents

List of Tables

List of Figures

List of Abbreviations and Acronyms

ANOVA	Analysis of variance
α-SMA	α-smooth muscle actin
BRCA	BReast CAncer susceptibility gene
CXC	Cystine X Cysteine
CXCL	CXC chemokine ligand
CSC	Cancer stem cell
CTACK	Or CCL27; Cutaneous T-cell-attracting chemokine
DMEM	Dulbecco's modified Eagle's minimal essential medium
dH_2O	Distilled water
EDTA	Ethylenediaminetetraacetic acid
EGF	Epidermal growth factor
EGFP	Enhanced green fluorescent protein
ELISA	Enzyme-linked immunosorbent assay
EMT	Epithelial-mesenchymal transition/transdifferentiation
ER	Estrogen receptor
FACs	Fluorescence-activated cell sorting
FCS	Forward-scattered light
FBS	Fetal bovine serum
FISH	Fluorescence in situ hybridization
GM-CSF	Granulocyte-macrophage colony-stimulating factor
GRO	Growth Related Oncogene
Gy	Gray (radiation dose unit)
HER2	Human epidermal growth factor receptor 2
HGF	Hepatocyte growth factor
HR	Homologous recombination
IL-8	Interleukin 8 (CXCL8)
IR	Ionizing radiation
IV	Intravenous
LLC-Pk_1 cells	Proximal tubular epithelial cell line from pigs

LM2-4	Lung metastatic variant of human breast carcinoma cell line MDA-MB-231
MCF-7	Human breast carcinoma; non-metastatic
MFI	Mean Fluorescence Intensity
MDA-MB-231	Human breast carcinoma; metastatic
231-Ecadh	Human breast carcinoma expressing E-cadherin
MET	Mesenchymal-epithelial transition
MFP	Mammary fat pad
MMP	Matrix metalloproteinase
NHEJ	Non-homologous end joining
NK	Natural killer cell
NOD SCID	Non-obese diabetic severe combined immunodeficiency
OCT	Optimal cutting temperature compound
PAM50	Prediction Analysis of Microarray 50
PBS	Phosphate-buffered saline
PFA	Paraformaldehyde
PE	Plating efficiency
PgR	Progesterone receptor
REV	Reticuloendotheliosis Virus
RPMI	Roswell Park Memorial Institute medium (tissue culture media)
RRE	Rev/Rev Reponsive Element
RT	Radiation therapy
SDS PAGE	Sodium dodecyl sulfate polyacrylamide gel electrophoresis
SEM	Standard error mean
SF	Surviving fraction
TBS(T)	Tris-buffered saline (Tween 20)
TGF-β	Transforming growth factor-β
VSVG	Vesicular Stomatitis Virus Glycoprotein

Acknowledgements

I would like to sincerely extend my gratitude to Dr. Kevin L. Bennewith for his mentorship, encouragement and unwavering patience. I was able to grow immensely as a young scientist under Dr. Bennewith's support and guidance, thank you for taking a chance on me. To the members of the Bennewith lab (Nancy LePard, Melisa Hamilton, Liz Halvorsen, Brennan Wadsworth, Natalie Firmino, Jenna Collier and S. Elizabeth Franks), thank you for making the last 2.5 years so wonderful, I could not have imagined a more wonderful and brilliant group of people to work with. Thank you for all of your assistance with the studies in this thesis. I would like to thank my supervisory committee members Dr. Marcel Bally, Dr. Cal Roskelley and Dr. David Granville for their guidance, insight and persistence in asking the hard but necessary questions. I would also like to acknowledge and thank Dr. Marcel Bally and his lab members (Visia Dragowska and Wallace Yuen) for the use of their Essen Bioscience IncuCyte ZOOM system, Drs. Andrew Minchinton and Alastair Kyle for the use of their multi-attenuator insert and finally, Drs. Aly Karsan, Joanna Wegrzyn and Dr. Kate Slowski for the pLL3.7 EGFP expression vector and lentiviral CL3 training.

Last but not least, I would like to thank my family and friends for supporting me during this entire endeavor. Thank you for enduring my sometimes very weird experiment schedules, the rants about my experimental failures (and small successes) and my attempts to explain what it is I do. You have kept me sane, grounded and most importantly, alive and for that, you have nothing but my wholehearted thanks.

Dedication

I dedicate this thesis to my beloved family, friends, colleagues who became like family, and every person that I have come across during this journey. Whether profound or slight, your contribution to this thesis is significant and for that, I thank you.

Proverbs 16:9

Proverbs 3:6

Chapter 1: Introduction

1.1 Cancer

Cancer is defined by the National Cancer Institute as a collection of related diseases that can start almost anywhere in the human body; a disease where cells in the body divide uncontrollably, developing into growths called tumours. These tumours are either benign and contain cells that do not spread into nearby healthy tissues, or are malignant and produce cells that separate from the primary tumour mass by invading local tissue, which holds the potential for cancer cells to enter the circulation and travel to distant sites to form new tumours (metastasis).

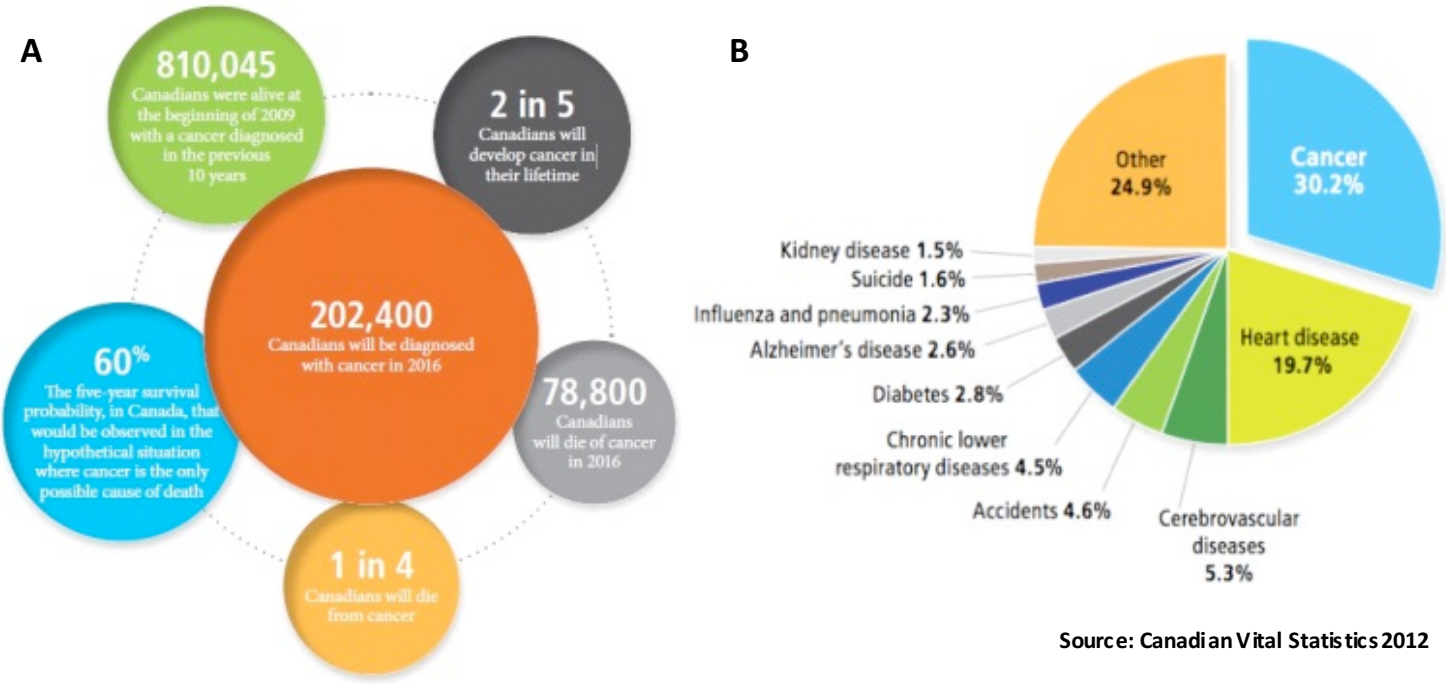

Figure 1.1 Overall cancer burden and proportion of cancer-related deaths in proportion to other causes (Canadian Cancer Statistics 2016 publication). Slightly more men than women are diagnosed with cancer and the majority of those diagnosed are over the age of 50. Cancer affects all age groups and is the leading cause of disease-related mortality [2]. Figure reprinted with permission: Canadian Cancer Society's Advisory Committee on Cancer Statistics. Canadian Cancer Statistics 2016. Toronto, ON: Canadian Cancer Society; 2016.

The Canadian Cancer Society estimates that 202,400 Canadians will be diagnosed with cancer in 2016, with 78,800 of those diagnosed succumbing to the disease, making it the leading cause of death in Canada (Figure 1.1). The five-year survival rate across all cancer types is 60% in Canada, with pancreatic, esophageal and lung cancer patients having the lowest five-year survival estimates. Female patients diagnosed with cancer exhibit a significant survival advantage compared to males, with a 13% lower excess risk of death for all cancers combined. Those patients that survive their diagnosis and treatment continue to face personal cost and challenges even when they are in remission. Cancer as a disease is a burden to the Canadian society as a whole due to the major economic ramifications; cancer is the source of both direct healthcare costs that cover drug and physician fees and indirect healthcare costs to help patients during times of low productivity due to side effects of treatment, illness or unfortunately, premature death. Although research and technological advancements are greatly enhancing the quality of diagnosis, treatment and disease management, progress is still required to prepare for the aging population in Canada that will be increasingly susceptible to developing cancer in the coming years, and will create a high demand for more effective treatments.

1.1.1 The hallmarks of cancer

One of the most recognized and highly cited pieces of literature in the cancer field is "The Hallmarks of Cancer" [3], first published in 2000 by Doug Hanahan and Robert A. Weinberg. This comprehensive literature review puts into perspective why cancer is such a difficult disease to diagnose and treat. Cancer is not a single disease that originates from a single organ, but rather cancer is the result of dynamic genetic changes that shift the balance between regulated cell growth and uncontrollable proliferation. Tumourigenesis relies on the ability of cancer cells to

both evolve over time and interact effectively with the host and the local tumour microenvironment; six mechanistic pillars of tumourigenesis were proposed by the Hallmarks of Cancer [3] which outlines the capabilities that most cancers, despite the vast heterogeneity of the disease, can acquire and exhibit. Since the initial publication, this review has been updated to produce "Hallmarks of Cancer: The Next Generation" [4], published in 2011, to expand on the previous six mechanistic strategies. Below is a summary of the ten hallmarks:

Table 1.1 Summary of the Hallmarks of Cancer. Adapted from references [3] and [4].

Hallmark	Description
1. Self-Sufficiency in Growth Signals/ Sustaining proliferative signaling:	Cancer cells have acquired the capability to synthesize their own growth signals such that they are able to sustain their own growth without reliance on an exogenous source; they function as a positive feedback signaling loop (autocrine and paracrine stimulation) that is further amplified when cancer cells also overexpress the cell surface receptors to these growth factors.
2. Evading Growth Suppressors:	Genetic mutations in tumour suppressor genes that normally negatively regulate cell proliferation; these genes are responsible for cells either entering a proliferative or senescent/apoptotic state.
3. Resisting Cell Death:	Programmed cell death by apoptosis is attenuated by tumour cells such that events that would normally trigger apoptosis, such as imbalances caused by increased oncogene signaling or DNA damage, are circumvented.
4. Enabling Replicative Immortality:	A capability as a result of cancer cells being able to overcome two barriers to proliferation; first is senescence, where cells are non-proliferative but viable, and subsequently, cell death or the crisis phase.
5. Inducing Angiogenesis:	During tumorigenesis, tumours hijack the process of vasculature development (angiogenesis) to constantly sprout new blood vessels to aid in nutrient delivery and removal of metabolic waste.
6. Activating Invasion and Metastasis:	A capability initiated by the loss of key proteins involved in cell-to-cell and cell-to-matrix adhesion, responsible for anchoring cells to each other and to the extracellular matrix, that eventually cascades into local invasion, intravasation of cancer cells into blood and lymphatic vessels, circulation, extravasation from vessels into distant tissues, the formation of micrometastases and eventually the growth of these small

	nodules into macroscopic tumours.
7. Genome Instability and Mutation:	Not a capability but an enabling characteristic that allows for the acquisition of the multiple hallmarks mentioned above by conferring selective advantage(s) to some subclones within a population of tumour cells that promotes their growth and subsequent dominance
8. Tumour Promoting Inflammation:	The presence of inflammatory cells in tumours can function as an enabling characteristic; instead of mounting an immune response against tumour cells, immune cells provide growth and survival factors that can promote metastasis and facilitate tumour-promoting angiogenesis.
9. Reprogramming Energy Metabolism:	An emerging capability describing how tumour cells are able to reprogram their energy production to adapt to the nutrient availability in the tumour microenvironment. Of note, some cancers have adapted to using glutamine (glutaminolysis) for cellular bioenergetics and metabolism. The resultant metabolites are important for the TCA cycle and as a result, these cancers become "addicted" to glutamine as their primary energy source.
10. Evading Immune Destruction:	An emerging capability recognizing that the immune system's basally functions to eliminate tumour cells in the body, thus tumours that are able to form have acquired mechanisms to evade active immune surveillance.

In summary, both reviews critically highlighted the challenges we face not only in understanding cancer and all of the intricate processes and events that lead to the manifestation of the disease, but also in designing therapies with all the knowledge that we have and will amass. To that end, in order for therapies to be effective, multiple hallmarks may have to be considered or targeted.

1.2 Breast cancer

One in four women in Canada will be diagnosed with breast cancer, according to the 2016 Canadian Cancer Statistics released by the Canadian Cancer Society [2]. Breast cancer is the 3rd most common cancer in Canada (2nd most in the world) and is the second most common cause of cancer-related mortalities in Canadian women, with a 1 in 30 chance of mortality [2].

Although the majority of women diagnosed with breast cancer are over 60 years of age, women aged 30-59 are at the greater risk for cancer-related mortality. The 5-year net survival for 2006-2008 was estimated to be 87% in females and 79% in the rare cases of male breast cancer [2].

Breast cancer develops in the lobules or ducts of the breast, which normally function as producers of milk and as a conduit for milk respectively [5]. Breast cancer either remains in the breast tissue (carcinoma in situ) or evolves into invasive carcinoma and eventually metastasizes to other organs, often the bone, lungs, regional lymph nodes, liver and brain [5-7]. Age, a family history of breast cancer, genetic predisposition (BRCA1 and BRCA2 gene mutations), the use of hormone therapy for postmenopausal women and a history of abnormal hyperplasia increases the risk of developing both carcinoma in situ and invasive breast cancer [8]. The uncontrolled proliferation is the consequence of genetic mutations that result in a disease that is not only genetically but also histologically heterogeneous in its presentation [9]. Carcinoma in situ (ductal and lobular) can be clearly differentiated from normal tissue by alterations in the expression pattern of genes involved in processes like cell cycle regulation, growth factor response and apoptosis [9]. The transition from ductal or lobular carcinoma in situ into invasive breast cancer is not as obvious in the genetic signature, although the expression status of the estrogen receptor (ER), human epidermal growth factor receptor 2 (HER2) and progesterone receptor (PgR) are well established predictors of endocrine/hormone therapy response and prognosis of invasive breast cancer [10-12]. This diversity in genetic and histological presentation is used to categorize breast cancer into distinct subtypes that have different clinical outcomes [7].

1.2.1 Diagnosis, stages and subtypes of breast cancer

In Canada, the most common breast cancer staging system is the TNM (tumour, nodes, metastasis) system; TNM describes the primary tumour based on size, the number and location of regional lymph nodes where cancer cells have invaded into and whether the cancer has disseminated to a different organ [13]. Each of these categories are also described with two classifications; the clinical classification of TNM describes the disease before treatment and is essential for therapy selection and evaluation, whereas the pathological classification is used to classify the disease post-surgery, inform adjuvant therapy and estimate prognosis [13]. Within the main categories are subdivisions; numbers (1-4) indicate the extent of malignant disease and letters (a-d) confer greater specificity. The three categories of the TNM system used to describe the anatomical extent of the cancer are then grouped into stages (I-IV); stage I describes localized tumours, stage II is disease with locally extended spread, stage III is disease that has spread to regional lymph nodes and finally, stage IV is disease with distant metastasis. Each stage encompasses groups with similar survival rates, with each increasing stage having worse survival [13].

Breast cancer is diagnosed using a combination of clinical examinations, imaging and pathological assessment [8]. Initially, clinical examinations through breast and locoregional lymph node palpations are used to establish the possible presence of a tumour, in addition to assessing signs and symptoms of distant metastases [8]. Screening mammography and ultrasound of the breast and regional lymph nodes are the most commonly used imaging techniques to define the location and extent of cancer spreading. Immunohistochemical analysis is the most commonly used pathological assessment technique used to identify breast cancer subtypes in the

clinic [14-16]; genetic/microarray profiling can also be used but are not as common [17-20]. These techniques are conducted using patient derived samples from the primary tumour, which are obtained using core needle biopsies before patients undergo treatment [8]. Immunohistochemical analysis provides detection of well-characterized markers associated with breast cancer. Patient biopsies are paraffin embedded, stained with antibodies against ER/PgR and fluorescent *in situ* hybridization (FISH) is used to detect HER2 gene amplifications [8, 21]. Based on the test results, patient samples are classified into one of four groups: Luminal B, Luminal A, Basal-like and HER2/neu overexpression [8, 21]. Tissue microarrays are used to analyze patient samples for genetic signatures, allowing for further subtyping [22]. Microarray genetic signatures produce 5 subtypes [18]: normal-breast like, basal-like, HER2+, luminal B and luminal A [18, 20, 22, 23]. Immunohistochemical, and to a much lesser extent genetic/microarray profiling subtypes, are used for treatment planning and have been associated with prognostic and clinical implications [7, 15, 21, 22].

Each of the five different subtypes identified through immunohistochemical and gene signature methods have been shown to be clinically distinct in their overall and relapse-free survival. Below is a table summarizing the subtypes with corresponding hormone receptor status, prognosis/relapse free survival and recommended therapy.

Table 1.2 Breast cancer subtypes and clinical features.

Intrinsic subtype	Clinicopathologic surrogate definition	Prognosis and relapse-free survival (RFS)	Recommended systemic therapy
Luminal A	**Luminal subtype** Luminal A-like ER^+ and PgR^{low} $HER2^-$ $Ki67^{low}$	Best/favourable clinical outcome and 10-year RFS Lower grade tumours	Endocrine therapy
Luminal B	**Luminal subtype** *Luminal B-like (HER2 negative):* ER^+/PgR^{low}, $HER2^-$, $Ki67^{high}$ *Luminal B-like (HER2 positive):* ER^+/PgR^+, $HER2^+$, $Ki67^{high}$	Worst prognosis and 10-year RFS of the two luminal subtypes	Endocrine therapy and chemotherapy ($HER2^{negative}$) Endocrine therapy, anti-HER2 therapy and chemotherapy ($HER2^{positive}$)
Basal-like	**Basal subtype** Triple-negative $ER^{negative}/PgR^{negative}$ $HER2^{negative}$	Poor survival; worst overall and disease-free survival	Chemotherapy
HER2 overexpression	**Basal/non-luminal subtype** HER2-positive $ER^{negative}/PgR^{negative}$ $HER2^{positive}$	Poor survival	Chemotherapy and anti-HER2 therapy

*Table adapted from tables from reference [8] and data from [17, 21]

1.2.2 Treatment

Treatment options are recommended based on the diagnosis (immunohistochemical and molecular profiling), the location and extent of the tumour, and the age and overall health of the patient [8]. Surgery is the most common treatment option for patients with localized tumours, with breast-conserving surgery and mastectomy (complete breast tissue removal) being the most common forms. Most importantly in relation to the research aims of this thesis, for patients undergoing breast-conserving surgery (and sometimes mastectomy), radiation therapy (RT) is strongly recommended afterwards to reduce the risk of reoccurrence at the site of resection. RT

has been shown to have a beneficial effect on survival [8] and is further discussed below in Chapter 1.2.3. Finally, adjuvant systemic treatments, such as chemotherapy, endocrine therapy and HER2-targeted therapy, are prescribed to patients based on their risk of relapse and/or their potential sensitivity to specific treatment methods; for patients who are ER+, where expression is found in ≥1% of invasive cancer cells, endocrine/hormone therapy is prescribed [8]. Personalized medicine in breast cancer refers to the use of genetic profiling, prognostic biomarker expression, and hormone receptor status as predictive factors to design the most effective treatment regimen for an individual patient [24]. The shift away from non-targeted therapies towards personalized medicine is occurring along with the emergence of assays that utilize high-throughput genomic technology to discover new potential markers and develop gene expression profiles that can provide prognostic and predictive data about a patient's tumour such that it can be used to tailor their treatment. Although not commonly used in the clinic and still undergoing rigorous validation, gene expression signatures like PAM50 [25], Oncotype DX [26], and MammaPrint [27, 28] are commercially available gene expression tests that use a formula of various genes related to proliferation and hormone receptor expression to obtain prognostic information relating to outcome, treatment sensitivity and recurrence.

1.2.3 Radiation therapy

Radiation therapy (RT) is an essential cancer therapy for curative, adjuvant, and palliative treatment. In the clinic, ionizing radiation (IR) treatment is usually in the form of X-rays delivered to the tumour tissue in focused beams coming from several directions. When cells (normal and tumour) are treated with radiation, DNA damage is incurred that ultimately results

in proliferative cell death if not repaired (Figure 1.2). DNA damage caused by IR results in single and double strand breaks (DSBs).

Double strand breaks in tumour suppressors or oncogenes, or essential genes, if erroneously repaired may lead to tumorigenesis or cell death respectively [29]. RT relies on the basic principle that tumour cells are inefficient in DNA damage repair in comparison to normal tissue cells, and are therefore more susceptible to IR-induced cell death [30]. DNA double strand break repair can occur through two distinct and complementary mechanisms: homologous recombination (HR) and non-homologous end-joining (NHEJ) [29]. HR begins with nucleases resecting the exposed DNA ends in the 5' to the 3' direction. Subsequently, the resultant 3' single-stranded tails are extended by DNA polymerase after insertion into a DNA double helix of a homologous partner. Once the exposed DNA ends have been elongated using the homologous partner as a template, the resultant DNA crossovers are resolved to produce two intact DNA molecules. In NHEJ, an undamaged homologous partner is not required. The two exposed DNA ends are instead ligated together and thus, often prone to error. This ligation step also results in small sequence deletions. The presence of DSBs signals cells to slow down progression through the cell cycle, providing time for repair and preventing propagation of mutations that could potentially be tumorigenic. With proper planning and design of RT delivery, cumulatively large radiation doses can be delivered to tumour tissue in a focused beam to induce the most damage, while minimizing risk for normal tissue [30].

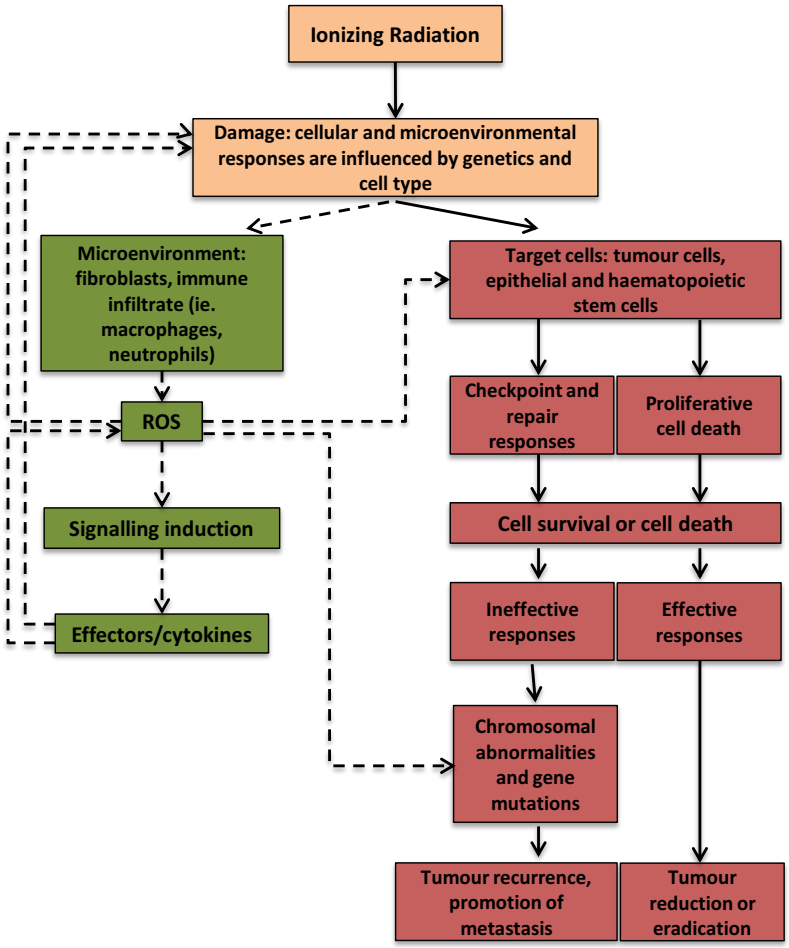

Figure 1.2 Cellular and microenvironmental responses induced by ionizing radiation (IR). IR induces a cascade of changes and responses that not only affect the tumour cells but also the tumour microenvironment. Feedback between the microenvironment (green boxes) and target/tumour cells (red boxes) lead to responses that either result in cell survival or cell death. In the case of tumour cells, ineffective response after IR treatment can lead to pathological consequences ie. local recurrence at site of treatment. Adapted with permission from **Barcellos-Hoff, M.H., C. Park, and E.G. Wright, *Radiation and the microenvironment–tumorigenesis and therapy.*** [30].

1.2.4 Radiation therapy in breast cancer treatment

In breast cancer, IR prevents local recurrence after breast conserving surgery by killing any remaining microscopic tumour foci, and has been shown to improve overall survival [31, 32]. Traditionally, a large total dose (between 40-50Gy) of IR is given after breast conserving surgery in fractionated doses of 1.8-2Gy each. Dose fractionation takes advantage of the DNA repair discrepancy between tumour and normal tissue. Between each radiation treatment, normal tissue can recover while tumour cells undergo proliferative cell death. Treatment lasts between 5-6

weeks (5 days/week), while some patients may receive an additional 10-15Gy dose boost [33]. Emerging RT strategies are applying hypofractionation, which utilizes larger doses per fraction, reducing total treatment time and total doses given. Studies comparing traditional versus hypofractionation treatment schedules have shown that local tumour control, recurrence and long-term outcomes were similar between the two groups (reviewed here [33]).

Radiation is also a well-known carcinogen and when used ineffectively, may be cancer and/or metastasis promoting. Meta-analysis of a large cohort of breast cancer patients (10,801 women from 17 randomized trials) stratified based on receiving RT or not after breast-conserving surgery found that radiation treatment reduced the 1-year recurrence risk of patients with node positive breast cancer (26.0% to 5.1%) but the effects of RT diminished after year 5; the 10-year absolute risk of locoregional or distant recurrence was halved with RT [31]. Most importantly, it was determined through this meta-analysis that both node-negative and node-positive disease patients who only received breast-conserving surgery had their first recurrence locoregionally compared to patients allocated to the RT after surgery group. A slightly higher percentage of patients with recurrence in the radiotherapy group developed recurrence at distant sites compared to the surgery only group (12% and 10% respectively) [31]. This suggests that although RT's main effect is to reduce locoregional recurrence, it may potentially be promoting distant metastases in some patients. With this potential risk, it is evident that further work needs to be conducted to better identify patients that would require additional therapy (like chemotherapy) to prevent potential radiation-induced dissemination of tumour cells and/or enhancement of distant metastases. Currently there are no radiation-induced biomarkers used to guide treatment decisions, due in part to breast cancer heterogeneity and thus, overtreatment and/or negative side effects may be possible [32].

1.3 Metastasis

1.3.1 The metastatic cascade

Metastasis is defined as the dissemination of malignant cells from the primary tumour to distant organs of the body. The basic steps of metastasis involve local invasion, intravasation to and survival within the circulatory system, extravasation and colonization of the distant organ by the tumour cells (summarized in Figure 1.3) [34]. The metastatic cascade involves intrinsic molecular and cellular processes that cause the loss of cellular adhesion, enhanced cell motility and invasion, and enhanced proliferative ability during colonization of the distant site [34]. Extrinsic influences from the tumour microenvironment including nutrient and oxygen availability, immune cell infiltrate and extracellular matrix components, also apply selective pressures that may promote metastasis in a sub-population of more aggressive tumour cells within the tumour [35]. Both intrinsic and extrinsic changes are responsible for the acquisition of malignant traits, but whether or not this progression is the inevitable fate of primary tumour evolution is still a widely contested topic.

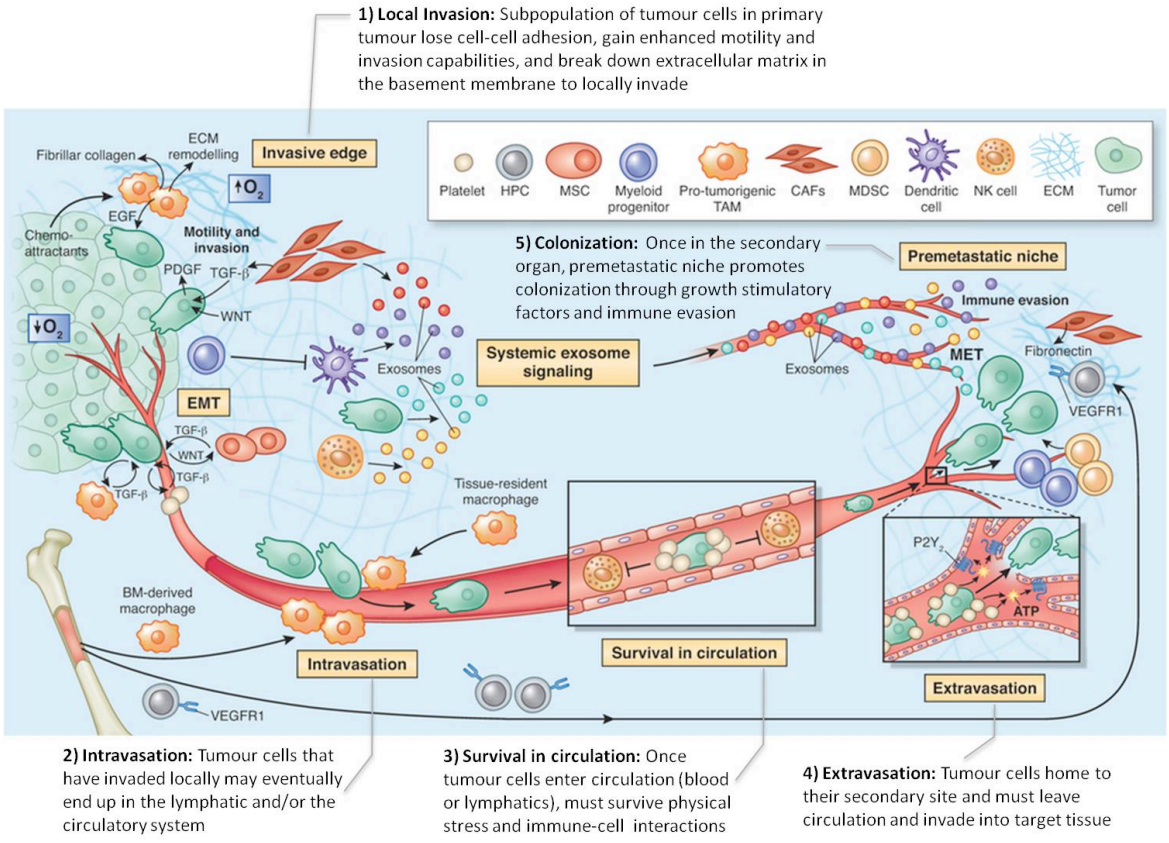

Figure 1.3 The metastatic cascade and the microenvironmental components that support and promote metastasis. In addition to genetic and cellular changes in tumour cells, tumour microenvironmental components (cells and secreted factors) contribute to tumorigenesis, metastasis and formation of the premetastatic niche. Adapted with permission from **Quail, D.F. and J.A. Joyce, *Microenvironmental regulation of tumor progression and metastasis.* Nature medicine, 2013.**

Multiple theories have been proposed to explain the initiation of the metastatic cascade. The clonal expansion perspective postulates that cancer cells acquire genetic and epigenetic alterations that provide them with a survival advantage, which can overlap with selection for expression of pro-metastatic genes [36]. The theory of cancer stem cells (CSCs) has also been proposed; these cells have enhanced tumour-initiating capabilities relative to other tumour cells, demonstrate self-renewal potential, and have the ability to give rise to non-CSC progeny, thus tumour cells must possess attributes of CSCs in order to colonize distant sites [37]. Collective migration and invasion is also a mechanism by which tumour cells can metastasize. *In vivo*

experiments have demonstrated that tumour cells can remain connected to each other via cell-cell junctions while invading locally into nearby tissue or break off from the primary tumour, forming clusters or single-cell files that can be isolated from the lymphatic or circulatory system during the course of tumour progression (reviewed in [38]).

One of the most well studied, and sometimes controversial, mechanisms to explain how the metastatic cascade is initiated is epithelial-to-mesenchymal transition (EMT). This cellular program involves the activation of transcription factors involved in cell-cell adhesion, cell migration and invasion, and the upregulation of mesenchymal markers [1]. Epithelial cells exhibit apical-basal polarity and possess membrane-associated complexes (tight junctions, adherens junctions and desmosomes) that allow for cell-cell adhesion and display keratin filaments [39, 40]. Functional EMT is used by cells during embryonic development, where polarized epithelial cells are able to switch to mesenchymal states via EMT and return to an epithelial state via mesenchymal-to-epithelial transition (MET) [1]. Mesenchymal cells are spindle-shaped, display vimentin filaments, and possess enhanced migratory and invasive capacity and are more resistant to apoptosis compared to polarized epithelial cells [40, 41]. Studies have shown that epithelial-like tumour cells are able to metastasize by undergoing EMT (summarized in Figure 1.4); the mesenchymal capabilities are conducive to single cell dissemination from the primary tumour and colonization in secondary organs [1].

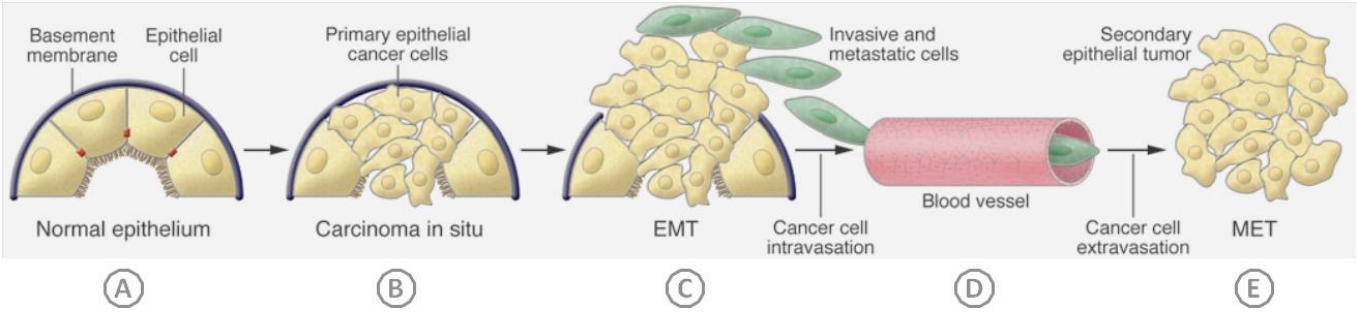

Figure 1.4 Epithelial-mesenchymal transition and its role in the metastatic cascade. A) Normal epithelium maintain cell-cell adhesion and are attached to the basement membrane. **B)** Primary epithelial cancer cells begin to over-proliferate, lose their polarity and begin detaching from the basement membrane. **C)** Epithelial cancer cells undergo EMT and become malignant. **D)** Resultant mesenchymal cells migrate to and intravasate into the circulatory (or lymphatic) system. **E)** Mesenchymal tumour cells extravasate into a secondary organ and undergo MET to form secondary epithelial tumour colonies. Adapted with permission from **Kalluri, R. and R.A. Weinberg, *The basics of epithelial-mesenchymal transition.* The Journal of clinical investigation, 2009.** [1].

The EMT program involves the activation of multiple transcription factors that allow epithelial-like carcinoma cells to break away from neighboring cells and invade into adjacent cell layers (Step C of Figure 1.4). The loss of cell-cell adhesion is the result of the loss of E-cadherin expression. A reliable epithelial cell marker, E-cadherin is a component of cellular adherens junctions, which are large protein complexes responsible for cell-cell adhesion [42]. Transcription factors of the EMT program generally function to down-regulate the expression of E-cadherin. EMT transcription factors can be activated by factors in the tumour microenvironment, whether acting as a paracrine or autocrine signal. Hepatocyte growth factor (HGF), epidermal growth factor (EGF), platelet-derived growth factor (PDGF) and transforming growth factor β (TGF-β) all play a role in activating EMT-inducing transcription factors [43]. Notably, TGF-β activity has been shown to be sufficient to induce EMT in tumour cells through the transcription factors Snail, Slug and SIP1 [42, 43]. These three factors subsequently repress the expression of E-cadherin. As previously stated, the function of TGF-β is both context and stage dependent; in the normal mammary gland, it functions to inhibit epithelial cell proliferation

and increase extracellular matrix production [44]. In a dose-dependent manner, TGF-β is able to induce a reversible EMT in the non-transformed mammary epithelial cell line NMuMG; TGF-β treatment caused the cells to become elongated/fibroblastic and immunofluorescence revealed the loss of cell-surface expression of E-cadherin and zonula occludens-1 (ZO-1) that would normally be found as a continuous line between neighbouring cells [44]. The actin skeleton of TGF-β-treated NMuMG cells was also reorganized into longitudinal fibers that made cells more spindle-shaped; the mesenchymal marker vimentin was also found to be increased in expression. Upregulation of proteins that increase cell motility and invasiveness follows the loss of cell-cell adhesion, and researchers use these proteins as mesenchymal markers. Thus, EMT is a multi-step process and not a simple switch between epithelial and mesenchymal, but rather a process that moves cells along a spectrum. Vimentin is a mesenchymal intermediate filament that has been traditionally used as a critical marker of complete EMT, as if it were the final step in becoming mesenchymal, although some data has shown TGF-β to induce vimentin expression in primary epithelial cells without acquiring expression of other traditional mesenchymal markers [42]. Alpha smooth muscle actin (α-SMA) is a transitional marker for cells undergoing EMT *in vivo* but only expressed in a subpopulation of cells characterized by myofibroblastic behavior. TGF-β has been shown to induce α-SMA synthesis as a consequence of EMT induction in renal epithelial cells [45]. Although both vimentin and α-SMA are well-cited markers of a mesenchymal phenotype, they are not unequivocal mesenchymal markers as studies have shown that their function and expression is contextual [42]. In addition to promoting migration of tumour cells, EMT also promotes the invasive capabilities of tumour cells (reviewed in [40]. Metalloproteinases (MMPs) are a family of secreted and transmembrane proteins with an enzymatic activity to degrade extracellular matrix and basement membrane [46]. MMP activity

has been shown to be necessary for both the intravasation and extravasation steps of the metastatic cascade, as studies have shown that synthetic inhibitors to MMPs reduce the formation of primary and metastatic tumours [46], and its activity has been associated with EMT [47, 48]. With these caveats in mind, I studied how the expression of E-cadherin, vimentin, α-SMA and MMPs is altered in the context of ionizing radiation-enhanced metastasis, and whether these alterations are a result of a tumour cell intrinsic response to direct radiation treatment or induced as a result of secreted factors, like TGF-β, with both mechanisms converging on the commonality of inducing EMT.

High doses of radiation are thought to enhance migration and/or invasion by inducing epithelial-mesenchymal transition (EMT) [49-52], typically through triggering a signaling cascade [50, 53-56]. Zhou et al. [49] observed induction of EMT in the epithelial-like tumour cell lines MCF-7 (breast) and A549 (lung) treated with 2Gy; Western blot analysis revealed a decrease in E-cadherin expression while N-cadherin expression (a mesenchymal marker) was increased; increased vimentin expression by both cell lines after 2Gy IR was demonstrated through immunocytochemistry. Scratch wound assays and transwell chamber assays revealed migration and invasion enhancement; radiation treatment increased TGF-β activity/SMAD-signaling, which subsequently led to EMT-induction [49]. Other studies citing EMT-induction after IR have also implicated other growth factors and/or signaling pathways; epithelial-like cervical cancer cell lines Siha and C33A observed a decrease in E-cadherin expression and an increase in vimentin expression after 20Gy IR treatment [52]. This EMT-induction subsequently led to enhancements in motility assayed through chemotactic migration and invasion assays, and found to be caused by increased NF-κB transcriptional activity and p65 signaling causing the initial decrease in E-cadherin expression [52].

An important observation in the histopathology of secondary metastases is the resemblance to the primary tumour, including the epithelial-like status. It is possible that a metastasized tumour cell from an epithelial-like primary tumour underwent EMT in order to metastasize as a single cell and then underwent MET upon colonization of the secondary organ [57]. However, difficulty in locating cells in primary human tumour samples that have undergone EMT brings into question the necessity of EMT [43]. To this point, two studies published in 2015 by separate research groups demonstrated that EMT is dispensable for metastasis. One group showed this in the context of breast cancer and the other in pancreatic cancer and although EMT did occur in their mouse models, it was not required for metastasis but did contribute to chemotherapy resistance in both cancer types [58, 59]. The murine-based spontaneous breast-to-lung metastasis study revealed, through a lineage-tracing system that allowed for the tracking of cells that have undergone EMT, that the lung metastases mainly comprised cells that maintained their epithelial features and did not exhibit evidence of of EMT [59]. Genetically modified mouse models of pancreatic cancer, where transcription factors involved in EMT and the repression of E-cadherin expression (Snail and Twist) were deleted, developed primary tumours that eventually became invasive and metastastic [58]. Remaining controversy over the importance for EMT includes the method of migration and invasion, specifically the contribution of single-cell versus collective migration and invasion. Although studies investigating the role of EMT in metastasis are controversial, EMT is one of the leading hypotheses used to explain how high doses of ionizing radiation may be enhancing metastasis in some types of cancer as treated cells lost or down-regulated E-cadherin expression while gaining expression of mesenchymal markers like N-cadherin and vimentin ([49, 50, 52, 55], reviewed in [60] and further discussed in Chapter 3). The studies that cited radiation-induced EMT also noted

changes in cell morphology, migration and invasion. For these reasons, EMT is a focus of the studies in this thesis as I am interested in whether a relatively lower, but clinically relevant, dose of IR is sufficient to induce an EMT in a breast cancer cell lines of interest, subsequently enhancing migration and invasion both *in vitro* and *in vivo*.

1.3.2 Tumour models of breast cancer used in this study

Animal and cell line models of breast cancer have been used extensively to study breast cancer, from development and therapeutic response, to the roles of oncogenes and tumour suppressors in the various breast cancer subtypes. Genetically modified mouse models have been developed to closely model human breast cancer development and are utilized extensively in scientific studies [61]. The genetic modifications involve the deletion of tumour suppressor genes (PTEN, BRCA1, Trp53) or the insertion of oncogenes (ie. PyMT, ErbB2, Wnt1, Ras) under a promoter that specifically drives gene expression in the mammary gland of the mice [62-64]. The resultant transgenic mice recapitulate human cancer stages and metastatic patterns, develop spontaneous tumours and even mirror estrogen receptor loss as in some human breast cancers. Even though these models have been helpful, they are not perfect; there is not a single transgenic mouse model that fully recapitulates all the characteristics and expression patterns found in human breast cancer. This thesis aims to address how a 2.3Gy dose of radiation would alter the growth and metastatic pattern of tumour cells, independent of the tumour microenvironment. However the use of transgenic mouse models of breast cancer in our radiation studies would introduce multiple confounding factors when the whole tumour is irradiated, thus making it difficult to deduce the radiation-induced changes to tumour cells alone.

An alternative to transgenic mice is xenograft transplantation, the method of transplanting human cancer cells to immune compromised mice. This is the method I chose to conduct animal studies and is a widely used method to monitor and study the genes and processes involved in metastasis, at the primary tumour and in secondary sites and as such, is the more appropriate method for my research aims [61]. In my studies, female NOD SCID (Non-obese diabetic Severe Combined Immunodeficiency) mice were used primarily because the studies involved the use of human breast cancer cell lines. These mice lack a fully functional immune system; T and B cell lymphocyte development is impaired, in addition to defective natural killer (NK) cell function. The added benefit to using immune compromised mice was also that it eliminated the possible influence immune cells may have on tumour development and metastasis after radiation treatment. As primary human breast cancer cells are difficult to acquire and culture, immortalized human breast cancer cell lines have been developed and used extensively [65-67]. The variety of immortalized breast cancer cell lines currently available for use in research has aided in the advancement of understanding breast cancer biology, but studies have found through comprehensive evaluation that gaps in how well cell lines are mirroring breast cancer heterogeneity still exist [65, 67]. Some of the most commonly used breast cancer cell lines are MCF-7 and MDA-MB-231, employed in more than two-thirds of all published breast cancer related studies [67]. The most important features to consider, when designing studies representative of the breast cancer subtypes, is the steroid receptor status and the origin of the cell line (whether it was from a primary tumour or metastatic site) [65, 67, 68]. With these considerations in mind, my study used the following human cell lines in both *in vitro* and *in vivo* (using immune compromised female NOD SCID mice) experiments to study potential ionizing radiation-enhanced metastasis.

Table 1.3 Characteristics of human breast cancer cell lines used in this study.

Cell line	Origin/Type of breast cancer [67]	Subtype classification [65]	Steroid receptor status [65]	EMT status [67]	Secondary metastatic site [65]
MCF-7	Pleural effusion/Invasive ductal carcinoma	Luminal A	ER^+ PgR^+ $HER2^-$	Epithelial	Poorly invasive and non-metastatic
MDA-MB-231	Pleural effusion/Invasive ductal carcinoma	Basal	ER^- PgR^- $HER2^-$	Mesenchymal	Lung, lymph nodes, brain, bone
MDA-MB-231 LM2-4 [69]	Lung metastatic variant derived from serial transplanted MDA-MB-231	Basal	ER^- PgR^- $HER2^-$	Mesenchymal	Lung, liver, tumour draining lymph nodes

These cell lines were chosen based on their difference in EMT status and metastatic potential. The cell lines also represent two contrasting subtypes of breast cancer; the Luminal A subtype is a low grade tumour with favourable outcome and relapse-free survival, whereas the Basal-like subtype has very poor overall and disease-free survival. The use of these cell lines with such distinct features in my studies will allow for the examination of the degree to which ionizing radiation can alter metastatic potential.

1.4 Hypothesis and aims

The tumour microenvironment plays a significant role in tumour response to radiation therapy treatment. The diversity of the immune cell infiltrate before and after radiation treatment can dictate how effective radiation treatment will be and stromal cells, such as fibroblasts and endothelial cells, have also been shown to respond to radiation therapy through the secretion of factors that may promote metastasis [30]. My study focused on whether radiation treatment itself is initiating EMT-dependent or independent tumour cell intrinsic responses that are enhancing migration and/or invasion. **I hypothesize that tumour cells that survive radiation therapy have a higher propensity to migrate, invade and eventually metastasize to secondary sites, independent of radiation-induced changes in the solid tumour microenvironment.**

The aims of this study are as follows:

Aim 1: To determine whether breast cancer cell lines that survive ionizing radiation treatment demonstrate increased migration and/or invasion *in vitro.*

> ***Aim 1a:*** *To determine whether breast cancer cell lines directly treated with a sub-lethal dose of ionizing radiation exhibit changes in migration through single cell tracking.*
>
> ***Aim 1b:*** *To determine whether migratory changes in breast cancer cell lines directly treated with a sub-lethal dose of ionizing radiation can be further supported by automated cell tracking systems.*
>
> ***Aim 1c:*** *To determine whether breast cancer cell lines directly treated with a sub-lethal dose of ionizing radiation exhibit changes in invasion.*

Aim 2: To determine whether there is a subpopulation within irradiated cell lines that undergoes EMT (non-metastatic cell line) or exhibits an increased expression of mesenchymal markers.

Aim 2a: *To determine through Western blot analysis whether 2.3Gy is sufficient to induce a loss of E-cadherin expression and an increase in mesenchymal marker expression in MCF-7 cells (thus an induction of EMT)*

Aim 3: To determine if secreted factors in conditioned media from irradiated cells may enhance the migratory phenotype of non-metastatic and metastatic breast cancer cell lines.

Aim 3a: *To determine whether conditioned media from irradiated MDA-MB-231 cells is sufficient to induce an enhanced migratory phenotype in viable, untreated MDA-MB-231 cells.*

Aim 3b: *To determine what possible secreted factors are present in conditioned media from irradiated MDA-MB-231 cells that may be enhancing migration.*

Aim 4: To determine whether pre-irradiated breast cancer cell lines, when implanted orthotopically or IV injected into mice, demonstrate an increase in loco-regional invasion and/or an increase in lung extravasation respectively *in vivo*.

Chapter 2: Materials and methods

2.1 Cell lines and media

The mesenchymal and metastatic MDA-MB-231, and epithelial-like, non-invasive MCF-7, both human breast carcinoma cell lines, were purchased from ATCC and cultured in DMEM (Gibco) supplemented with 10% FBS (Gibco). The lung metastatic variant breast carcinoma cell line MDA-MB-231 LM2-4 (LM2-4) was a kind gift from Dr. Robert Kerbel's laboratory (University of Toronto) and cultured in phenol red free RPMI (Gibco) supplemented with 10% FBS.

2.1.1 Genetically modified cell lines

Cell lines stably expressing EGFP were produced via lentiviral transduction of the pLL 3.7 EGFP construct [70], kindly provided by Dr. Aly Karsan's laboratory. Calcium phosphate transfections were used to transfect 293T cells with the lentiviral packing components (RRE, VSVG, REV) and the plasmid of interest. The resultant viruses produced were collected, filtered and concentrated over a span of 2 days before target breast tumour cells were transduced with the virus. Transduced breast tumour cell lines were subsequently FACs sorted on the FACs Aria II for further enrichment to produce the cell lines MDA-MB-231 EGFP, MCF-7 EGFP and MDA-MB-231 LM2-4 EGFP (LM2-4 EGFP).

2.1.2 Clonogenic survival assay and radiation dose determination

Both unlabeled parental and EGFP-stable breast tumour cell lines were plated into 60mm tissue culture plates, irradiated with various doses of radiation (300kV and 10mA, dose rate of 5.21Gy/min) using the Precision X-ray Model X-RAD320 (North Branford, Connecticut, USA)

and incubated for 2 weeks (5% CO_2, 37°C) before the plates were stained with Crystal Violet (5g Crystal Violet dissolved in 25% Methanol) and colony counts conducted (colonies with greater than 50 cells were counted). Surviving fraction (SF) was determined using the equation SF = Total colonies counted/(Number of cells plated*Plating Efficiency), where plating efficiency (PE) is calculated by dividing the resultant number of colonies in the untreated plate (0Gy) and dividing the value by the number of cells initially plated.

Table 2.1 Clonogenic plating density for human breast cancer cell lines.

Cell line	Seeding density (cells/plate)		
	0-2 Gray	4-6 Gray	8-10 Gray
MDA-MB-231 (EGFP)	100	500	4000
MDA-MB-231 LM2-4 (EGFP)	100	500	4000
MCF-7 (EGFP)	500	5000	50,000

The Minchinton Laboratory multi-attenuator insert [71] was used in all studies involving the direct radiation treatment of breast tumour cell lines. The initial premise for utilizing this piece of equipment was for the possibility of studying radiation induced effects on migration at multiple radiation doses. The multi-attenuator insert allows for multiple radiation dose treatments in a single administration; designed and built for a 24-well tissue culture plate by Dr. Alastair Kyle in the Minchinton lab, each column of wells receives one radiation dose, for a total of 6 different radiation doses administered to a single plate. The 2.3Gy radiation dose used in all the studies mentioned in this thesis was determined based on what a 10Gy dose, attenuated across the plate by the multi-attenuator insert, would produce. The amount of attenuation achieved with the insert

was previously determined and 10Gy attenuated across a 24-well plate format was calculated as follows:

Table 2.2 Calculations for 10Gy dose attentuation on the Minchinton Lab Multi-attentuator insert.

24-well plate column	Attenuating agent	Background subtracted TLD reading (arbitrary units)	Percent attenuation of administered dose	Final dose after attenuation of single 10Gy
1	None	8073	0%	10Gy
2	0.25 mm brass	6089	25%	7.5Gy
3	0.76 mm brass	4513	44%	5.6Gy
4	1.52 mm brass	3614	55%	4.5Gy
5	1.52 mm brass, 0.38 mm lead	1867	77%	**2.3Gy**
6	1.52 mm brass, 11.38 mm lead	436	95%	0.5Gy

2.2 Migration and invasion assays

2.2.1 Single cell tracking (*in vitro*)

Direct low-dose radiation exposure study:

Cell lines stably expressing EGFP were seeded into 24-well tissue culture plates 24 hours before a plate of each cell line was placed into a radiation multi-well attenuator apparatus designed by the Minchinton lab. Each plate was exposed to different radiation doses in a single administration of 10Gy and subsequently, along with its control/sham treated plate, placed into the Essen Bioscience IncuCyte ZOOM (Ann Arbor, Michigan, USA) for imaging. Plates were imaged at 1-hour intervals for a total of 72-74 hours. Images were exported and single cell tracking was facilitated in FIJI [72] using the MTrackJ plugin function [73]. Between 30-70 cells total were single cell tracked across multiple wells (>3) for each cell line studied, for each biological replicate (n=3). Equal numbers of sham treated and 2.3Gy treated cells were used in statistical analysis. The resultant migration and displacement values (0.8178 pixels/um) were

plotted in Graphpad Prism 6.0. In addition, at 72 hours after radiation treatment, dead and dying cells were visually counted using the Cell Counter (Kurt De Vos, University of Sheffield, Academic Neurology, available at: https://imagej.nih.gov/ij/plugins/cell-counter.html) function on FIJI to determine approximate differences in cell death percentage compared to clonogenic assays.

2.2.2 Chemotaxis migration/invasion assays

EGFP-expressing cells lines were plated into 100mm plates 48-hours before 70-80% confluent plates were irradiated with 2.3Gy and subsequently serum-starved for 24h before being resuspended in culture media (migration) without FBS or Cultrex 3-D Culture Matrix Reduced Growth Factor Basement Membrane extract (Trevigen Cat. #3445-005-01; Gaithersburg, Maryland, USA), at a final concentration of 5.0 mg/ml (invasion), and placed into the Essen Bioscience Clearview 96-well Chemotaxis plate (Cat. no. 4582; Ann Arbor, Michigan, USA). This modified Boyden chamber 96-well plate allows for real-time imaging of both the upper and lower chamber of each well, allowing for quantification of migration and/or invasion of cell from the upper chamber into the lower chamber containing the chemoattractant. The chemoattractant for both the Chemotaxis migration and invasion assay was cell culture media (DMEM or phenol-red RPMI) supplemented with 10% FBS. Chemotactic migration and/or invasion were imaged at 2-hour intervals for 72 hours. Equipment specific software (IncuCyte ZOOM 2015A Rev1) was used to analyze and quantify changes in cell count over time, normalized to the initial top chamber cell count at the start of the assay.

2.2.3 MMP2/9 zymography

MDA-MB-231 parental cells were seeded into 100mm tissue culture plates 48-hours before the plates were either sham treated or irradiated with 2.3Gy of ionizing radiation. Immediately after cells were treated, tissue culture plates were rinsed with 5ml of sterile PBS before 5ml of fresh serum-free culture media (to reduce background in subsequent assays where samples were to be analyzed) was plated onto the cells. Supernatant from sham-treated or irradiated cells were collected 8, 16, 24, 30, 38, 48, and 72 hours after treatment, filtered using a 0.22um filter and stored at -70°C in 3 different aliquots. Total protein content of all supernatant samples were quantified using a modified Lowry Assay (Bio-rad *DC* Protein Assay Kit II, Cat. No. 5000112; Mississauga, Canada) and a total of 11µg of protein from each sample condition was loaded and separated using a 10% SDS-polyacrylamine gel containing 1% gelatin (1mg/ml). The gel was run at 125 mV, with the apparatus placed on ice, for 2.5h. After protein separation, the gel was washed in Wash Buffer (2.5% Triton X-100 in dH_2O) before being placed into activation buffer (10mM Tris-HCl, pH 7.5, 1.25% Triton X-100, 9.8µM $ZnCl_2$, 4.9mM $CaCl_2$) for 41 hours at 37°C on a rocking platform. Activated gels were placed into Coomassie Blue R-250 for 3 hours before being destained in destain solution (50% MeOH, 16.6% glaciel acetic acid) for 5 hours to reveal enzymatic bands. Gels with resultant enzymatic bands were scanned on a flatbed scanner for visualization and Adobe Photoshop was used to enhance the contrast of all gels at the same time.

2.3 EMT marker western blot

MDA-MB-231 EGFP and MCF-7 EGFP cell lines were seeded into 100mm tissue culture plates, 48-hours before they were irradiated with 2.3Gy of ionizing radiation. Whole cell lysates were

collected at various time points (pre-treatment, 8, 24, 48 and 72 hours) after radiation treatment using RIPA buffer (10mM Tris ph7.5, 150mM NaCl, 1% Triton X-100, 0.1% SDS, 0.5% sodium deoxycholate, 1mM EDTA, 1X protease inhibitors (Roche)) and stored at -70°C. Standard Western blot protocol was followed, using the following primary antibodies: mouse monoclonal antibody against human E-cadherin (BD Biosciences, #610181; 1:2000; Mississauga, Canada), mouse monoclonal antibody against human vimentin (abcam 8978, 1:1000) and rabbit monoclonal antibody against human α-smooth muscle actin (abcam 32575, 1:5000; Cambridge, MA, USA), with rabbit monoclonal antibody against human α-tubulin (ab4074, 1:10,000; Cambridge, MA, USA) as the loading control. Briefly, 25µg of cell lysate for each sample was separated using a 10% SDS-polyacrylamide gel electrophoresis. The separated proteins were transferred onto a nitrocellulose membrane before kept in blocking buffer (5% w/v non-fat dry milk in 1X TBST) overnight at 4°C. Membranes were subsequently incubated with the above primary antibodies in blocking buffer (overnight, 4°C) before washes with 1X TBS-T were done 3 times, 5 minutes each wash. Secondary horseradish peroxidase (HRP)-linked antibodies were incubated with membranes overnight at 4°C (goat anti-mouse HRP diluted in blocking buffer at 1:3000 for E-cadherin and vimentin primary antibodies; 1:5000 for α-SMA and α-tubulin). Blots were washed 5 times in 1X TBS-T for 5 minutes each time. Antibody reactions to proteins present on the blots were detected by enhanced chemiluminescence (ECL; PerkinElmer Inc, Waltham, MA). Western blots were developed onto X-ray film using a film developer. Developed film was scanned to image files using a flatbed scanner.

2.4 EMT marker flow cytometry

MDA-MB-231 parental and MCF-7 parental cell lines were seeded into 100mm tissue culture plates at pre-determined seeding densities 48-hours before treatment with 2.3Gy of ionizing radiation. Irradiated and sham treated cells were collected using cell dissociation buffer (Gibco, Cat. No. 13151014) and flow cytometry analysis was used to look at expression of EMT markers E-cadherin (eBioscience, eFluor 660 conjugated clone DECMA-1; 1:200; San Diego, Ca, USA), vimentin (abcam 8978, 1:100; Goat Anti-mouse 594 secondary) and α-smooth muscle actin (eBioscience, AlexaFluor 488 conjugated clone 1A4, 1:50). All samples for each biological replicate were run on the BD Bioscience Fortessa I in the TFL Flow Core using FACs Diva II. FlowJo (ver. 7.6) software was used to analyze all events collected and to determine changes in the percentage of the cell population expressing the aforementioned markers.

2.5 Conditioned media co-culture experiment

MDA-MB-231 EGFP cells were seeded into 150mm (18ml total volume) plates 48-hours before the 70-80% confluent plate was irradiated with 2.3Gy of radiation (3553Mu/Gy) or sham treated. Culture media was replaced with 18ml of serum-free culture media supplemented with 0.1% BSA after the plate was rinsed twice with 5ml of sterile PBS. FBS was initially excluded from the culture media to reduce potential background effects on factors secreted by irradiated and sham treated cells. Conditioned media was collected 48-hours after treatment and filtered through a 0.22μm filter before storage at -20°C. Viable, un-irradiated MDA-MB-231 EGFP cells were seeded into 24-well plates 24-hours before cells were co-cultured with conditioned media supplemented with 10% FBS. Plates were imaged at 1-hour intervals for a total of 72-74 hours. Images were exported and single cell tracking was facilitated in FIJI using the MTrackJ (ver.

1.5.1; https://imagescience.org/meijering/software/mtrackj/) plugin function. The resultant migration and displacement values (0.8178 pixels/μm) were plotted in Graphpad Prism 6.0.

2.6 TGF-β1 ELISA

TGF-β1 levels in the supernatant collected from sham and 2.3Gy treated MDA-MB-231 for the MMP2/9 Zymogram was also analyzed using the human/mouse TGF-β1 Ready-SET-Go! ELISA 2nd Generation kit (e-Bioscience, Cat. No. 88-8350-22). Standards were done in triplicate and all time point supernatant samples were run in duplicate for each biological replicate (n=3). Briefly, 200μl of supernatant from time points 30, 38, 48 and 72 hours after treatment (sham and 2.3Gy) were acid-treated (1M HCl) and neutralized (1M NaOH) to release TGF-β1 from latency-associated peptide (LAP) before samples were evaluated following the kit's outlined protocol. The ELISA plate was read on the a plate reader using the SoftMax Pro software, with the output being mean optical density (once background subtraction was conducted). Using the 4-parameter logistic regression algorithm ($y=d+a-d/1+(x/c)^b$) on www.elisaanalysis.com to fit the standard curve (recombinant human TGF-β1 protein standard provided by the kit was diluted to a working stock of 1000ρg, and serially diluted 1:2 for a total of 8 standard points), raw mean optical density values from the plate reading was used to generate mean concentration values. After factoring in the dilution factor from the acidification-neutralization step (dilution factor of 1.4) and back calculating to determine total TGF-β1 concentration in each 100μl of sample analyzed, resultant values were normalized to total protein content in each supernatant. Data is presented as ρg TGF-β1/μg total protein for each time point analyzed.

2.7 Human chemokine antibody array

Supernatant, generated for the MMP2/9 zymogram and TGF-β1 ELISA from irradiated and sham-treated MDA-MB-231 cells, were also analyzed using the Abcam Human Chemokine antibody array's manufacturer protocol (abcam169812). Supernatant collected from 72 hours post treatment (sham/control or 2.3Gy irradiated) was analyzed. Antibody array blots were developed onto X-ray film using a film developer. Developed film was scanned to image files using a flatbed scanner and densitometric analysis of resultant dot plots on film were analyzed using the "Protein Array Analyzer" tool on FIJI, a macro developed by G. Carpentier (Carpentier G., Contribution: Protein array analyzer for ImageJ. ImageJ News. 2010; Available at: https://imagej.nih.gov/ij/macros/toolsets/Protein%20Array%20Analyzer.txt). Protein targets were analyzed in duplicate on antibody array and resultant mean signal intensity (MSI) values from the analysis tool (performed by integrating the grey level of pixels contained in the circular selection) were averaged and the average negative control MSI was subtracted from all values to account for background and non-specific binding. The equation $X(Ny)= X(y) * P1/P(y)$, included in the protocol and recommended by the antibody array kit to normalize all MSI values to the positive control signal intensities on each blot, was used to calculate the normalized values. The control blot was used as the reference blot. Resultant expression levels were graphed to compare changes induced by radiation treatment.

2.8 *In vivo* mouse experiments

2.8.1 Mammary fat pad tumour implants

To study the local invasion of 2.3Gy pre-irradiated vs untreated/sham treated MDA-MB-231 EGFP and MCF-7 EGFP cells, cell lines of each type from multiple 150mm plates were

trypsinized, counted and split into 2 tubes. One tube was sham treated while the second tube was irradiated with 2.3Gy using the "New" tube jig on the 9th floor X-ray room. Tubes were submerged in cold water during the duration of treatment. After treatment, cells resuspended in complete culture media were resuspended with an equal volume of Matrigel (Standard formulation, Corning Cat. No.356234; Bedford, MA, USA) to facilitate tumour formation. Resuspended cells in complete culture media/Matrigel mixture of both treatment conditions were implanted into the fourth mammary fat pad (MFP) of 8-week old female NOD SCID mice (The Jackson Laboratory) using a 26 gauge needle in a total volume of 100µl. For mice that received MCF-7 EGFP tumour cells, estrogen pellets, kindly provided by Jennifer Baker from the Minchinton Laboratory, were implanted subcutaneously into the nape of the neck 4 days before tumour cells were implanted. 2.3Gy pre-irradiated cells were implanted into the left MFP while sham treated MDA-MB-231 cells were implanted into the contralateral MFP of the same mouse, acting as an internal control. Tumours with their accompanying MFP were resected 3, 7, 14, and 21 days after implant and placed into 4% PFA (16% PFA diluted into sterile PBS) overnight at 4°C for fixation. Tumours were subsequently placed into 30% sucrose solution (250g sucrose dissolved in 500ml of sterile PBS) for 48 hours in 4°C before they were frozen in Optimal Cutting Temperature compound (Tissue-Tek O.C.T. Compound, VWR Cat. No. 25608-930; Edmonton, Alberta). 12µm tumour sections were mounted on microscope slides and stained with DAPI (1µg/ml) before imaging on the epifluorescent microscope (ZEISS Axiovert S100, Germany) to visualize EGFP expressing tumour cells and single cells that have invaded into surrounding fat tissue. Only qualitative observations were made on images.

2.8.2 Tail vein IV injection of 2.3Gy or sham treated MDA-MB-231 EGFP cells

MDA-MB-231 EGFP cells were plated onto 150mm plates 48 hours before treatment. Media on cells were replaced 4 hours before treatment (18ml); plates 70-75% confluent were either sham or 2.3Gy treated, and media volume was topped up to a total of 25ml. Cells were incubated for 40 hours after treatment before being trypsinized and counted for tail vein intravenous (IV) injections. 500,000 cells in a total volume of 200µl was injected into the lateral tail vein of 9-10 week old female NOD SCID mice (The Jackson Laboratory) using a 27 gauge needle. A total of 12 mice per treatment group were injected and at 2, 4, and 8 hours after injection, mice from both groups were euthanized, resected and the largest lobe of each lung were set aside for tissue sectioning, while the rest of the lungs were dissociated for subsequent flow cytometry analysis of EGFP positive tumour cells. The large lung lobe set aside from each lung sample was fixed in 4% PFA (16% PFA diluted into sterile PBS) overnight at 4°C for fixation. Lung lobes were subsequently placed into 30% sucrose solution (250g sucrose dissolved in 500ml of sterile PBS) for 48 hours in 4°C before they were frozen in OCT. 10µm lung sections were mounted on microscope slides and imaged using an inverted fluorescent microscope.

2.8.3 Lung tissue processing and flow cytometry

Lung tissues were minced finely with scalpels before being digested with a mixture of 3ml sterile PBS, 1ml of Trypsin (25mg/ml, Gibco) and 1ml Collagenase II (4mg/ml, Gibco) at 37°C for 40 minutes on agitation. Digested lungs were treated with 1ml DNase (3mg/ml) and vortexed before 5ml of culture media with serum was added to inhibit further enzymatic activity. Digested lung tissue mixtures were filtered through a 100µm filter and any remnants left in the filter were further broken down before filters were rinsed with 10ml of complete media. Samples were

centrifuged for 10 minutes at 850rpm before liquid was aspirated off the resultant pellet. Cell pellets were gently resuspended with 1ml sterile PBS until no clumps were visible. To lyse red blood cells, 9ml of NH_4Cl was added and incubated on ice for 9 minutes. Cold, sterile PBS was added to a total volume of 40ml to dilute out the NH_4Cl and samples were centrifuged at 850rpm to pellet cells. NH_4Cl and PBS were aspirated off and cell pellets were gently resuspended with 1ml sterile PBS. 3.4ml of sterile complete culture media was added to each sample before samples were filtered through a syringe cell filter. Single cell suspensions were counted on the Coulter Counter (Beckman Coulter Z1 Coulter Counter; Brea, CA); 10µl of the single cell suspension was diluted in 9ml of PBS and 3 cell counts were taken on the Coulter Counter before total cell number was calculated using the formula: # average cell count * 1800 * total volume.

Single cell suspensions from processed lung tissues were resuspended to a final concentration of 10^7cells/ml and stained with Fixable Viability Dye eFluor 780 (eBioscience, San Diego, CA). *In vitro* cultured MDA-MB-231 EGFP cells were dissociated and used to approximate the gate for the EGFP positive tumour cells in the lung tissue samples. Samples were run on the FACSCalibur in the Flow Cytometry Core and collected events analyzed using FlowJo software. 200,000 events were collected per sample and back calculations were conducted to determine the percentage of IV injected EGFP positive tumour cells present in the lungs.

2.9 Statistics

All statistical analysis was conducted on GraphPad Prism 7.0. All data is presented as the mean ±SEM, where $p<0.05$ is considered significant. $p<0.05$ is *; $p<0.01$ is **; $p< 0.001$ ***; $p< 0.0001$ is ****. Where only two different treatment groups were compared (as in all single cell tracking migration and displacement studies), unpaired two-tailed Student's t-test was used. Statistical analysis of single cell tracking migration and displacement kinetic analyses, and chemotaxis migration assay, was conducted by first drawing a linear regression before the slopes were tested for significance. Ordinary two-way ANOVA was used to determine significance for chemotaxis invasion assays. In co-culture studies, comparison of the migration and displacement kinetics between multiple co-culture conditions were done using Tukey's multiple comparisons test.

Chapter 3: Cell intrinsic responses to radiation: clinically-relevant, sub-lethal ionizing radiation induces enhancement of migration in non-metastatic and metastatic breast cancer cell lines.

A version of this Chapter has been submitted for publication (January 2017)

3.1 Introduction

Ionizing radiation (IR) can enhance migration and invasion of multiple tumour cell lines *in vitro* (reviewed in [60]). However many past studies have used relatively high doses of radiation, up to 12Gy per dose instead of the 2Gy per dose used in conventional radiation therapy regimens, without accounting for the high percentage of cell kill induced. Multiple *in vitro* studies have reported that 1-3Gy IR can increase migration to varying degrees in some brain (U87 [74], UN3 [75], GM2 [75], U87MG [76], T98G [77], LN-18 [76], LN-229 [76]), pancreatic (MIAPaCA-2 [78]), and head and neck (CAL-27 and HN [79]) cancer cell lines, while also decreasing migration of some lung (A549 [80]), pancreatic (PANC-1 [78, 81], SUIT-2 [81]), colon (HCT116 [74]), and sarcoma (HT1080 [82]) cancer cell lines. In these studies, migration was assessed using transwell or scratch wound assays, in time frames that ranged from 1 to 48 hours after treatment. The breast tumour cell line MDA-MB-231 has been shown in the literature to exhibit enhanced migration when scratch wound assays were performed after 10Gy IR [83] and 2Gy IR was sufficient in enhancing the migration of non-metastatic MCF-7 cells [49]. Despite the accumulated evidence of variability in migration response after 1-3Gy IR in other cancer cell lines, MDA-MB-231 migration response to IR doses lower than 10Gy has not been studied.

Enhanced invasion has also been reported in literature after ionizing radiation treatment [76, 78, 81]. First developed to study the chemotactic migration of leukocytes to specific soluble

substances, the Boyden assay utilizes a chamber with two compartments separated by a filter membrane of a known pore size [84]. Cells are placed into the upper chamber and will migrate into the lower chamber if it contains a soluble substance with a chemotactic effect to induce active migration of the cells through the pores and into the lower chamber side of the membrane. After allowing the cells to migrate, the membrane is fixed and stained to enable quantification of the migrated cells [84]. A variation of this involves coating the filter membrane with basement membrane (Matrigel) such that the cells must invade through the basement membrane in order to reach the lower chamber with the chemoattractant, thereby assessing cellular migration and invasion capabilities. A number of scientific papers that have studied how the microenvironment influences radiation-enhanced invasion of breast cancer cell lines have used the Boyden assay. 5Gy irradiated 3T3 fibroblasts seeded in the lower chamber enhanced the invasion of untreated MDA-MB-231 placed in the upper chamber, dependent on upregulation of COX-2, a protein that stimulates the activity of matrix metalloproteinase 2 (MMP2) [85]. Pre-irradiation of the Boyden chamber coated with Matrigel with as low as 5Gy was also found to enhance MDA-MB-231 invasion by releasing proteins that increased MMP-2 activity on the surface of untreated tumour cells [86]. Supernatant collected from cells irradiated with 20Gy has also been shown to enhance invasion in untreated cells in multiple cell lines [87]. These studies provided foundation for an indirect effect of radiation treatment that produces a tumour microenvironment more conducive to invasion. This is in part due, at least *in vitro*, to increased tumour cell matrix metalloproteinase (MMP) activity, the key protein required for extracellular matrix degradation and thus, invasion. Further supporting the importance of MMP proteins, the direct IR treatment of various brain and pancreatic tumour cell lines (dose range 3-10Gy) also induced enhanced invasion through increased MMP2 or MMP9 activity [76, 78, 81]. Although the aforementioned studies

collectively reveal the potential metastasis-promoting abilities of radiation and importance of MMPs, it remains unclear whether the reported increased migration is capturing the response of dying cells or the very small fraction of cells that survive these relatively high radiation doses. What has been demonstrated in the literature is that the effect of radiation on cell migration and/or invasion is for the most part cell line dependent.

The majority of literature studying the effects of IR on cell migration have used scratch wound assays, which measure collective cellular migration and therefore cannot relate to the EMT hypothesis IR-induced migration because the EMT phenotype is defined as single cell detachment and migration away from the primary tumour mass [43]. The scratch wound assay is a highly utilized *in vitro* assay to study migration based on the simple observation that when an artificial gap or "wound" is made in a confluent monolayer of cells as a result of a "scratch", the cells at the edge of the wound will migrate inwards until the space is once again filled with cells [88]. Imaged over time, the closure of the wound can be used to quantify how fast cells are migrating towards each other at the edge of the wound [88]. Therefore the migration output of the scratch wound assay is the collective migration of each wound edge. As such, the majority of radiation enhanced migration studies using the scratch wound assay have been quantifying collective migration enhancement. As an alternative to scratch wound assays, the studies in this thesis will employ single cell migration tracking, which has not been used previously to study radiation induced alterations to tumour cell migration. Cell or particle tracking was developed as a method to quantify cell behavior and molecular changes under varying conditions that influence cell fate [89]. Although labour intensive, as reliable automated methods of cell tracking are still being developed, manual single cell tracking produces numerical outputs such as total trajectory length/migration distance and displacement for each cell tracked or as mean values for

each treatment group (illustrated in Figure 3.1) [73]. Plotted against time, these two parameters can also be used to reveal changes in the migration kinetics and behavior of treated versus untreated cells. **With these current gaps in knowledge highlighted, the data presented in this chapter aims to address Aims 1 and 2 of the thesis. Specifically, whether breast cancer cell lines, when treated with 2.3Gy ionizing radiation, exhibit changes in migration and invasion associated with radiation-induced EMT and/or an upregulation of mesenchymal markers.**

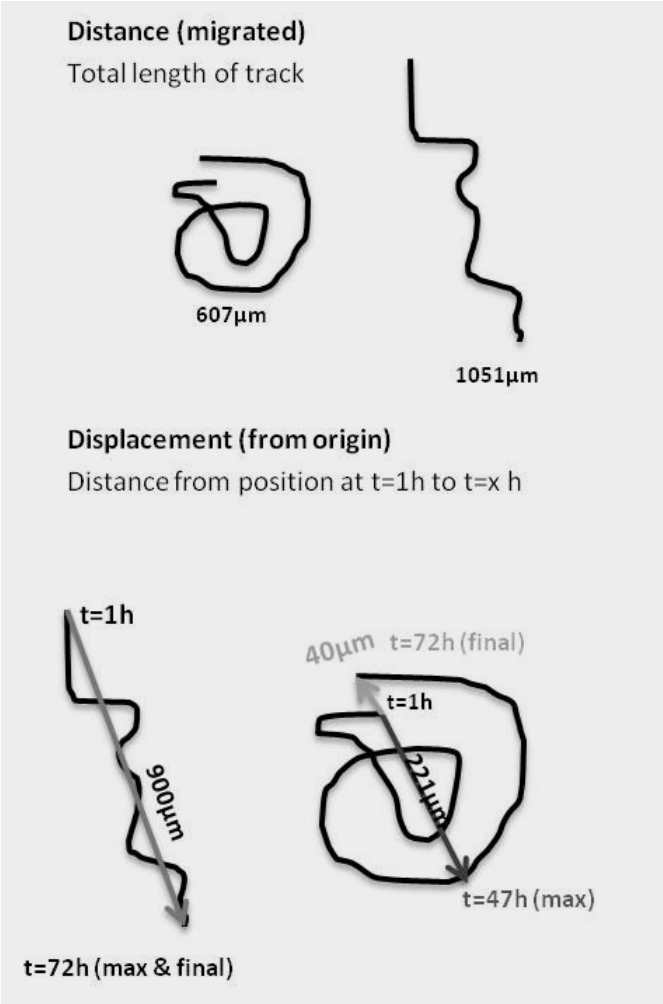

Figure 3.1 The differentiation and quantification of distance vs. displacement. Illustrating total distance migrated and cellular displacement from the initial point of origin.

3.2 Results

3.2.1 Clonogenic survival assays – the effect of ionizing radiation on breast tumour cell survival

Human breast carcinoma cells (MDA-MB-231, MDA-MB-231 LM2-4 and MCF-7) were engineered to stably express EGFP to help facilitate single cell tracking after imaging was conducted in the IncuCyte ZOOM system. It is important to determine what percentage of cells survive various doses of radiation treatment in order to select a radiation dose to study that is not only clinically relevant in a conventional treatment schedule but also exhibits a high percentage of cell survival. Figure 3.1 shows the clonogenic survival curves of all 3 cell lines used throughout this study, with cell lines treated with a range of radiation doses from 0 to 10 Gray. Although there is some discrepancy in survival in the MDA-MB-231 (Figure 3.1A and Table 3.1) and its lung metastatic variant MDA-MB-231 LM2-4 (LM2-4, Figure 3.1B and Table 3.1) between the parental and EGFP expressing cell lines at higher radiation doses, at 2Gy, there is still an appreciable amount of cell survival 2 weeks after radiation treatment. Parental and EGFP-stably expressing MCF-7 cells exhibited no apparent difference in clonogenic survival (Figure 3.1C and Table 3.1). Additional biological replicates would be required to make a firm conclusion about potential differences in radiation sensitivity between EGFP-expressing and parental cell lines. A radiation dose of ~2Gy (2.3Gy) was used in all subsequent studies.

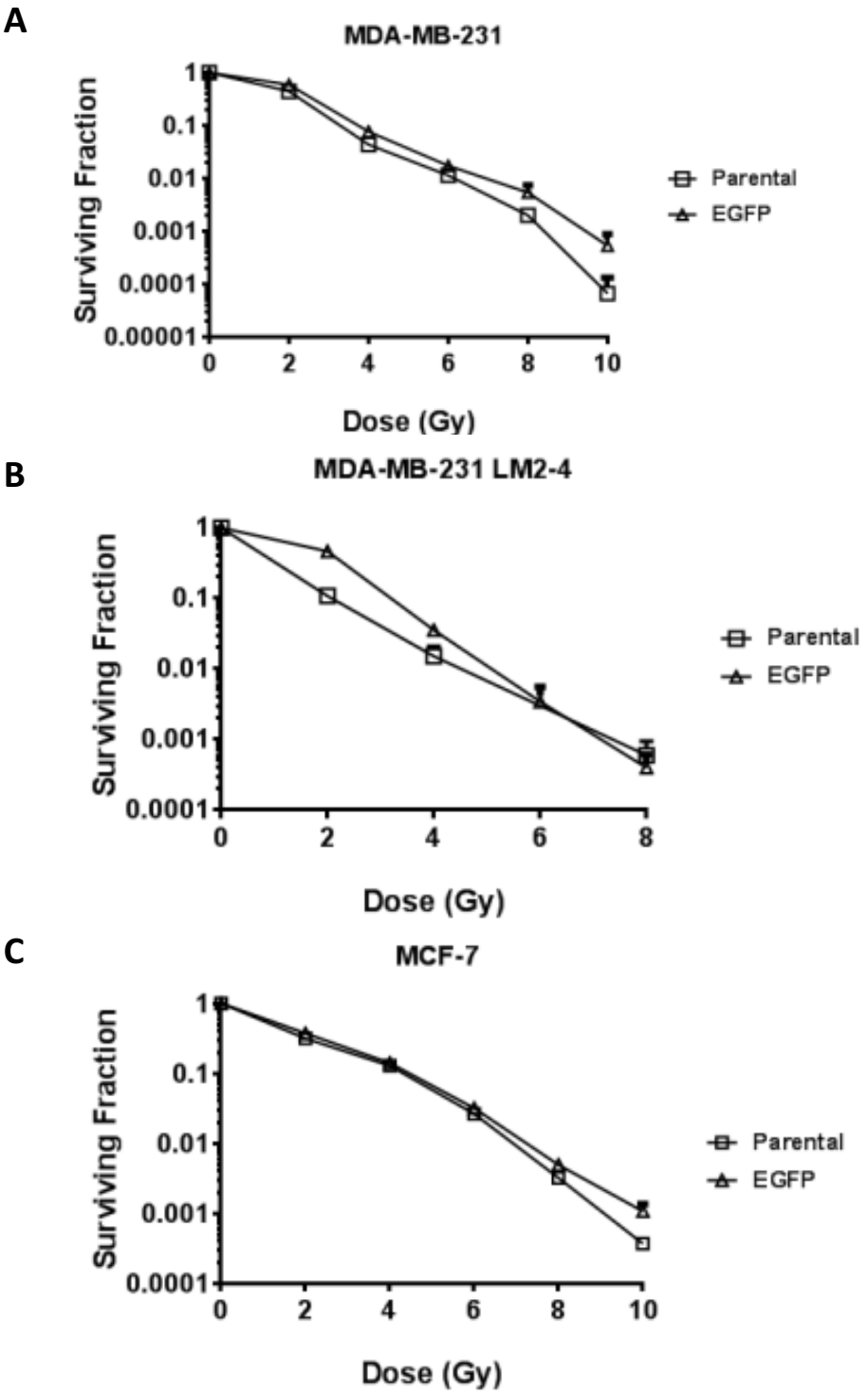

Figure 3.2 Clonogenic analysis of breast carcinoma cell lines following radiation treatment. Surviving fractions (SF) of (A) MDA-MB-231, (B) MDA-MB-231 LM2-4, and (C) MCF-7 cells after irradiation with the indicated radiation doses were stained with Crystal Violet, counted 2-weeks after radiation exposure and compared to untreated control cells (SF=colonies counted/(cells plated * plating efficiency). Plots from one biological replicate per cell line (EGFP and parental) are shown (3 technical replicates per dose). Data are mean±SEM.

Table 3.1 Surviving fraction comparison between parental and EGFP-stable human breast tumour cell lines after 2Gy IR treatment.

Cell line	Parental	EGFP-stable
MDA-MB-231	0.444 ±0.050	0.594 ±0.048
MCF-7	0.316 ±0.027	0.372 ±0.015
MDA-MB-231 LM2-4	0.108 ±0.027	0.466 ±0.032

3.2.2 Quantification of enhanced migration phenotypes following radiation of breast cancer tumour cell lines

Through single cell tracking, migration and displacement of all three cell lines were quantified over 72-74 hours after 2.3Gy radiation. The non-metastatic, epithelial-like breast carcinoma cell line MCF-7 and the metastatic, mesenchymal line LM2-4 exhibited no enhancement in their migration but both maximally displaced further in 2.3Gy radiation treated cells compared to the sham treated cells (Figure 3.3A-B, Table 3.2). The metastatic and fully mesenchymal MDA-MB-231 cell line, when treated with 2.3Gy radiation, robustly exhibited both an enhanced migration and displacement phenotype compared to sham treated cells (Figure 3.3C, Table 3.2). Irradiated MDA-MB-231 cells migrated a greater total distance, and exhibited a greater maximal displacement from the cellular point of origin compared to their sham treated counterparts. Therefore, 2.3Gy radiation treatment induces an enhanced single-cell displacement in all three human breast cancer cell lines (summarized in Table 3.2).

Table 3.2 Comparison of migration and displacement between sham treated and 2.3Gy treated breast cancer cell lines (n=3 with 30-70 cells analyzed per condition)

	Migration (μm)			
Cell Line	**Control**	**2.3Gy Irradiated**	**Significance**	**p-value**
MCF-7 EGFP	901.2 ± 46.17	916.5 ± 76.36	NS	
LM2-4 EGFP	1647 ± 39.96	1652 ± 39.98	NS	
MDA-MB-231 EGFP	1315 ± 38.65	1622 ± 83.71	*	<0.05
	Maximal displacement (μm)			
Cell Line	**Control**	**2.3Gy Irradiated**	**Significance**	**p-value**
MCF-7 EGFP	108.3 ± 5.657	133.1 ± 7.369	*	<0.05
LM2-4 EGFP	289.3 ± 20.05	364.7 ± 19.98	*	<0.05
MDA-MB-231 EGFP	194.9 ± 10.89	293.1 ± 24.81	*	<0.05

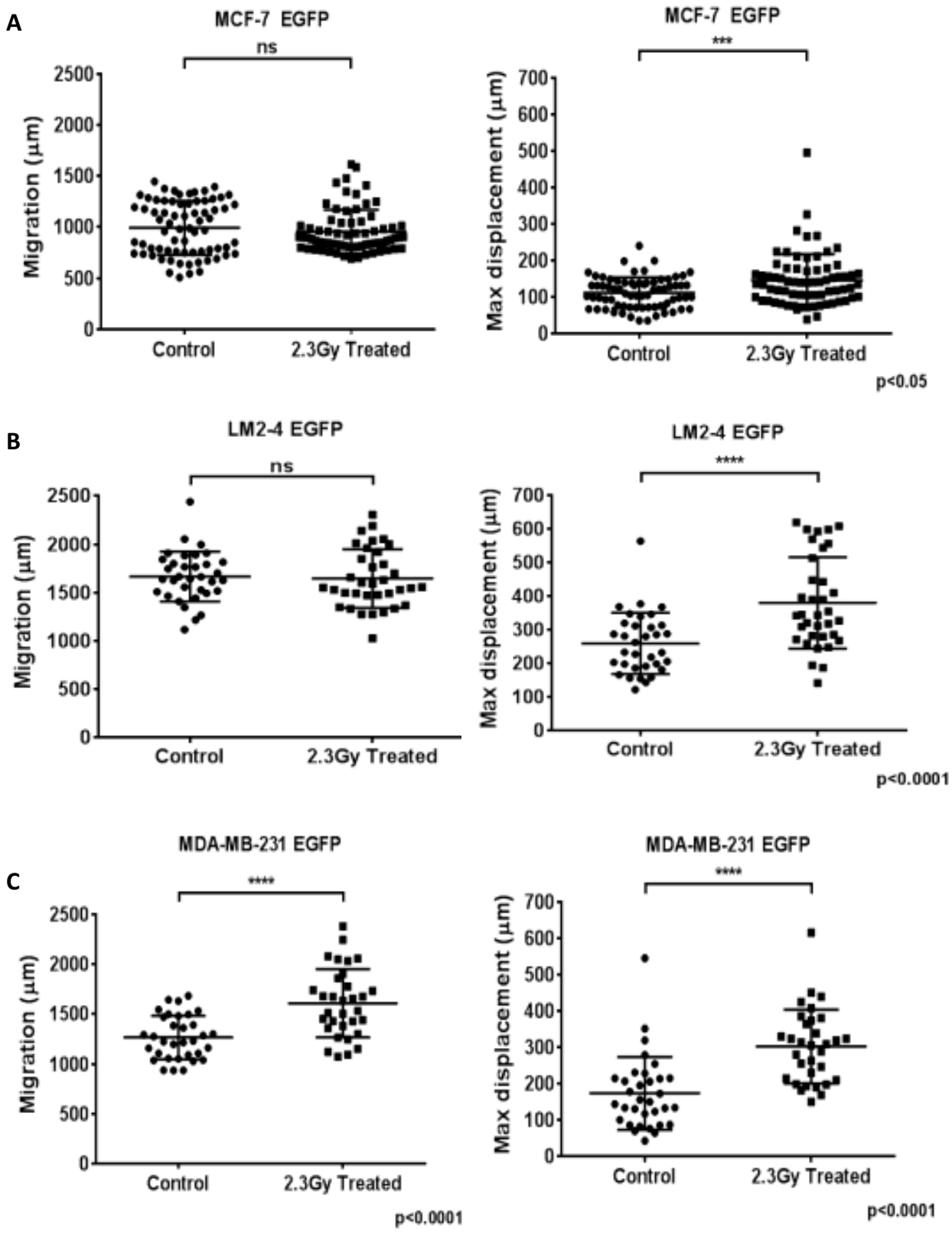

Figure 3.3 2.3 Gy IR enhances migration of breast cancer cells. (A) MCF-7, **(B)** LM2-4, and **(C)** MDA-MB-231 cells were sham-treated or irradiated with 2.3Gy and imaged at 1 hour intervals for 72 hours. 30-70 single cells (across 2-3 wells) were tracked to determine total distance migrated and maximal displacement over a 72 hour timeframe post-treatment. Data are mean±SEM ($p<0.05$-0.0001 unpaired two-tail t-test). Representative plots from one experiment are displayed (n=3).

3.1.1 Effects of 2.3Gy radiation dose on migration and displacement kinetics

Analysis of migration and displacement kinetics revealed different time points in which irradiated cells diverged from sham treated cells. MDA-MB-231 cells diverged in their migration and displacement at approximately 38 hours after radiation treatment compared to sham treated cells (Figure 3.4A). The slope of both irradiated curves increases significantly over time with a distinguishable inflection point at 38 hours, representing the time point in which the velocity of the irradiated cells increases. MCF-7 and LM2-4 cells demonstrated an enhancement in maximal displacement after treatment with 2.3Gy, and when this is plotted over time there are clear time points in which the enhancement occurs, at 25 hours after treatment for MCF-7 cells and at about 31 hours for LM2-4 cells (Figure 3.4B-C). It is clear 2.3Gy radiation treatment has cell line dependent effects on migration.

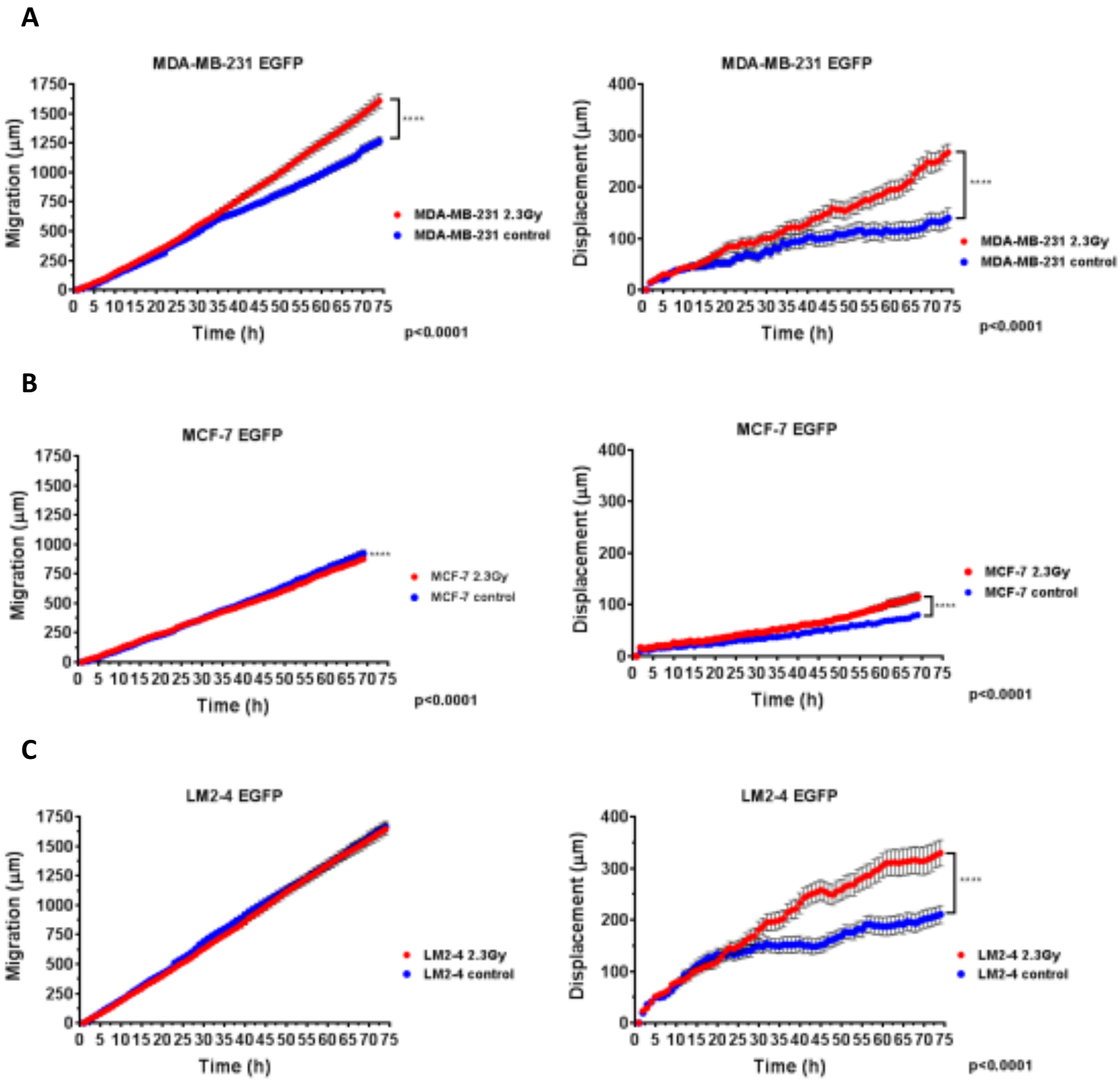

Figure 3.4 Kinetic analyses of radiation-induced single cell migration and displacement. Mean distances migrated and displacement of all cells single cell tracked were plotted over time for sham-treated or 2.3Gy irradiated (A) MDA-MB-231, (B) MCF-7, and (C) LM2-4 cells. Data are mean±SEM (Linear regression analysis with comparison of slopes). Representative plots from one experiment (same experiment as Figure 3.3) are displayed (n=3).

3.1.2 Automated quantification of how a 2.3Gy dose of radiation alters chemotactic migration and invasion

Real-time automated tracking of chemotactic migration of the 3 breast cancer cell lines recapitulated what was seen in the single cell tracking migration data. Briefly, breast cancer cell lines were serum-starved for 24 hours after 2.3Gy IR or sham treatment before being seeded into a 96-well modified transwell plate for imaging; the lower chamber wells contained 10% FBS. 2.3Gy treated MDA-MB-231 cells displayed enhanced migration towards the FBS in the lower chamber of the transwell compared to sham treated controls (Figure 3.5A) whereas MCF-7 cells and LM2-4 cells demonstrated no significant enhancement (Figure 3.5B-C). As all 3 cell lines were serum-starved for 24 hours before the start of the assay, the chemotaxis migration assay further supports what I observed in the kinetic analysis of migration from single cell tracking. After 24 hours of serum starvation, at 14 hours into the chemotaxis migration assay, the rate at which 2.3Gy treated MDA-MB-231 cells were migrating towards the chemoattractant (FBS) began to increase compared to sham treated cells (Figure 3.5A). This coincides with the 38-hour time point in which I observed the divergence in the migration kinetics of the single cell tracking data in Figure 3.4A. MCF-7 and LM2-4 cells did not chemotactically migrate faster towards FBS when treated with 2.3Gy radiation and this corresponds to the single cell tracking migration kinetics data (Figure 3.4B-C).

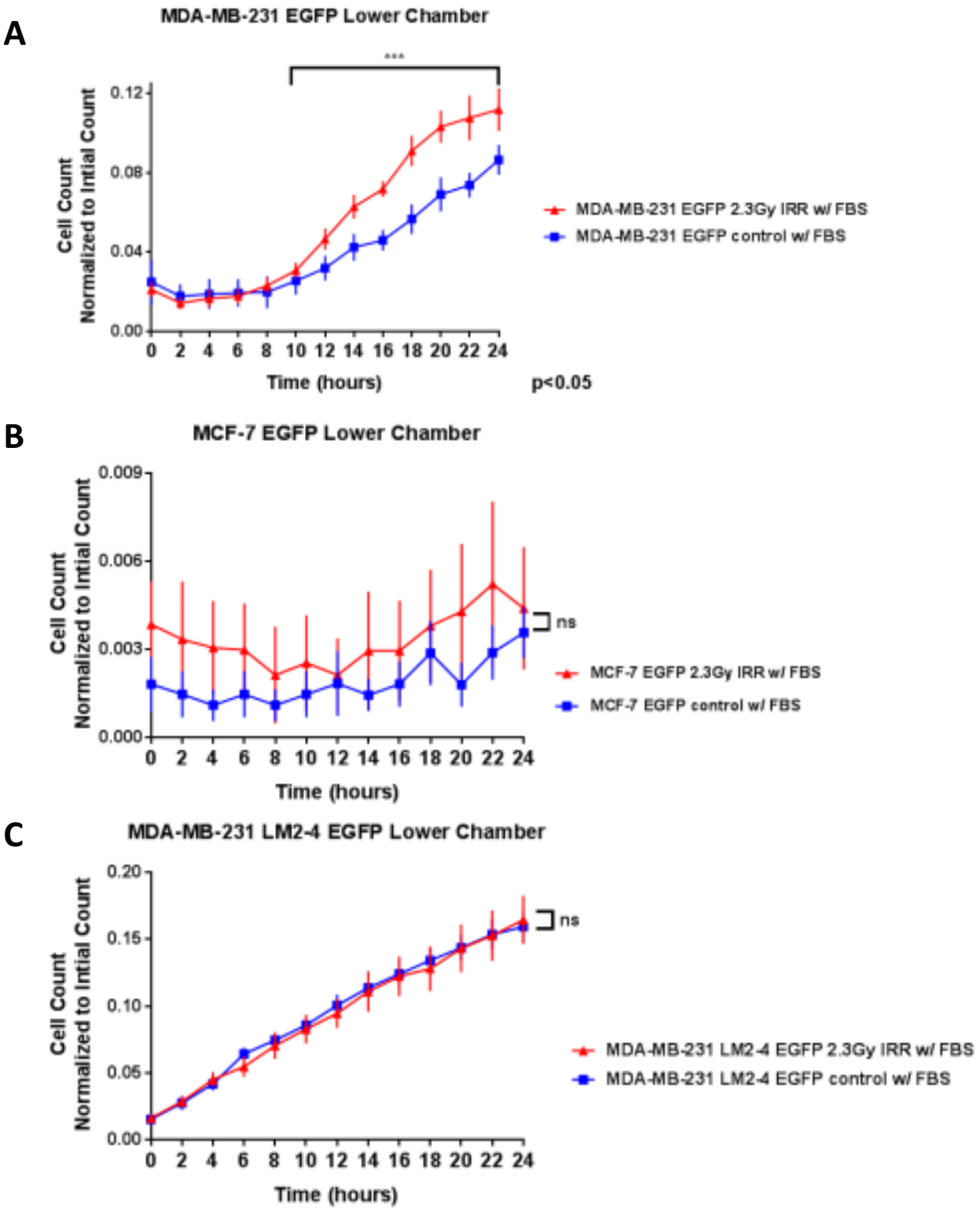

Figure 3.5 Automated chemotaxis migration assay recapitulates single cell tracking observations. (A) MDA-MB-231, **(B)** MCF-7, and **(C)** LM2-4 cells were sham-treated or irradiated with 2.3Gy prior to 24 hours serum starvation and plating in transwell chambers with 10% FBS as chemoattractant. Cells that underwent chemotactic migration to the bottom of the chambers were quantified (cell count on Y-axis of graph) over time (hours). Data are mean±SEM (Linear regression analysis with comparison of slopes was conducted between times points 10h to 24h).

EMT-induced enhanced invasion after radiation treatment has also been reported in the literature [49, 52] but as I did not observe a substantial enhancement in migration in MCF-7 cells, I did not look at potential changes in invasiveness. The fully mesenchymal MDA-MB-231 cells exhibited a robust radiation-induced migration enhancement, are invasive *in vitro* but are poorly metastatic *in vivo* [68], which prompted further study into whether radiation treatment would further enhance MDA-MB-231 invasiveness and thus, overall metastatic potential. Real-time chemotactic invasion assays on the IncuCyte ZOOM system were used to monitor changes in the invasive ability of MDA-MB-231 cells after 2.3Gy radiation treatment compared to sham treated cells. Using a modification of the chemotaxis migration assay above, cells were resuspended in basement membrane instead of culture media after 24 hours of serum starvation and treated with sham protocol or 2.3Gy, before being placed into the modified 96-well Boyden chamber plate. Therefore, cells in both treatment groups had to migrate and invade through the basement membrane in the upper chamber towards the pores that led to the lower chamber containing the chemoattractant. Low-dose ionizing radiation does not enhance the invasive phenotype of MDA-MB-231 cells (Figure 3.6A).

3.1.3 Characterization of MMP2/9 activity change after 2.3Gy radiation treatment

Gelatin zymography of supernatant collected from irradiated and sham treated MDA-MB-231 cells was conducted to examine how the enzymatic activity of proteins involved in extracellular matrix degradation, a process necessary for invasion through tissue and basement membrane, changes in response to radiation treatment. MMP2/9 enzymatic activity was similar in both treatment conditions at all time points (Figure 3.6B), further supporting the lack of enhanced invasion observed in Figure 3.6A. Supernatants analyzed were from time points with

the greatest difference in invasion between irradiated and sham treated cells in chemotaxis invasion assays (30-72 hours after treatment).

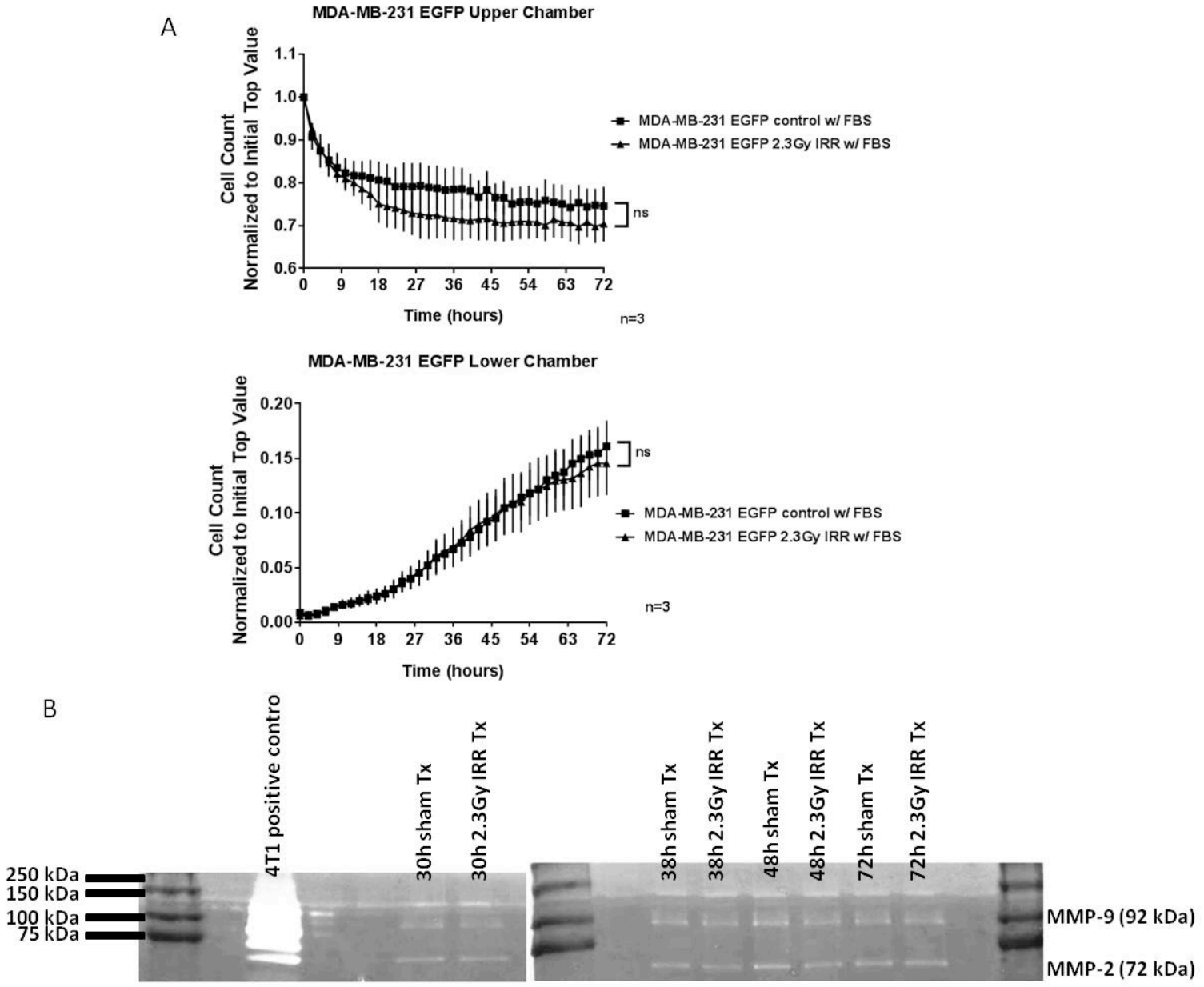

Figure 3.6 Chemotactic invasion of MDA-MB-231 cells. **(A)** MDA-MB-231 cells were sham-treated or irradiated, serum starved for 24 hours, and plated in basement membrane in transwell chambers. The upper and lower chambers were imaged at 2 hour intervals over 72 hours. Cells that underwent chemotactic invasion from the upper chambers (upper plot) to the bottom chambers (lower plot) were quantified (Y-axis of graph) over time (hours). No significant difference was observed by two-way ANOVA. **(B)** Gelatin zymogram of MMP2 and MMP9 secreted by sham-treated or irradiated MDA-MB-231 cells. 4T1 murine mammary carcinoma cells were used as a positive control due to well characterized MMP2/9 activity [90].

3.1.4 Characterization of EMT markers after 2.3Gy radiation treatment in non-metastatic and metastatic breast cancer cell lines through Western Blot analysis

To characterize possible molecular changes that may explain the observed enhanced migration phenotype in single cell tracking, Western blot analysis was conducted using well-characterized markers of EMT. Cell lysates from MCF-7 and MDA-MB-231 cells were collected pre-treatment and at multiple time points after 2.3Gy radiation treatment (8, 24, 48 and 72 hours). Three different markers of EMT were analyzed: vimentin, highly expressed in mesenchymal cells and involved in maintaining cell integrity; E-cadherin, involved in cell to cell adhesion and highly expressed in epithelial cells; and α-smooth muscle actin (α-SMA), highly expressed in mesenchymal cells and involved in cell motility. Short exposures of Western blot membranes reveal that MCF-7 cells retain E-cadherin expression and do not up-regulate vimentin in response to 2.3Gy at any time point, suggesting that 2.3Gy radiation treatment is not sufficient to induce EMT (Figure 3.7A). MCF-7 cells did not exhibit a marked increase in their migratory phenotype through single cell tracking and displayed low expression of α-SMA across all samples. In response to 2.3Gy radiation, MDA-MB-231 cells, a fully mesenchymal cell line (that therefore does not express E-cadherin), demonstrated a slight up-regulation of E-cadherin expression at 48 hours after radiation treatment and an even greater up-regulation at 72 hours (Figure 3.7B bottom panel). Correlatively, with shorter membrane exposures, vimentin expression decreased in the 48-72 hour time points. α-SMA increased in expression over time in lysates from irradiated MDA-MB-231 cells compared to pre-treatment lysates (Figure 3.7A). This steady increase in α-SMA may contribute to the enhanced migratory phenotype observed in MDA-MB-231 cells after treatment with 2.3Gy radiation, while the loss of vimentin and modest

increase in E-cadherin suggest a potential MET that would run counter to the increased migration observed in these cells after radiation treatment.

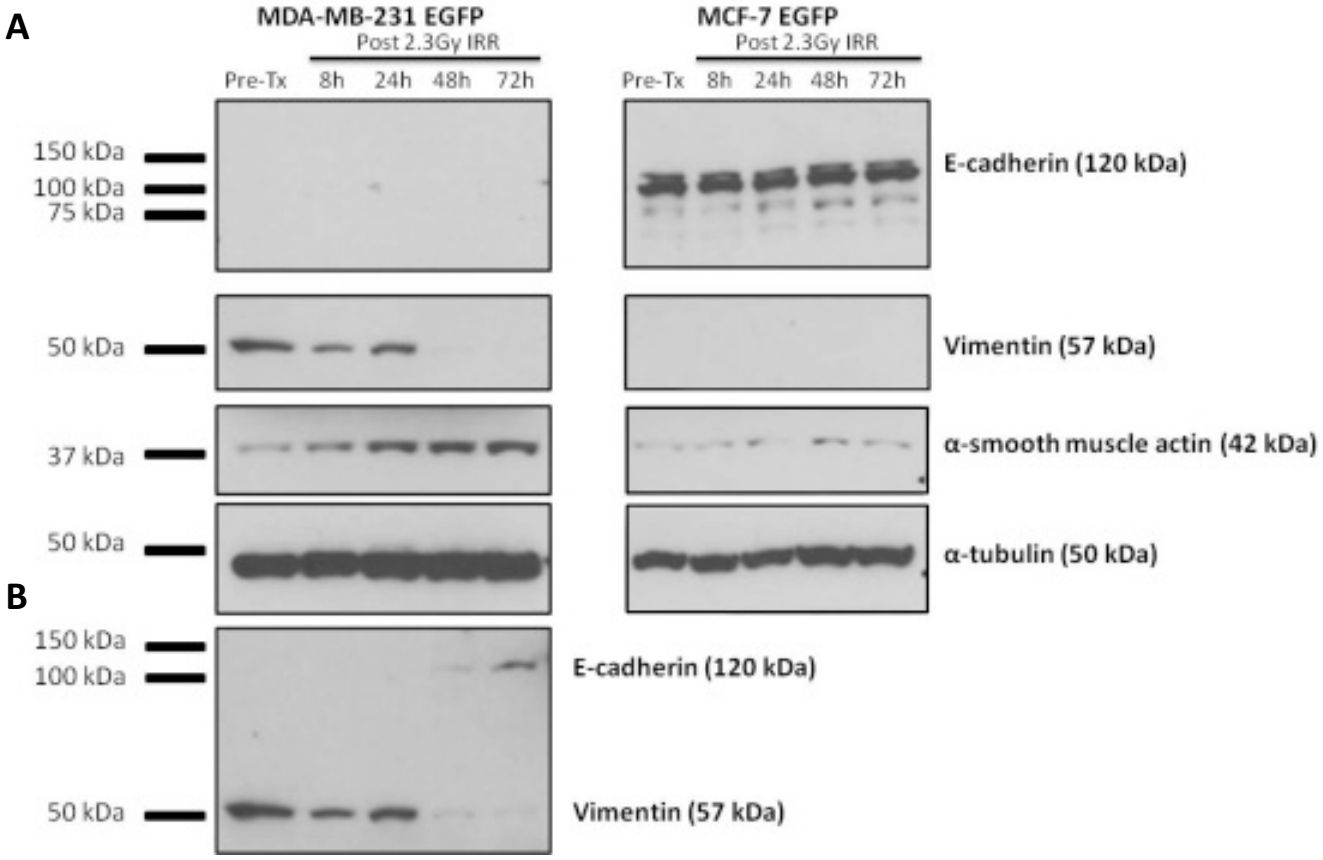

Figure 3.7 Radiation-induction of EMT markers by Western blot. (A) MDA-MB-231 and MCF-7 cell lysates from various time points after sham or 2.3Gy irradiation were probed for the presence of EMT markers E-cadherin, vimentin, and α-smooth muscle actin, with α-tubulin as a loading control. 25μg of total protein was loaded per sample. (B) Longer exposure time of the MDA-MB-231 Western blot showing the presence of E-cadherin (n=1).

3.1.5 Characterization of EMT marker changes after 2.3Gy radiation treatment in non-metastatic and metastatic breast cancer cell lines through flow cytometry analysis

Single cell tracking data (Chapter 3, section 3.2.2) showed a high range of cellular movement after IR (lows of ~1000 μm to highs of ~2500μm), and Western blot analysis assessed the EMT marker protein levels of the cell population as a whole. I followed Western blot analysis with flow cytometric analysis to determine whether IR changes EMT marker expression

in a subpopulation of cells; due to the capacity of flow cytometry analysis to detect rare expression events at the single cell level, it is highly sensitive. Single stain controls (viability, E-cadherin, vimentin and α-sma) were used to draw the gates around the population of cells positive for the marker of interest; cells used for single stains were a mixture of cells from all treatment time points. Single stains also allowed us to determine whether the presence of multiple fluorophores in a single sample would cause a whole population shift that could be mistaken as a positive staining of the whole population; as this did occur during the analysis of E-cadherin in the MDA-MB-231 samples, the positive gate was drawn to take this artificial shift into account (Figure 3.9A). An additional control time point (72h post shamTx/control) was analyzed in addition to the Pre-sham Tx/control (a replicate of the pre-treatment control analyzed in our Western blot) to take into account the possible affect confluency may have on cell surface marker expression. In accordance with Western blot results, epithelial-like MCF-7 cells maintained the same level of E-cadherin expression at all time points after 2.3Gy treatment and this was not significantly different compared to sham treated cells at corresponding time points (Figure 3.8A). Vimentin expression was detected in irradiated MCF-7 cells but was not significantly increased compared to controls (Figure 3.8B). As was also observed by Western blot analysis, α-SMA expression was detectable but did not increase significantly in irradiated cells compared to sham-treated control cells. There was no significant change in MDA-MB-231 vimentin or α-SMA expression; these proteins are highly expressed in all sham treated and 2.3Gy treated time points (Figure 3.9B-C), contradicting what I observed by Western blot analysis. A sub-population of MDA-MB-231 cells exhibited a significant, nearly two-fold, increase in E-cadherin expression at 72 hours after 2.3Gy radiation treatment compared to its matching 72h

post sham treated control cells (Figure 3.9A), recapitulating what was observed by Western blot analysis in Figure 3.7B.

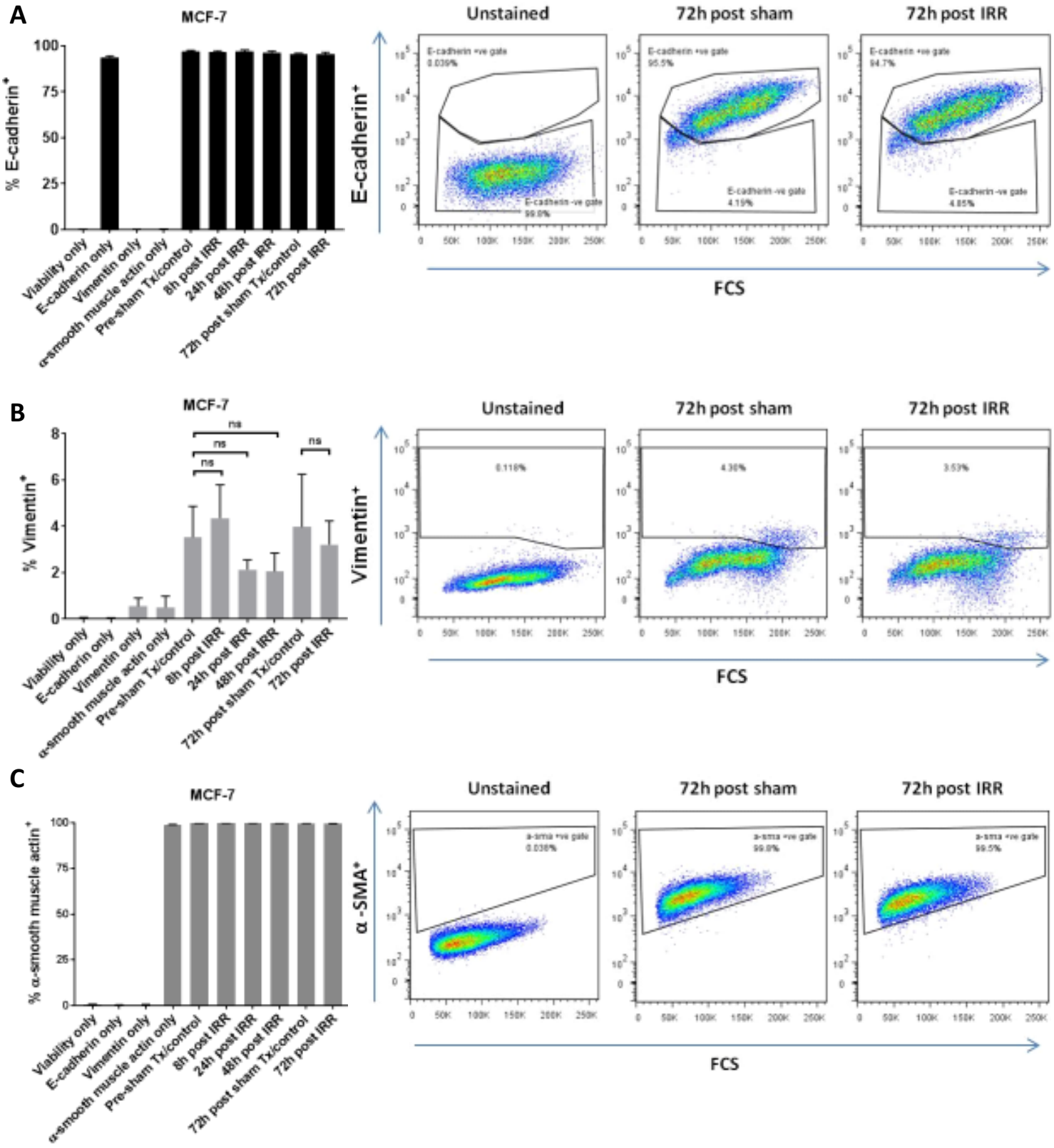

Figure 3.8 Radiation-induction of EMT markers by flow cytometry. Flow cytometric analysis of EMT marker changes in **(A-C)** MCF-7 cells after 2.3Gy irradiation or sham treatment at various time points. The expression of E-cadherin, vimentin and alpha smooth muscle actin on irradiated cells are compared to pre-irradiated control cells and cells 72 hours after sham-treatment. Data are mean±SEM (n=4); unpaired one-tail t-test.

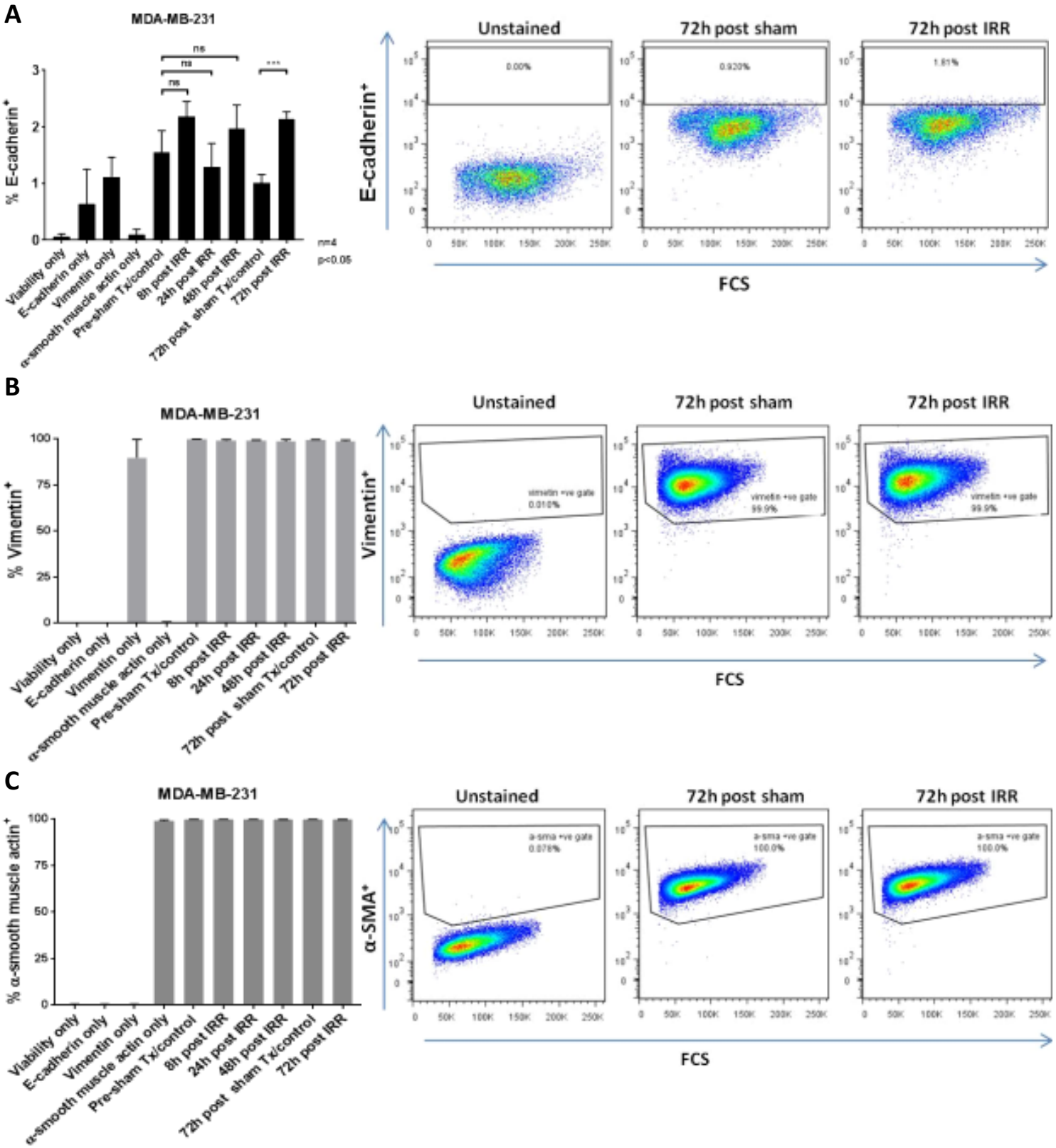

Figure 3.9 Radiation-induction of EMT markers by flow cytometry. Flow cytometric analysis of EMT marker changes in **(A-C)** MDA-MB-231 cells after 2.3Gy irradiation. The expression of E-cadherin, vimentin and alpha smooth muscle actin on irradiated cells are compared to pre-irradiated control cells and cells 72 hours after sham-treatment. Data are mean±SEM (n=4); unpaired one-tail t-test ***$p<0.05$.

3.2 Discussion

Previous studies have used ionizing radiation doses that ranged from 3-10Gy to conclude that radiation treatment induces an EMT-dependent migration and invasion enhancement across many cell types. Our clonogenic assays of breast cancer cell lines MDA-MB-231, MDA-MB-231 LM2-4 and MCF-7 revealed that at 10Gy, there is less than 0.001-0.01% survival two weeks after treatment. With such a small surviving fraction at higher single doses, I decided to study a radiation dose (2.3Gy) where the surviving fraction is higher in our cell lines of interest and would subsequently be more meaningful for future *in vivo* studies.

Previous studies of migration have used scratch wound assays, which are representative of collective migration and are unsuitable to study EMT as it is defined as single cell detachment from the tissue (normal or tumour) mass. Single cell tracking is a superior method for analysis of EMT-induced enhancement of migration and also revealed that even at a conventional dose of IR (2.3Gy), there was still an appreciable and significant migration enhancement in MDA-MB-231 cells, and displacement enhancement in all 3 breast cancer cell lines studied. It allowed for not only the quantification of total distance travelled by cells during the duration of the assay but also the displacement of cells from their cellular point of origin at any given time and the dynamic changes that occur over time. The cell intrinsic response to move away from its original location demonstrates the possible dissemination-inducing effect IR has on surviving tumour cells. Displacement enhancement was consistently statistically significant in all irradiated breast tumour cells studied. All breast cell lines studied possessed different metastatic abilities and each displayed a characteristic radiation-induced enhancement in displacement kinetics that was only appreciated through single cell tracking. Automated Boyden assays showed that irradiated MDA-MB-231 cells also have the enhanced ability to respond and migrate towards a chemoattractant,

although IR did not affect chemotactic invasion or MMP2/9 activity. This demonstrates that a dose of 2.3Gy ionizing radiation treatment can also enhance tumour cell response to chemokines that may be present in the microenvironment, in a temporal fashion.

Previous studies that focused on radiation enhanced migration and metastasis often associated the changes with the induction of EMT. Recently published literature [58, 59, 91] suggests that EMT is not necessary or sufficient for metastasis, and demonstrates that tumour cells are able to disseminate from the primary tumour and form metastatic nodules while retaining their epithelial-like phenotype [59]. The studies of this thesis provide new insight on radiation induced enhancement of migration in both non-metastatic and metastatic breast carcinoma cell lines by establishing that relatively low-dose ionizing radiation is sufficient to enhance migration and/or displacement. These changes occur within the first 72 hours after treatment as evidenced by kinetic increases in migration and/or displacement. In comparing EMT marker expression levels of MDA-MB-231 and MCF-7 cells at various time points after sham or 2.3Gy IR treatment, Western blot and flow cytometry analysis revealed different vimentin and/or α-SMA expression profiles. Western blot analysis was not used quantitatively in our studies to assess EMT marker expression; it was first used to qualitatively determine whether 2.3Gy IR treatment to MCF-7 cells was sufficient to induce EMT based on protein isolated from cell lysates. Through Western blot analysis, I made the observation that 2.3Gy treated MDA-MB-231 cells were expressing E-cadherin at later time points (48-72h) at higher exposure times. The expression of the mesenchymal markers vimentin and α-sma also changed in response to radiation, thus further studies were conducted using flow cytometry analysis, which is a more quantitative assay to assess changes in protein expression on intact cells. EMT marker-specific flow cytometry analysis of both MCF-7 and MDA-MB-231 cells was conducted multiple times

and I determined that contrary to Western blot results, 2.3Gy IR treatment did not down-regulate vimentin or up-regulate α-SMA expression. The gene that encodes α-SMA, *ACTA2*, is known to be involved in cell-generated mechanical tension and in the maintenance of cell movement and shape [92]. Downregulation of α-SMA expression in the lung adenocarcinoma cell line PC14PE6 by shRNA knockdown decreased transendothelial migration [92] and the expression of α-SMA has been directly correlated with the contractile activity of cells during wound healing [93]. Increased α-SMA expression (observed through Western blot analysis, Chapter 3) may have directly contributed to the increased cellular motility that was observed but high levels of α-SMA expression were observed across all time points and treatment conditions in flow cytometry analysis. This may be due to the gating strategy I employed to identify subpopulations and may have not allowed for me to observe the decrease in vimentin and the increase in α-SMA expression after IR treatment (as I had observed in Western blot analyses). The use of Mean Fluorescence Intensity (MFI) histograms to look at overall changes in the intensity of expression of these two markers in the whole population must be done in order to compare the results from Western blot and flow cytometry analysis. MFI histograms of the intensity of expression of α-SMA in MDA-MB-231 cells were two-fold higher than MCF-7 cells across all time points and treatment conditions (data not shown). This demonstrated that although α-SMA is present in MCF-7 cells, it is present at much lower levels compared to MDA-MB-231 cells. An additional method to determine whether the vimentin expression in my Western blot or my flow cytometry analysis is correct would be to conduct vimentin-specific immunocytochemistry at multiple times points to look at not only the level of expression but also the distribution of expression in sham treated and 2.3Gy treated breast cancer cells.

Cell-intrinsic responses as a result of IR treatment are EMT-independent as evidenced by the lack of EMT-induction in MCF-7 cells that demonstrated enhanced displacement and the migration and/or displacement enhancement of MDA-MB-231 and LM2-4 cells that are fully mesenchymal. Ionizing radiation also sufficiently induced molecular phenotypic changes (increase in E-cadherin expression confirmed by both Western blot and flow cytometry analysis, and a decrease in vimentin expression) that may suggest Mesenchymal to Epithelial transition (MET) in a small percentage of mainly mesenchymal (vimentin positive) MDA-MB-231 cell population. Previous work has shown that re-expression of E-cadherin in MDA-MB-231 (231-Ecadh) cells altered cell morphology; cell-cell adhesions were formed and displayed cobblestone morphology, indicative of a reversion to a more epithelial-like phenotype [94]. 231-Ecadh cells also demonstrated a decrease in smooth muscle actin and vimentin expression [94]. In my studies, after 2.3Gy IR treatment, MDA-MB-231 cells remained fibroblastic in morphology and thus apparently remained mesenchymal in phenotype. Scratch wound assays of MDA-MB-231 cells expressing E-cadherin demonstrated a marked decrease in migration comparable to the low level migration of MCF-7 cells [94]. Based on the data shown in Figure 3.1A (MCF-7) and 3.1C (MDA-MB-231), comparing the range in migration and displacement of MDA-MB-231 and MCF-7 cells after 2.3Gy IR treatment argues against MET playing any major role in affecting cellular motility as the cells remained highly migratory.

It is possible for both epithelial and mesenchymal cells to coexist during the development of fibrosis in various organs [1]. Kidney, lung, intestine and liver epithelial cells expressing E-cadherin and cytokeratin can be found with epithelial cells expressing the mesenchymal markers fibroblast-specific protein 1 (FSP-1), α-sma, and vimentin due to EMT-induction as a result of chronic inflammation. These epithelial cells maintain their epithelial-specific morphology while

transitioning through EMT [1]. I can see from my flow cytometry analysis that in sham treated (Pre-sham and 72h post sham treatment) MDA-MB-231 cells there is a baseline level of E-cadherin expression that coexists with cells expressing high levels of vimentin. MET is also a complex mechanism that is not well understood [57, 95] and the upregulation of E-cadherin expression in a small percentage (based on flow cytometry analysis, 2% of the total population) of 2.3Gy radiation treated MDA-MB-231 cells is insufficient to fully support radiation-induced MET. Although flow cytometry confirmed and quantified the radiation induced increase in E-cadherin expression that I observed in Western blots, further analysis with other epithelial markers shown to be upregulated after MET would help strengthen the possible radiation-induced MET observation as E-cadherin upregulation alone is insufficient to support MET. For example, an increase in the expression of proteins that form the complexes necessary for cell-cell adhesion would provide stronger evidence for MET. To confirm the presence and localization of adherens junction proteins such as E-cadherin, catenins (β, α, and p120) and for the anchoring of the actin cytoskeleton at these points between adjacent cells, time course flow cytometry analysis and immunocytochemistry of irradiated and sham treated MDA-MB-231 cells would support the possibility of radiation-induced MET [96]. From the studies in this chapter, I can conclude that radiation increases MCF-7 cell displacement independent from EMT. IR increases the migration and displacement of MDA-MB-231 cells but does not affect MDA-MB-231 invasion. The displacement of LM2-4 cells is enhanced by 2.3Gy IR treatment. Finally, as further experiments are required, I cannot conclude whether or not IR is sufficient to induce an EMT in MDA-MB-231 cells. I next focused my subsequent studies on potential secreted factors induced by ionizing radiation that may be promoting a pro-migratory phenotype.

Chapter 4: Low-dose radiation induces secretion of factors sufficient to promote enhanced migration in metastatic breast cancer cell line

4.1 Introduction

In addition to cell intrinsic responses that are observed when tumour cells are directly irradiated, it may be possible that irradiated tumour cells are secreting factors that promote migration as well. Radiation treatment induces the secretion of a multitude of factors that include pro-inflammatory cytokines [97], GM-CSF [87], and TGF-β [98, 99]. Whether this is the result of dying tumour cells releasing their cytoplasmic contents or the result of signaling mechanisms to indicate DNA damage, both tumour cells and the tumour microenvironment are responsive to these cytokines. In chapter 3, my data revealed that the fully mesenchymal human breast carcinoma cell line MDA-MB-231 displayed an enhanced migratory phenotype in response to 2.3Gy radiation treatment. It remains to be seen if 2.3Gy ionizing radiation can induce the production of secreted factors that may also be contributing to enhanced migration. Co-culture experiments with conditioned media from irradiated cells were used to answer this question.

Other secreted factors induced by 2.3Gy radiation treatment that could promote migration of MDA-MB-231 cells may also be present. To investigate other possible secreted factors, supernatant collected from sham or 2.3Gy radiation treated MDA-MB-231 cells 72 hours post treatment was analyzed using a human chemokine antibody array looking at the following 38 targets:

Table 4.1 Human chemokine antibody array targets (38 total). Abcam human chemokine antibody array (ab169812) was used to analyze conditioned media from 2.3Gy treated and sham treated cells at multiple time points.

Targets: BLC/CXCL13, CCL28, Ck beta8-1/CCL23, CTACK, CXCL16, ENA-78/CXCL5, Eotaxin-1/CCL11, Eotaxin-2/CCL24, Eotaxin-3/CCL26, Fractalkin/CX3CL1, GCP-2/CXCL6, GRO/CXCL1+2+3, GRO alpha/CXCL1, HCC-4/CCL16, I-309/CCL1, I-TAC/CXCL11, IL-8/CXCL8, IP-10/CXCL10, Lymphotactin/XCL1, MCP-1/CCL2, MCP-2/CCL8, MCP-3/CCL7, MCP-4/CCL13, MDC/CCL22, MIG/CXCL9, MIP1 alpha/CCL3, MIP-1 beta/CCL4, MIP-1 delta/CCL15, MIP-3 alpha/CCL20, MIP-3 beta/CCL19, MPIF-1/CCL23, NAP-2/CXCL7/PPBP, PARC/CCL18, RANTES/CCL5, SDF-1 alpha/CXCL12alpha, SDF-1 beta/CXCL12beta, TARC/CCL17, TECK/CCL25

TGF-β is a well known radiation-induced cytokine and growth factor secreted by both tumour and stromal cells [98]. Ionizing radiation has been shown to induce the secretion of active TGF-β1 in glioma cells [100] through the production of reactive oxygen species (ROS) [101]. Even after large doses of radiation, malignant glioma cells maintain their ability to secrete TGF-β and activate latent TGF-β. TGF-β signaling has been shown to induce single cell motility in multiple murine mammary cancer cell lines *in vivo* in an EMT-dependent manner [102], where TGF-β signaling was found to be transient and localized to single cells disseminating from the primary tumour. Breast cancer patient samples, when stained with anti-TGF-β1 antibody, revealed a positive association with staining intensity and rate of disease progression (recurrence, progression and/or cancer-related mortality) [103]. Patient tumour samples with slight or intense staining for TGF-β1 were compared using Kaplan-Meier plots and patients with high TGF-β had worse progression-free survival (increased rate of disease progression) [103]. In immunohistochemical analysis of breast cancer patients with invasive carcinoma, a positive relationship between the staining intensity of TGF-β1 and metastasis to lymph nodes was observed [104]. Patients with non-invasive ductal carcinoma *in situ* demonstrated a much higher percentage of negative or slight staining, further implicating the potential pro-metastatic role of TGF-β [104]. Tumour cells are the primary target of radiation therapy and ideally would also receive the majority of the radiation dose. These studies do not differentiate the source of TGF-β but because its effects are widespread both locally at the primary tumour and potentially at secondary metastatic sites, as it is also found elevated in the plasma of breast cancer patients [105], a more comprehensive understanding of the molecular and cellular events that occur immediately after RT in breast tumour cells is important.

TGF-β has been implicated in both tumour suppressive and promoting roles. Although it has been shown that numerous carcinoma cell lines are reactive to endogenous TGF-β stimulation and produce both EMT-dependent and independent migration phenotypes, ionizing radiation-induced production of TGF-β and its impact on migration has not been well studied. I aimed to determine if low-dose radiation would induce TGF-β secretion and if this would produce similar enhancements to single cell motility in fully mesenchymal (thus EMT-independent) MDA-MB-231 cells. As TGF-β is well characterized to have both a tumour suppressive and tumour promoting function depending on the context, it could also be possible that a decrease in TGF-β secretion after radiation treatment may enhance tumour cell migration. To determine whether TGF-β secreted by irradiated cells is associated with migration of untreated MDA-MB-231 cells a time point analysis of TGF-beta concentration in culture medium was conducted using ELISA.

With these current gaps in knowledge highlighted, the data presented in this chapter aims to address Aim 3 of the thesis. Specifically, to determine whether IR induces the secretion of pro-migratory factors by MDA-MB-231 cells and what these factors may be.

4.2 Results

4.2.1 2.3Gy dose of ionizing radiation induces secretion of pro-migratory factors

I was interested in whether 2.3Gy IR treatment of MDA-MB-231 cells would induce the secretion of pro-migratory factors that would contribute to the enhanced migration I observed when cells were directly irradiated. During the process of conditioned media collection (after cells were treated with 2.3Gy IR), culture media was not supplemented with FBS to avoid

potential background affects it may have on radiation-induced secreted factors. Instead, the media was supplemented with 0.1% BSA to sustain cells during serum starvation and to prevent secreted factors from adhering to the tissue culture plate. Before untreated MDA-MB-231 cells were co-cultured with conditioned media, all conditioned media collected from treated cells was supplemented with 10% FBS . In addition to the most important migration and displacement comparison between cells co-cultured with conditioned media from sham treated or 2.3Gy treated cells, the potential effect of BSA in media on migration and displacement also required analysis. Untreated fresh media (with FBS) containing 0.1% BSA did enhance migration, but not displacement, when compared to untreated fresh media with FBS alone. When the migration and displacement of cells co-cultured with fresh media containing 0.1% BSA was compared to cells co-cultured with conditioned media from sham treated MDA-MB-231 cells, there was no difference (Figure 4.1A). Quantification of migration and displacement (measured as described in Chapter 3) of untreated and viable MDA-MB-231 cells co-cultured with conditioned media obtained from 2.3Gy irradiated MDA-MB-231 cell cultures 48 hours after radiation revealed that both were significantly enhanced compared to conditioned media from sham treated cells and fresh, untreated media with and without 0.1% BSA (Figure 4.1A). In the kinetic analysis of migration and displacement, all comparisons were made to untreated MDA-MB-231 cells co-cultured with 2.3Gy conditioned media as I was most interested in whether radiation-induced secreted factors also enhanced the kinetics of untreated cells. Analysis of the migration and displacement kinetics revealed that untreated MDA-MB-231 cells co-cultured with conditioned media from irradiated cells begin to observably diverge in their migration and displacement from cells co-cultured with sham treated conditioned media at 50 and 36 hours respectively, after co-culture began (Figure 4.1B). The 36 hour divergence in the displacement kinetics in co-culture

experiments is consistent with what was observed in the kinetics of cells treated directly with 2.3Gy radiation. The presence of BSA in both the fresh media and sham treated conditioned media did not have a significant effect on migration; migration enhancement observed in co-culture with 2.3Gy conditioned media can largely be attributed to pro-migratory factors present in the media after IR treatment. The presence of BSA did affect displacement during the later time points of the assay when comparing fresh media and sham treated conditioned media but the substantial increase in displacement of cells co-cultured with 2.3Gy conditioned media also strongly suggests that IR treatment induced pro-migratory factors play a much larger role in displacement enhancement. These data support the presence of pro-migratory factors in conditioned media from 2.3Gy-irradiated MDA-MB-231 tumour cells that are sufficient to enhance migration of untreated cells, and that the observed migration enhancement is of similar magnitude to the studies involving the direct radiation treatment of MDA-MB-231 cells.

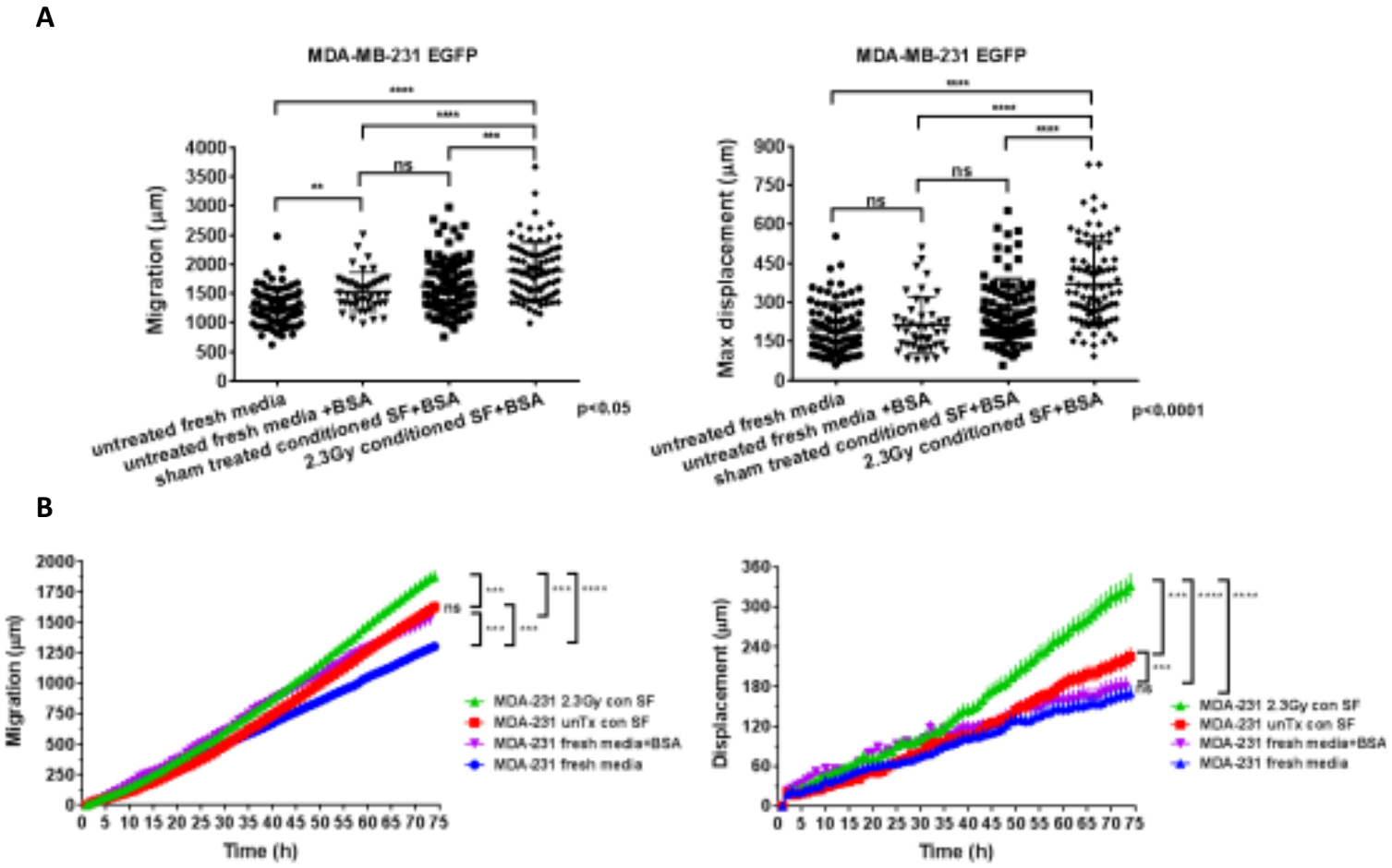

Figure 4.1 48-hour conditioned medium from irradiated MDA-MB-231 EGFP cells enhances migration of untreated MDA-MB-231 EGFP cells. Untreated MDA-MB-231 EGFP cells were co-cultured with media from various conditions. Cells were single cell tracked over a 72-hour period as in direct radiation experiments; migration and maximal displacement was quantified (µm). **(A)** Total distance migrated and maximal displacement of non-irradiated MDA-MBM-231 cells cultured with fresh medium, fresh medium + BSA, serum free (SF) medium + BSA from sham treated control MDA-MB-231 cells, or SF medium + BSA from MDA-MB-231 cells irradiated with 2.3Gy. **(B)** Kinetic analyses from the same experiments showing migration and displacement over time. Data are mean±SEM (*** $p<0.05$, **** $p<0.0001$, Tukey's multiple comparisons test).

4.2.2 Effect of ionizing radiation on secreted TGF-β1 by metastatic breast cancer cells

I performed ELISA analysis of supernatant collected from sham treated and 2.3Gy treated MDA-MB-231 cells over various time points to quantify the total TGF-β1 present over

time. ELISA results showed that there was no significant increase in total secreted TGF-β1 until 72 hours after treatment when compared to sham controls (Figure 4.2). Based on the kinetic analysis of MDA-MB-231 cell co-culture studies (Figure 4.1B), which concluded that migration and displacement between sham and irradiated cells diverged at 50 and 36 hours respectively, TGF-β1 may not be responsible for the observed enhanced migration phenotype based on the current assay protocol.

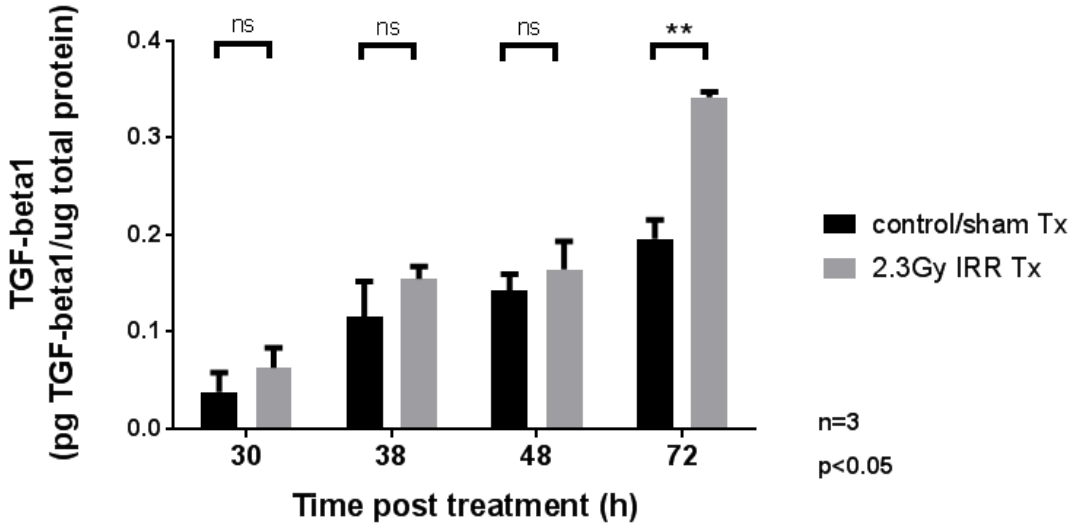

Figure 4.2 Secreted, mature TGF-β1 protein increases almost two-fold at 72 hours after 2.3Gy radiation treatment compared to sham treated control. TGF-β1 levels in supernatants collected from sham and 2.3Gy treated MDA-MB-231 (non-EGFP) cells were analyzed at several time points after treatment. Resultant levels (in ρg) were normalized to total protein (μg) in supernatant from sham treated or 2.3Gy irradiated cells. Data displayed as mean+/- SEM (**p<0.05, unpaired two-tailed t-test, n=3).

4.2.3 2.3Gy ionizing radiation induces secretion of pro-inflammatory factors in metastatic breast cancer cell line MDA-MB-231

I next performed a chemokine array analysis on supernatant collected from MDA-MB-231 cells with or without 2.3Gy irradiation. Chemokine array analysis revealed that IL-8 was highly upregulated in supernatant from 2.3Gy irradiated MDA-MB-231 cells (Figure 4.3). GRO (CXCL1-3), GROα (CXCL-1) and CTACK were upregulated in supernatant from 2.3Gy

irradiated MDA-MB-231 cells 72 hours after IR compared to supernatant from sham treated cells. Through the chemokine antibody array, I have identified 4 putative chemokines induced by 2.3Gy radiation with levels of expression that should be further validated by individual ELISA assays.

A

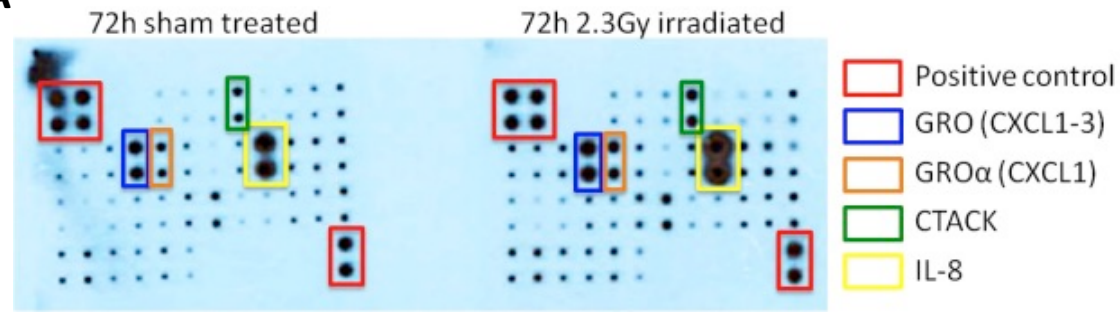

	A	B	C	D	E	F	G	H	I	J	K	L
1	POS	POS	NEG	NEG	BLC	CCL28	Ckβ8-1	CTACK	CXCL16	ENA-78	Eotaxin	Eotaxin-2
2	POS	POS	NEG	NEG	BLC	CCL28	Ckβ8-1	CTACK	CXCL16	ENA-78	Eotaxin	Eotaxin-2
3	Eotaxin-3	Fractalkine	GCP-2	GRO	GROα	HCC-4	I-309	I-TAC	IL-8	IP-10	Lymphotactin	MCP-1
4	Eotaxin-3	Fractalkine	GCP-2	GRO	GROα	HCC-4	I-309	I-TAC	IL-8	IP-10	Lymphotactin	MCP-1
5	MCP-2	MCP-3	MCP-4	MDC	MIG	MIP-1α	MIP-1β	MIP-1δ	MIP-3α	MIP-3β	MPIF-1	NAP 2
6	MCP-2	MCP-3	MCP-4	MDC	MIG	MIP-1α	MIP-1β	MIP-1δ	MIP-3α	MIP-3β	MPIF-1	NAP 2
7	PARC	RANTES	SDF-1α	SDF-1β	TARC	TECK	BLANK	BLANK	BLANK	BLANK	BLANK	POS
8	PARC	RANTES	SDF-1α	SDF-1β	TARC	TECK	BLANK	BLANK	BLANK	BLANK	BLANK	POS

B

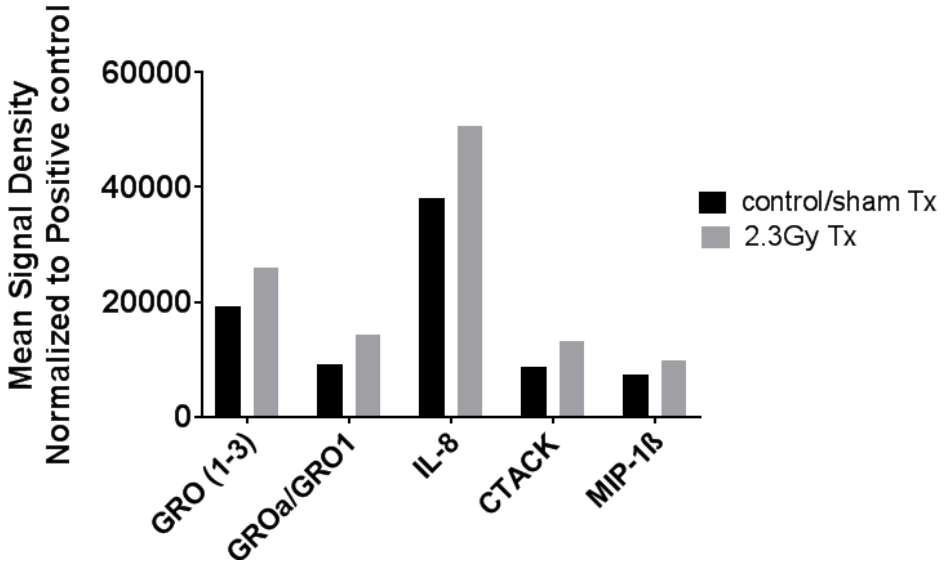

Figure 4.3 Pro-inflammatory chemokines are upregulated at 72 hours after 2.3Gy radiation treatment compared to sham treated control. Supernatant collected from sham and 2.3Gy IR treated MDA-MB-231 cells, 72 hours after treatment, was used to identify and quantify expression of chemokines upregulated by radiation treatment. **A)** Chemokines with the most obvious visual difference in signal between control and 2.3Gy treated cells were quantified. **B)** Mean Signal Density was normalized to the positive control after subtracking background (from negative control); comparisons were made between the control and 2.3Gy blots.

4.3 Discussion

Conditioned medium derived from MDA-MB-231 cells irradiated with 2.3 Gy caused increased migration of untreated MDA-MB-231 cells, indicating that radiation-induces the secretion of pro-migratory factors from irradiated cells. TGF-β is known to function as a tumour suppressor or metastasis-promoting factor, depending on tissue context and tumour progression. Kinetic analysis of conditioned media co-cultured MDA-MB-231 cells showed that irradiated and sham conditioned media co-cultured cells diverge in terms of migration and displacement at 50 and 36 hours post-treatment respectively (Figure 4B). Since no increase in secreted TGF-β1 was observed until 72 hours after irradiation, my data suggest that TGF-β may not be responsible for the radiation-induced enhancement in migration phenotype. Although our TGF-β ELISA did not indicate an increase during time points that correlated to divergence in migration and displacement in our co-culture studies, the functional duality of TGF-β as a pro-tumorigenic factor or as a tumour suppressor may explain this temporal variation and the functional role it may be playing during those key time points. The almost two-fold increase in secreted TGF-β in supernatant from irradiated MDA-MB-231 cells 72 hours after treatment correlated with the time point at which upregulation of α-SMA expression was observed to be greater than untreated cells in our Western blot data (Figure 3.7). TGF-β has been shown to be sufficient for the induction of α-SMA expression [106, 107]. TGF-β treatment of LLC-Pk_1 cells (proximal tubular epithelial cell line from pigs) in addition to inducing EMT, as indicated by the loss of cell-cell adhesion due to the dissociation of E-cadherin from the cell periphery and an elongated cell morphology, induced strong α-SMA expression by 72 hours after treatment. The newly expressed α-SMA also formed thick fibers in TGF-β-treated cells that were not found in untreated cells; TGF-β-treatment also became highly- polarized in cortactin distribution, resulting in large lamellipodia,

suggestive of increased migratory potential [45]. In my flow cytometry analysis of α-SMA, instead of an upregulation of expression over time after IR treatment like I observed in my Western blot data, irradiated MDA-MB-231 cells maintained a high and consistent level of α-SMA expression. This lack of agreement in expression between the two assays may be explained by the difference in what is being analyzed by the two methods. I determined that there is a significant upregulation of TGF-β1 secretion into the supernatant 72 hours after IR treatment and propose that this may be the factor responsible for upregulating α-SMA. Cell lysates to isolate protein from sham and irradiated MDA-MB-231 cells are prepared in a relatively short time after the supernatant is taken off the cells whereas in flow cytometry, after supernatant removal and dissociation from the tissue culture plate, cells are left sitting for a couple of hours during antibody incubation steps. The removal of the TGF-β-containing supernatant could thus reduce the induction of α-SMA expression back down to levels similar to sham treated cells. This hypothesis may explain the lack of agreement between Western blot and flow cytometry analysis of α-SMA expression.

The TGF-β1 ELISA protocol requires acidification of all samples to release mature TGF-β1 from the latency associated peptide (LAP), resulting in the quantification of total TGF- β1 present in the supernatant. Without this acidification step, levels of mature TGF- β1 would fall below the detection sensitivity of the kit. This acidification step prohibits the quantification of mature TGF- β1 that was actually released by ionizing radiation and consequently, the time-point comparison of secreted TGF-β1 levels between sham and 2.3Gy treated supernatants may not be reflective of what is actually active and functional. Further quantification of concentrated and non-acidified supernatant samples needs to be conducted to determine how IR is affecting the ratio of latent/inactive to mature/active TGF-β1 present; the role of radiation-induced TGF-β1 in

migration can subsequently be determined and thus, TGF-β1 may still have a potential role in radiation-induced migration enhancement. Studies have also shown that other growth factors work in conjunction with TGF-β to enhance migration. EGF, in combination with TGF-β, was previously found to increase migration of rat intestinal epithelial cells by four-fold, compared to the two-fold enhancement of EGF alone and the inhibitory effect of TGF-β alone on migration [108]. Thus, it is possible that the enhanced migration and displacement observed in co-culture experiments were dependent on TGF-β, but as part of an interaction between EGF and TGF-β1 signaling and not due to an independent TGF-β pathway. At 72 hours after 2.3Gy IR treatment, MDA-MB-231 cells were found to secrete almost two-fold more TGF-β1 than sham-treated cells.

The chemokine array in Figure 4.3 contains 38 chemokines (as shown in Table 4.1) with known involvement in cellular migration and chemotaxis. Based on the relative abundance and fold-increase induced by IR, we predict that IL-8 may be a potential target. Also known as neutrophil activating protein, IL-8 is a proinflammatory cytokine involved in the migration and activation of neutrophils and plays a significant role in inflammation along with platelet factor 4 (PF4) and macrophage inflammatory proteins (MIP1 & 2) [109]. IL-8 has been shown to induce the migration of tumour cells *in vitro* [109, 110], its overexpression in colorectal cancer cell lines promoted tumour angiogenesis, growth and metastasis [111], and it is produced by various tumour cell lines (reviewed here [112]). In breast cancer cell lines such as MDA-MB-231, which highly express IL-8 [113], IL-8 expression levels have been directly correlated with metastatic potential, invasiveness, and angiogenesis [114]. The emerging role of IL-8 in tumour progression and metastasis, due in part to its autocrine and paracrine signaling mechanisms that act as a feedback loop between tumour cells and inflammatory cells in the tumour microenvironment,

has made it not only a therapeutic target but published literature has also alluded to its possible role in resistance to chemotherapy [110, 115]. In the context of radiation therapy, the role of IL-8 has been predominantly in the inflammatory response following radiation [116], and for the most part has been categorized as having a bystander effect, even when it is secreted by tumour cells in response to direct IR treatment [117]. I show here for the first time that a dose of 2.3Gy IR is sufficient to induce increased secretion of IL-8 in the estrogen-receptor negative, metastatic breast cancer cell line MDA-MB-231. IL-8 expression levels have also been negatively correlated with ER-status; analysis of breast and ovarian cancer cell lines, and patient breast tumour samples revealed that IL-8 is highly expressed in ER-negative samples, a well known indicator of poor prognosis [118]. TGF-β1 has been shown to induce the expression of IL-8 in a dose-dependent manner in prostate cancer cells (PC-3MM2); at the highest TGF-β1 treatment dose (10ng/ml), IL-8 expression reached its maximal concentration before plateauing at 16h [119]. Taking into account what is already known regarding IL-8 and its role in promoting migration, metastatic potential, and angiogenesis, the enhanced expression of TGF-β1 and increased expression of IL-8 following 2.3Gy IR may act in a synergistic manner that contributes to metastasis and radioresistance of breast tumour cells.

Chapter 5: Low-dose ionizing radiation enhances lung colonization of MDA-MB-231 EGFP cells in female NODSCID mice.

5.1 Introduction

The potential impact of radiation on local tumour recurrence and distant metastatic dissemination has mainly been studied through irradiation of tumour bearing mice [120, 121] or pre-irradiation of mice before primary tumour development [122]. From these experiments the tumour microenvironment has been shown to play a significant role in radioresistance and treatment outcome. Whole tumour irradiation inevitably brings about a myriad of acute and chronic alterations to the microenvironment including, but not limited to, immune cell infiltration and inflammation, tumour cell clonal selection, and restructuring of ECM and vasculature [30]. These complex and diverse microenvironmental responses to radiation, both during and after radiation treatment, introduce difficulty in defining the cause of any enhanced metastatic phenotype when the whole tumour is irradiated. Rather, it is critical to study how radiation specifically affects tumour cells *in vivo,* including determining how tumour cells establish tumours after being directly treated with IR before orthotopic implant *in vivo*. By focusing on the tumour cell responses, therapy design could potentially anticipate and intervene against metastatic disease. More rigorous *in vivo* studies must also be conducted to better relate back to *in vitro* data that studies tumour cell response to radiation separate from the microenvironment; my studies have demonstrated that IR treated tumour cells exhibit enhanced migration through cell intrinsic and radiation-induced pro-migratory factors (Chapter 3 and 4). Pre-irradiating tumour cells, before being implanted into mice for *in vivo* study, will allow for distinguishing the response of tumour cells that survive a clinical dose of IR from the microenvironment response

in terms of altering tumour development/formation and structure, tumour cellularity and inflammation, production of secreted factors, and propensity for metastasis.

With these current gaps in knowledge highlighted, the data presented in this chapter aims to address Aim 4. Specifically in this chapter, I will use breast cancer cell lines irradiated before orthotopic implant or IV injection into mice to study loco-regional invasion and/or lung extravasation or colonization respectively in vivo.

5.2 Results

5.2.1 Pre-irradiation of breast cancer cell lines alters tumour formation *in vivo*

2.3Gy pre-irradiated and sham treated MDA-MB-231 EGFP or MCF-7 EGFP cells were implanted into the same female NOD SCID mice in contralateral mammary fat pads (MFPs) and allowed to form tumours. The tumour and its surrounding mammary fat pad (MFP) were resected as follows:

i. MDA-MB-231 EGFP tumours: 3, 7, 14, 21 days after implant
ii. MCF-7 EGFP tumours: 7, 14, 21, 28 days after implant

I had difficulty generating consistent data in these *in vivo* experiments. In both MDA-MB-231 EGFP and MCF-7 EGFP implanted mice, at 14 days post implant where tumours were at a good size (~0.3-0.5g) to section and adequate mammary fat pad tissue was still intact, no enhanced loco-regional invasion by 2.3Gy pre-irradiated EGFP cells into the surrounding fat tissue was observed compared to sham treated cells in the contralateral fat pad of the same mouse (Figure 5.1A-B). Arrowheads in Figure 5.1A-B indicate possible single cell invasion but as tumour margins were difficult to demarcate and the frequency of these invading single cells were

inconsistent between tumour samples, this is just an observation. Tumours resected at time points before and after the 14-day time point exhibited no difference between 2.3Gy and sham treated tumours for either cell type. Pre-irradiated tumours from both breast cancer cell lines exhibited poorly defined margins, sometimes almost non-existent, whereas tumours formed from sham treated cells developed an obvious tumour capsule with clearly defined margins (evidenced by the very strong DAPI staining around the EGFP expressing tumour). In this study, pre-irradiation of breast tumour cell lines before orthotopic implant into the MFP of female NOD SCID mice mildly altered tumour structure but did not enhance local invasion.

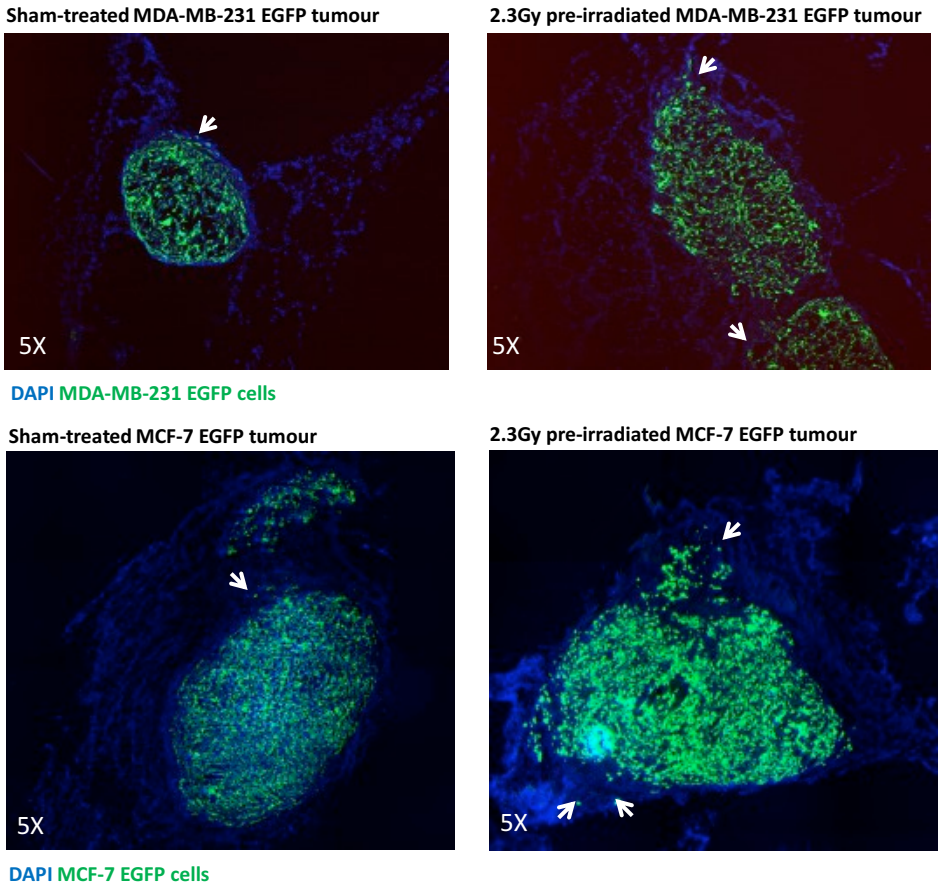

Figure 5.1 2.3Gy pre-irradiation of MDA-MB-231 EGFP or MCF-7 EGFP tumour cells before MFP orthotopic implant does not alter locoregional invasion and slightly alters tumour morphology compared to sham-treated cells. MDA-MB-231 or MCF-7 EGFP cells were either pre-irradiated (2.3Gy) or sham treated before orthotopic implant into the 4th mammary fat pad of female NOD SCID mice. Time point resections were conducted; tissue was fixed, placed in OCT and sectioned. Tumour sections from 14 days post implant are shown in this figure; arrowheads indicate areas with single cell locoregional invasion.

5.2.2 Pre-irradiation of metastatic breast cancer cell line alters its invasion *in vivo*

2.3Gy irradiated or sham treated MDA-MB-231 EGFP cells were IV injected into the tail vein of female NOD SCID mice 40 hours after irradiation. This time point was chosen to match the chemotaxis migration assay results, as it was where the greatest increase in migration rate was observed in irradiated cells (Figure 3.4-3.5). At 2, 4 and 8 hours after IV injection, mice from both treatment groups were euthanized and their lungs were resected to quantify tumour cell content in the lungs. The largest lobe of each lung in both treatment groups was removed, fixed, and embedded in OCT for fluorescent microscopy detection of fluorescent tumour cells; the remaining lung tissue was disaggregated into a single cell suspension to detect fluorescent tumour cells with flow cytometry. Based on the flow cytometry analysis of EGFP positive tumour cells in processed lung tissue from both treatment groups, at 8 hours after tail vein IV injection of tumour cells, there were significantly more EGFP positive tumour cells in the lungs of mice injected with 2.3Gy irradiated tumour cells compared to mice that were injected with sham treated cells (Figure 5.2C). There was no significant enhancement at 2 or 4 hours after IV injection (Figure 5.2A-B). Lung tissue sections from IV injected mice exhibited no difference between sham treated and 2.3Gy treated MDA-MB-231 tumour cells (Figure 5.3); multiple sections from each lung lobe of each treatment group needs to be sectioned and quantified to determine whether it can recapitulate flow cytometry analysis data. Pre-irradiation of mesenchymal breast tumour cell line MDA-MB-231 resulted in increased invasive capabilities compared to sham treated cells, suggesting that the clinically relevant dose of 2.3Gy IR is sufficient to enhance lung extravasation 8 hours after IV injection or 48 hours after initial radiation treatment.

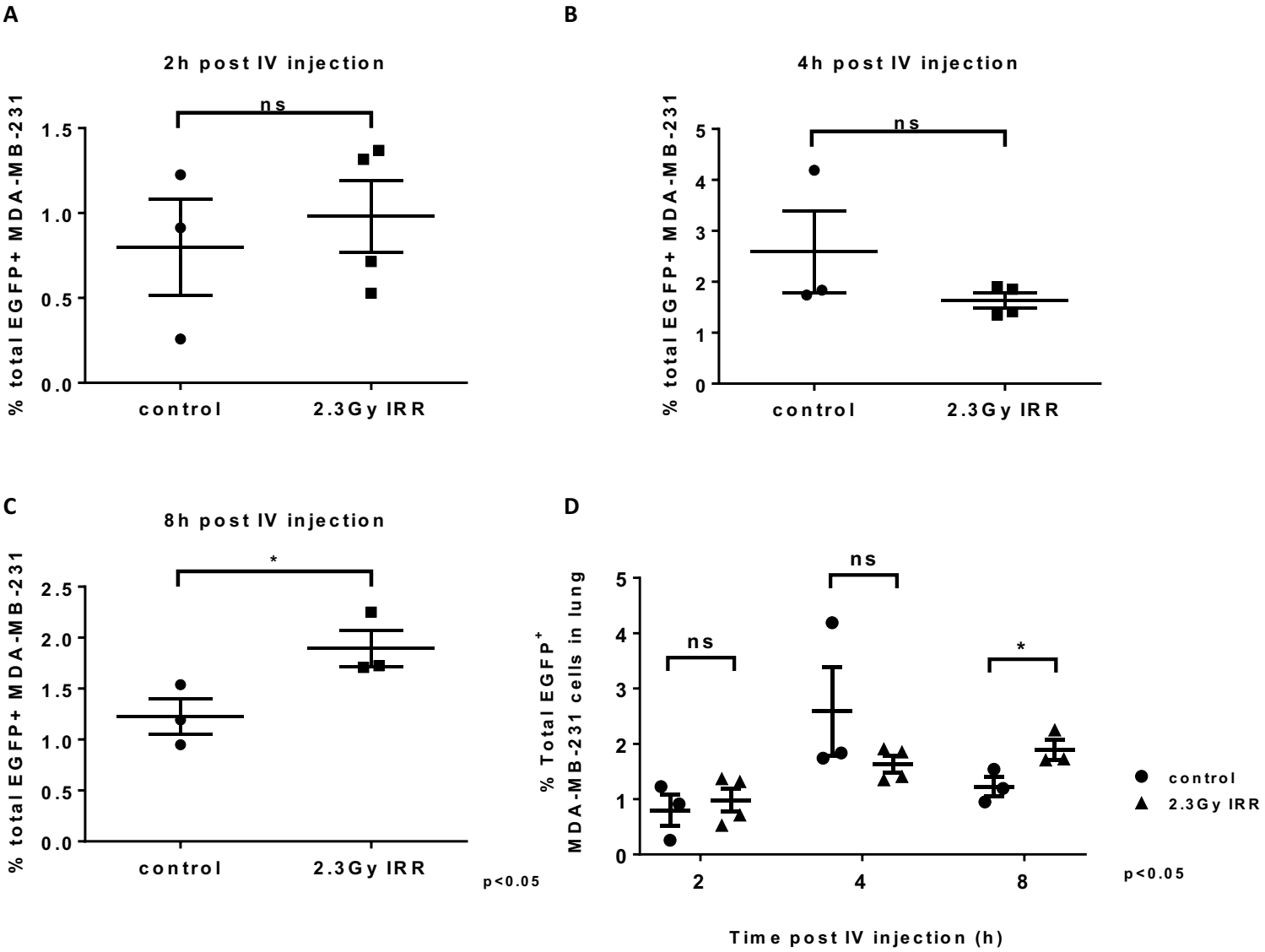

Figure 5.2 2.3Gy pre-irradiation of MDA-MB-231 tumour cells before tail vein IV injection enhances lung extravasation compared to sham-treated cells when quantified through flow cytometric analysis. Lung tissue from mice tail vein IV-injected with sham treated or 2.3Gy treated MDA-MB-231 EGFP cells were processed for flow cytometry analysis; % EGFP positive cells were quantified **A) 2 hours B) 4 hours and C) 8 hours after injection; D) all time points plotted on one graph.** Total % of MDA-MB-231 EGFP+ describes EGFP positive tumour cells that were in the lungs of mice after 500,000 MDA-MB-231 EGFP cells were injected via the tail vein (total of 200,000 events analyzed through flow cytometry). Data are mean±SEM ($p<0.05$; unpaired two-tail Student's t-test); n=3-4 mice per treatment group.

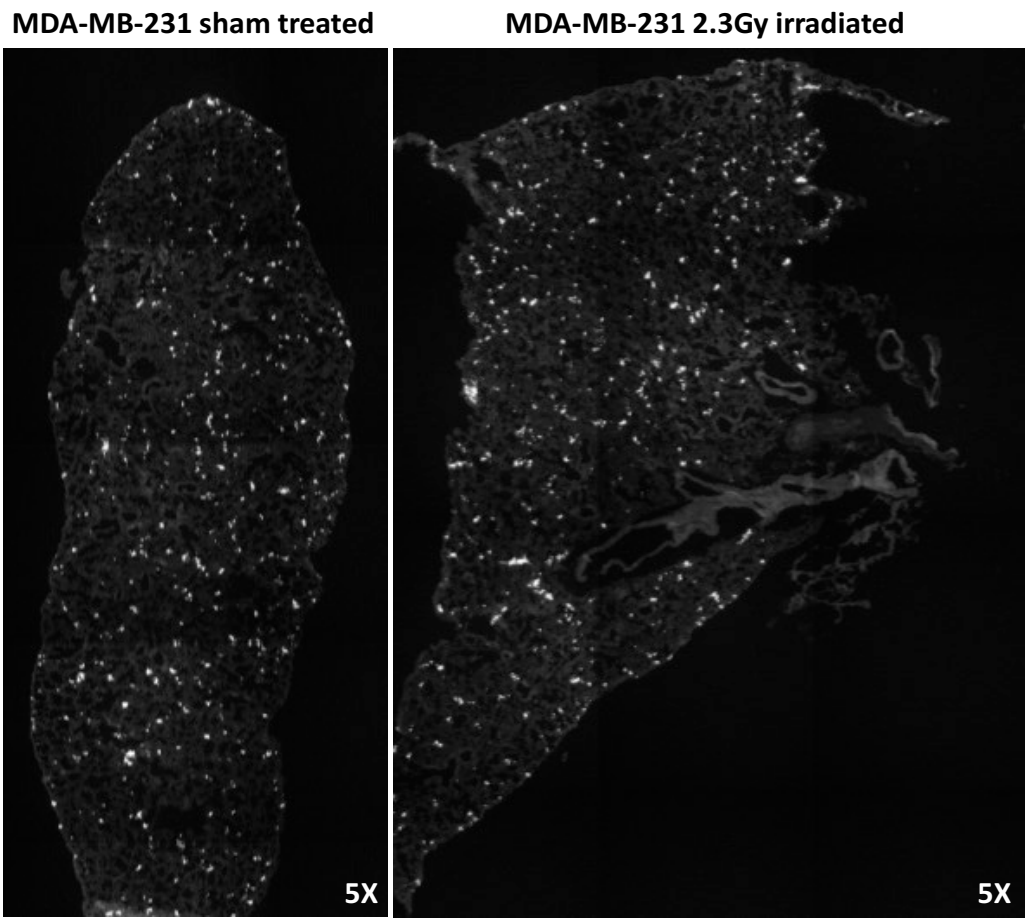

Figure 5.3 8 hours post 2.3Gy pre-irradiation of MDA-MB-231 tumour cells vs. sham treated MDA-MB-231 cells in the lungs after tail vein IV injection. Largest lung lobes from mice tail vein IV-injected with sham treated or 2.3Gy treated MDA-MB-231 EGFP cells were fixed in 4% PFA, placed in OCT and sectioned for fluorescent microscopy to visualize EGFP cells. Representative images are shown for each treatment group at 8 hours IV-injection (where flow cytometry analysis revealed significant increase in MDA-MB-231 EGFP+ cells after treatment with 2.3Gy compared to sham treatment). EGFP positive areas of lung tissue are white in contrast with the normal lung tissue (grey).

5.3 Discussion

Radiation treatment of non-metastatic MCF-7 and fully mesenchymal MDA-MB-231 cells may induce cell intrinsic effects that alter tumour structure and IV foci development when studied in pre-clinical mouse models. Pre-irradiation of these breast tumour cell lines prior to orthotopic implantation in mice revealed no obvious differences in local invasion at any of the time points examined. Tumours resected before day 14 for both breast tumour cell lines were too

small to observe any changes within the tumour and surrounding MFP. Further, at this time point the mammary fat pad (MFP) that surrounded the small tumour was difficult to section, meaning areas where there may have been single tumour cell invasion into fat tissue were difficult to locate. Tumours from time points after day 14 eventually overtook the majority of the MFP, resulting in further difficulty in locating loco-regional invasion for both tumour cell lines. At time points beyond day 14, tumours from 2.3Gy treated cells resembled sham treated tumours, suggesting that radiation induced changes to breast tumour cell lines may persist at least 14 days post treatment but diminish thereafter.

IV injection of pre-irradiated tumour cells demonstrated the greatest lung colonization 8 hours after injection, or 48 hours after 2.3Gy IR treatment; this time point coincides with the greatest increase in migration I observed in the *in vitro* assays in Chapter 3 (Figure 3.3-3.5) and where total TGF-β levels were not significantly different between sham and 2.3Gy IR treated cells (Figure 4.2). The role of TGF-β in enhancing lung extravasation cannot be completely ruled out because as discussed in Chapter 4, the acidification step in my ELISA protocol prohibited the quantification of mature TGF- β1 that was actually released by ionizing radiation. Thus, the time-point comparison of secreted TGF-β1 levels between sham and 2.3Gy treated supernatants may not be reflective of what is actually active and functional, and this applies to how the TGF-β1 results can be used to interpret my *in vivo* extravasation study. Further quantification of concentrated and non-acidified supernatant samples needs to be conducted to determine how IR is affecting the ratio of latent/inactive to mature/active TGF-β1 present It is also possible that microenvironmental influences after tumour cells are injected into mice may alter their phenotype and the secretion of TGF-β by pre-irradiated cells may be induced earlier than the 72 hour time point where I observed the most significant increase in TGF-β levels *in vitro*.

I assessed tumour cell content in the lungs between 2 and 8 hours after iv injection, which is a timeframe used in previous work to study the process of tumour cell extravasation from the vasculature into lung tissue. Tumour cells have been shown to extravasate within this timeframe [123, 124], and tumour cell numbers in the lungs would not be significantly affected by tumour cell proliferation after IV injection. Regardless, a detailed immunohistochemical analysis of lung sections to quantify tumour cell content within the vasculature compared to the surrounding lung tissue would be required to conclusively assess whether pre-irradiation influences tumour cell extravasation. The steady increase in EGFP positive cells observed over time after IV injection into mice may speak to the potential enhanced ability of irradiated breast tumour cells to develop secondary metastases in the lungs, a common secondary site for breast cancer patients with metastatic disease. Past studies have observed a greater incidence of pulmonary metastases when breast tumour cells were pre-irradiated with two fractions of 3.5Gy before being subcutaneously implanted in mice, although local recurrence was not significantly altered [121]. In a similar study, radiation treatment of subcutaneously implanted Lewis Lung Carcinoma tumours found that in mice treated with large doses of IR, either in single or multiple fractions (40Gy in 1 fraction, 30Gy in 1 fraction, 40Gy in 2x20Gy fractions or 50Gy in 5x10Gy fractions), the primary tumour was eradicated regardless of IR dose, but lung metastatic burden was significantly enhanced compared to un-irradiated animals [120]. These studies demonstrate that although IR treatment is very effective in primary tumour eradication, the potential for promoting distant metastases warrants further concern and study. Elucidating the initial response of pre-irradiated tumour cells *in vivo* and subsequently building on these findings with the incorporation of the rest of the tumour microenvironment components may help inform why certain doses of radiation and treatment schedules are able to enhance the development of

metastatic disease. Furthermore, the scientific findings would highlight the possible need for concurrent secondary targeted therapies during IR treatment to prevent dissemination or to inhibit pro-metastatic factors upregulated as a result of IR.

Chapter 6: Conclusion

6.1 Summary of research

There is a disconnect in the scientific literature addressing radiation-enhanced metastasis; *in vitro* studies clearly demonstrate that direct IR treatment of tumour cells with high doses enhances migration and invasion without taking survival into consideration. *In vivo* studies that have observed enhanced development of distant metastases after direct IR treatment to whole tumours are more likely due to reoxygenation of previously hypoxic tumour cells coupled with direct IR damage to tumour vasculature, allowing tumours cells to escape into the circulation, and due to the influx of immune cells that produce factors facilitating metastatic dissemination (reviewed extensively in [87]). The studies described in this thesis collectively demonstrate that IR induced enhancement of migration of the mesenchymal MDA-MB-231 breast tumour cell line *in vitro*, an observation that was recapitulated *in vivo* as increased tumour cell content in the lungs after iv injection when cells were pre-irradiated. These enhancements may be a result of a combination of cell intrinsic responses, demonstrated through our single cell tracking studies and EMT marker analysis, and the secretion of pro-migratory and pro-metastatic factors, demonstrated in my co-culture studies and human chemokine array respectively. Thus, my *in vitro* and *in vivo* findings support my hypothesis; breast tumour cells that survive radiation therapy have a higher propensity to migrate and colonize lung tissue after tail vein IV injection, and I demonstrated that this is independent from radiation-induced changes to the solid tumour microenvironment by directly irradiating tumour cells and pre-irradiating tumour cells for *in vivo* experiments.

6.2 Future directions

My studies were focused on breast cancer cell lines. As radiation is used to treat a variety of cancers, future studies will need to extend my observations to cell lines of other cancer types. Other tumour models of cancers routinely treated with radiation should be assessed *in vitro* to determine if the same migration phenotype occurs and whether upregulated factors that I observed are induced in a similar manner. Of particular interest for future studies employing single-cell tracking will be comparing time lines of speed and velocity changes across tumour cell lines and whether divergences between treatment groups occur within similar time frames.

My choice of *in vitro* methods to assess migration not only improved the quantification of radiation enhanced migration, but also revealed that although migration was not able to enhance the total distance migrated by some breast tumour cells (MCF-7 and LM2-4), IR consistently enhanced the total displacement of all irradiated cell lines studied. These observations suggest that cell intrinsic responses following irradiation are driving subpopulations of breast tumour cells, regardless of metastatic potential, to migrate away from the irradiated location. Further mathematical modeling may allow for the determination of directionality in the migration patterns of irradiated cells to further support this conclusion.

Numerous *in vitro* and *in vivo* follow-up studies can be conducted to further elucidate what the tumour cell specific response, *in vitro* and *in vivo*, is after IR treatment to anticipate what possible immune cell infiltrates and other changes to the tumour microenvironment will occur. A limitation of my data is the potential of tracking dead and dying cells. The use of a fluorescent dye to identify dead and dying cells during single cell tracking would help to lessen the impact of tracking dead cells, but as the assay time of 72 hours is still much shorter than the 2 weeks typical of clonogenic assays, the tracking of cells that may eventually die is inevitable.

The observations made from the *in vivo* studies in Chapter 5 should be replicated in future studies interested in the *in vivo* enhancement of migration by IR in order to confirm if there is a stronger and more reproducible phenotype, as both treatment groups in the lung extravasation study exhibited a great degree of spread in the data at the 2 and 4 hour time points. However, the spread in our *in vivo* data is further support of the heterogeneity and presence of sub-populations that I observed with our *in vitro* experiments. Thus, a potential direction for future research could attempt to identify and isolate sub-populations of irradiated tumour cells prior to *in vivo* testing of invasive and metastatic ability, with the aim of determining factors necessary for radiation-induced migration enhancement.

Kinetic analysis of migration and displacement after IR of breast cancer cell lines, made possible through single cell tracking, allowed me to define specific time points where I observed divergence in the speed and velocity of irradiated cells. These time points can potentially inform when secondary treatments can be introduced before, during, or after IR to contain/prevent dissemination of tumour cells from the primary tumour. My analysis of radiation-induced secreted factors by tumour cells demonstrated that tumour cells are able to respond to a 2.3Gy dose of radiation with pro-migratory and pro-metastatic proteins that act in an autocrine, and most likely paracrine, fashion and that these inductions are temporal, as evidenced by the TGF-β1 ELISA where TGF-β1 levels were the highest 72 hours after IR compared to earlier time points and to sham treated levels. Further quantification of MDA-MB-231 production of active TGF-β1 induced by IR treatment by not conducting the acidification and neutralization step outlined in the TGF-β1 ELISA protocol could help determine whether, in the time points (38-48 hours after IR treatment) where no difference in TGF-β1 concentration was observed between sham and 2.3Gy treated samples, TGF-β1 is present. Chemokine array analysis of supernatant

from earlier time points (before 72 hours) would reveal whether the upregulated factors (IL-8 in particular) identified at 72 hours was present earlier or differentially expressed.

Direct treatment of un-irradiated breast cancer cell lines with TGF- β1 to determine whether it has the same effect on migration and displacement through single cell tracking as 2.3Gy irradiated cells would support its radiation-induced role in migration. Subsequently, genetic modification (gene knock down or knock out) or treatment with primary antibody against TGF-β1 should be employed to determine if TGF-β1 upregulation following 2.3Gy IR treatment plays a role in either migration and invasion enhancement *in vitro*, or the increased secretion of IL-8 from irradiated cells. If the increased secretion of IL-8 is found to be independent of TGF-β1 upregulation after IR, direct treatment of un-irradiated cells with IL-8, and antibody therapy or genetic alterations against IL-8 expression in tumour cells of interest (before radiation treatment) could be used to further examine the potential role of IL-8 in radiation enhanced migration and invasion *in vitro*. Subsequently, if it is determined that TGF-β1 and/or IL-8 play a major role *in vitro* in different tumour cell lines as singular or synergistic factors, pre-clinical mouse models using more aggressive tumour models that observe ineffective disease eradication with IR alone could be used to determine whether the incorporation of antibody or small molecular therapies before, during or after IR treatment would affect the formation of distant metastases and produce prognostic biomarkers that would inform disease progression. These *in vivo* studies will hopefully further support the need to review and improve current clinical IR practices, in particular with cancer patients where radiation is the main therapeutic option and the response to IR is uncertain.

References

1. Kalluri, R. and R.A. Weinberg, *The basics of epithelial-mesenchymal transition.* The Journal of clinical investigation, 2009. **119**(6): p. 1420-1428.
2. Advisory, C.C.S.s. and C.o.C. Statistics *Canadian Cancer Statistics 2016*. 2016.
3. Hanahan, D. and R.A. Weinberg, *The hallmarks of cancer.* cell, 2000. **100**(1): p. 57-70.
4. Hanahan, D. and R.A. Weinberg, *Hallmarks of cancer: the next generation.* cell, 2011. **144**(5): p. 646-674.
5. Sims, A.H., et al., *Origins of breast cancer subtypes and therapeutic implications.* Nature Clinical Practice Oncology, 2007. **4**(9): p. 516-525.
6. Polyak, K., *Breast cancer: origins and evolution.* The Journal of clinical investigation, 2007. **117**(11): p. 3155-3163.
7. Kennecke, H., et al., *Metastatic behavior of breast cancer subtypes.* Journal of clinical oncology, 2010. **28**(20): p. 3271-3277.
8. Senkus, E., et al., *Primary breast cancer: ESMO Clinical Practice Guidelines for diagnosis, treatment and follow-up.* Annals of Oncology, 2013: p. mdt284.
9. Burstein, H.J., et al., *Ductal carcinoma in situ of the breast.* New England Journal of Medicine, 2004. **350**(14): p. 1430-1441.
10. Richard, J., et al., *Epidermal-growth-factor receptor status as predictor of early recurrence of and death from breast cancer.* The Lancet, 1987. **329**(8547): p. 1398-1402.
11. Slamon, D., et al., *Human breast cancer: correlation of relapse and.* science, 1987. **3798106**(177): p. 235.
12. Nguyen, P.L., et al., *Breast cancer subtype approximated by estrogen receptor, progesterone receptor, and HER-2 is associated with local and distant recurrence after breast-conserving therapy.* Journal of Clinical Oncology, 2008. **26**(14): p. 2373-2378.
13. Sobin, L.H., M.K. Gospodarowicz, and C. Wittekind, *TNM classification of malignant tumours*. 2011: John Wiley & Sons.
14. Allred, D., et al., *Prognostic and predictive factors in breast cancer by immunohistochemical analysis.* Modern pathology: an official journal of the United States and Canadian Academy of Pathology, Inc, 1998. **11**(2): p. 155-168.
15. Blows, F.M., et al., *Subtyping of breast cancer by immunohistochemistry to investigate a relationship between subtype and short and long term survival: a collaborative analysis of data for 10,159 cases from 12 studies.* PLoS Med, 2010. **7**(5): p. e1000279.
16. Nielsen, T.O., et al., *Immunohistochemical and clinical characterization of the basal-like subtype of invasive breast carcinoma.* Clinical cancer research, 2004. **10**(16): p. 5367-5374.
17. Sotiriou, C., et al., *Breast cancer classification and prognosis based on gene expression profiles from a population-based study.* Proceedings of the National Academy of Sciences, 2003. **100**(18): p. 10393-10398.
18. Hu, Z., et al., *The molecular portraits of breast tumors are conserved across microarray platforms.* BMC genomics, 2006. **7**(1): p. 96.
19. Cheang, M.C., et al., *Ki67 index, HER2 status, and prognosis of patients with luminal B breast cancer.* Journal of the National Cancer Institute, 2009. **101**(10): p. 736-750.

20. Sørlie, T., et al., *Repeated observation of breast tumor subtypes in independent gene expression data sets.* Proceedings of the National Academy of Sciences, 2003. **100**(14): p. 8418-8423.
21. Onitilo, A.A., et al., *Breast cancer subtypes based on ER/PR and Her2 expression: comparison of clinicopathologic features and survival.* Clinical medicine & research, 2009. **7**(1-2): p. 4-13.
22. Sørlie, T., et al., *Gene expression patterns of breast carcinomas distinguish tumor subclasses with clinical implications.* Proceedings of the National Academy of Sciences, 2001. **98**(19): p. 10869-10874.
23. Perou, C.M., et al., *Molecular portraits of human breast tumours.* Nature, 2000. **406**(6797): p. 747-752.
24. Van't Veer, L.J. and R. Bernards, *Enabling personalized cancer medicine through analysis of gene-expression patterns.* Nature, 2008. **452**(7187): p. 564-570.
25. Nielsen, T.O., et al., *A comparison of PAM50 intrinsic subtyping with immunohistochemistry and clinical prognostic factors in tamoxifen-treated estrogen receptor–positive breast cancer.* Clinical Cancer Research, 2010. **16**(21): p. 5222-5232.
26. Cronin, M., et al., *Analytical validation of the Oncotype DX genomic diagnostic test for recurrence prognosis and therapeutic response prediction in node-negative, estrogen receptor–positive breast cancer.* Clinical chemistry, 2007. **53**(6): p. 1084-1091.
27. Paik, S., et al., *A multigene assay to predict recurrence of tamoxifen-treated, node-negative breast cancer.* New England Journal of Medicine, 2004. **351**(27): p. 2817-2826.
28. Van De Vijver, M.J., et al., *A gene-expression signature as a predictor of survival in breast cancer.* New England Journal of Medicine, 2002. **347**(25): p. 1999-2009.
29. Khanna, K.K. and S.P. Jackson, *DNA double-strand breaks: signaling, repair and the cancer connection.* Nature genetics, 2001. **27**(3): p. 247-254.
30. Barcellos-Hoff, M.H., C. Park, and E.G. Wright, *Radiation and the microenvironment–tumorigenesis and therapy.* Nature Reviews Cancer, 2005. **5**(11): p. 867-875.
31. Group, E.B.C.T.C., *Effect of radiotherapy after breast-conserving surgery on 10-year recurrence and 15-year breast cancer death: meta-analysis of individual patient data for 10 801 women in 17 randomised trials.* The Lancet, 2011. **378**(9804): p. 1707-1716.
32. Langlands, F., et al., *Breast cancer subtypes: response to radiotherapy and potential radiosensitisation.* The British journal of radiology, 2013. **86**(1023): p. 20120601.
33. Jagsi, R., *Progress and controversies: Radiation therapy for invasive breast cancer.* CA: a cancer journal for clinicians, 2014. **64**(2): p. 135-152.
34. Gupta, G.P. and J. Massagué, *Cancer metastasis: building a framework.* Cell, 2006. **127**(4): p. 679-695.
35. Quail, D.F. and J.A. Joyce, *Microenvironmental regulation of tumor progression and metastasis.* Nature medicine, 2013. **19**(11): p. 1423-1437.
36. Greaves, M. and C.C. Maley, *Clonal evolution in cancer.* Nature, 2012. **481**(7381): p. 306-313.
37. Jordan, C.T., M.L. Guzman, and M. Noble, *Cancer stem cells.* New England Journal of Medicine, 2006. **355**(12): p. 1253-1261.
38. Friedl, P., Y. Hegerfeldt, and M. Tusch, *Collective cell migration in morphogenesis and cancer.* International Journal of Developmental Biology, 2004. **48**(5-6): p. 441-449.

39. Savagner, P., *Leaving the neighborhood: molecular mechanisms involved during epithelial-mesenchymal transition.* Bioessays, 2001. **23**(10): p. 912-923.
40. Christiansen, J.J. and A.K. Rajasekaran, *Reassessing epithelial to mesenchymal transition as a prerequisite for carcinoma invasion and metastasis.* Cancer research, 2006. **66**(17): p. 8319-8326.
41. Mani, S.A., et al., *The epithelial-mesenchymal transition generates cells with properties of stem cells.* Cell, 2008. **133**(4): p. 704-715.
42. Zavadil, J. and E.P. Böttinger, *TGF-β and epithelial-to-mesenchymal transitions.* Oncogene, 2005. **24**(37): p. 5764-5774.
43. Yang, J. and R.A. Weinberg, *Epithelial-mesenchymal transition: at the crossroads of development and tumor metastasis.* Developmental cell, 2008. **14**(6): p. 818-829.
44. Miettinen, P.J., et al., *TGF-beta induced transdifferentiation of mammary epithelial cells to mesenchymal cells: involvement of type I receptors.* The Journal of cell biology, 1994. **127**(6): p. 2021-2036.
45. Masszi, A., et al., *Central role for Rho in TGF-β1-induced α-smooth muscle actin expression during epithelial-mesenchymal transition.* American Journal of Physiology-Renal Physiology, 2003. **284**(5): p. F911-F924.
46. Chambers, A.F. and L.M. Matrisian, *Changing views of the role of matrix metalloproteinases in metastasis.* Journal of the National Cancer Institute, 1997. **89**(17): p. 1260-1270.
47. Radisky, D.C., et al., *Rac1b and reactive oxygen species mediate MMP-3-induced EMT and genomic instability.* Nature, 2005. **436**(7047): p. 123-127.
48. Yoo, Y.A., et al., *Sonic hedgehog pathway promotes metastasis and lymphangiogenesis via activation of Akt, EMT, and MMP-9 pathway in gastric cancer.* Cancer research, 2011. **71**(22): p. 7061-7070.
49. Zhou, Y.-C., et al., *Ionizing radiation promotes migration and invasion of cancer cells through transforming growth factor-beta–mediated epithelial–mesenchymal transition.* International Journal of Radiation Oncology* Biology* Physics, 2011. **81**(5): p. 1530-1537.
50. Jung, J.-W., et al., *Ionising radiation induces changes associated with epithelial-mesenchymal transdifferentiation and increased cell motility of A549 lung epithelial cells.* European Journal of Cancer, 2007. **43**(7): p. 1214-1224.
51. Kawamoto, A., et al., *Radiation induces epithelial-mesenchymal transition in colorectal cancer cells.* Oncology reports, 2012. **27**(1): p. 51.
52. Yan, S., et al., *Low-dose radiation-induced epithelial-mesenchymal transition through NF-κB in cervical cancer cells.* International journal of oncology, 2013. **42**(5): p. 1801-1806.
53. Chang, L., et al., *Acquisition of epithelial–mesenchymal transition and cancer stem cell phenotypes is associated with activation of the PI3K/Akt/mTOR pathway in prostate cancer radioresistance.* Cell death & disease, 2013. **4**(10): p. e875.
54. He, E., et al., *Fractionated ionizing radiation promotes epithelial-mesenchymal transition in human esophageal cancer cells through PTEN deficiency-mediated akt activation.* PloS one, 2015. **10**(5): p. e0126149.

55. Andarawewa, K.L., et al., *Ionizing Radiation Predisposes Nonmalignant Human Mammary Epithelial Cells to Undergo Transforming Growth Factor β–Induced Epithelial to Mesenchymal Transition.* Cancer research, 2007. **67**(18): p. 8662-8670.
56. Valerie, K., et al., *Radiation-induced cell signaling: inside-out and outside-in.* Molecular cancer therapeutics, 2007. **6**(3): p. 789-801.
57. Gunasinghe, N.D., et al., *Mesenchymal–epithelial transition (MET) as a mechanism for metastatic colonisation in breast cancer.* Cancer and Metastasis Reviews, 2012. **31**(3-4): p. 469-478.
58. Zheng, X., et al., *Epithelial-to-mesenchymal transition is dispensable for metastasis but induces chemoresistance in pancreatic cancer.* Nature, 2015.
59. Fischer, K.R., et al., *Epithelial-to-mesenchymal transition is not required for lung metastasis but contributes to chemoresistance.* Nature, 2015. **527**(7579): p. 472-476.
60. Moncharmont, C., et al., *Radiation-enhanced cell migration/invasion process: A review.* Critical reviews in oncology/hematology, 2014. **92**(2): p. 133-142.
61. Kim, I.S. and S.H. Baek, *Mouse models for breast cancer metastasis.* Biochemical and biophysical research communications, 2010. **394**(3): p. 443-447.
62. Jonkers, J., et al., *Synergistic tumor suppressor activity of BRCA2 and p53 in a conditional mouse model for breast cancer.* Nature genetics, 2001. **29**(4): p. 418-425.
63. Guy, C., R. Cardiff, and W. Muller, *Induction of mammary tumors by expression of polyomavirus middle T oncogene: a transgenic mouse model for metastatic disease.* Molecular and cellular biology, 1992. **12**(3): p. 954-961.
64. Ursini-Siegel, J., et al., *Insights from transgenic mouse models of ERBB2-induced breast cancer.* Nature Reviews Cancer, 2007. **7**(5): p. 389-397.
65. Subik, K., et al., *The expression patterns of ER, PR, HER2, CK5/6, EGFR, Ki-67 and AR by immunohistochemical analysis in breast cancer cell lines.* Breast cancer: basic and clinical research, 2010. **4**: p. 35.
66. Neve, R.M., et al., *A collection of breast cancer cell lines for the study of functionally distinct cancer subtypes.* Cancer cell, 2006. **10**(6): p. 515-527.
67. Lacroix, M. and G. Leclercq, *Relevance of breast cancer cell lines as models for breast tumours: an update.* Breast cancer research and treatment, 2004. **83**(3): p. 249-289.
68. Holliday, D.L. and V. Speirs, *Choosing the right cell line for breast cancer research.* Breast Cancer Research, 2011. **13**(4): p. 215.
69. Munoz, R., et al., *Highly efficacious nontoxic preclinical treatment for advanced metastatic breast cancer using combination oral UFT-cyclophosphamide metronomic chemotherapy.* Cancer research, 2006. **66**(7): p. 3386-3391.
70. Rubinson, D.A., et al., *A lentivirus-based system to functionally silence genes in primary mammalian cells, stem cells and transgenic mice by RNA interference.* Nature genetics, 2003. **33**(3): p. 401-406.
71. Lindquist, K.E., et al., *Selective radiosensitization of hypoxic cells using BCCA621C: a novel hypoxia activated prodrug targeting DNA-dependent protein kinase.* Tumor Microenvironment and Therapy, 2013. **1**: p. 46-55.
72. Schindelin, J., et al., *Fiji: an open-source platform for biological-image analysis.* Nature methods, 2012. **9**(7): p. 676-682.
73. Meijering, E., O. Dzyubachyk, and I. Smal, *Methods for cell and particle tracking.* Methods Enzymol, 2012. **504**(9): p. 183-200.

74. Goetze, K., et al., *The impact of conventional and heavy ion irradiation on tumor cell migration in vitro.* International journal of radiation biology, 2009.
75. Zhai, G.G., et al., *Radiation enhances the invasive potential of primary glioblastoma cells via activation of the Rho signaling pathway.* Journal of neuro-oncology, 2006. **76**(3): p. 227-237.
76. Wild-Bode, C., et al., *Sublethal irradiation promotes migration and invasiveness of glioma cells Implications for radiotherapy of human glioblastoma.* Cancer research, 2001. **61**(6): p. 2744-2750.
77. Steinle, M., et al., *Ionizing radiation induces migration of glioblastoma cells by activating BK K+ channels.* Radiotherapy and Oncology, 2011. **101**(1): p. 122-126.
78. Fujita, M., et al., *X-ray irradiation and Rho-kinase inhibitor additively induce invasiveness of the cells of the pancreatic cancer line, MIAPaCa-2, which exhibits mesenchymal and amoeboid motility.* Cancer science, 2011. **102**(4): p. 792-798.
79. Pickhard, A.C., et al., *Inhibition of radiation induced migration of human head and neck squamous cell carcinoma cells by blocking of EGF receptor pathways.* BMC cancer, 2011. **11**(1): p. 388.
80. Ogata, T., et al., *Carbon ion irradiation suppresses metastatic potential of human non-small cell lung cancer A549 cells through the phosphatidylinositol-3-kinase/Akt signaling pathway.* Journal of radiation research, 2011. **52**(3): p. 374-379.
81. Qian, L.-W., et al., *Radiation-induced increase in invasive potential of human pancreatic cancer cells and its blockade by a matrix metalloproteinase inhibitor, CGS27023.* Clinical Cancer Research, 2002. **8**(4): p. 1223-1227.
82. Ogata, T., et al., *Particle irradiation suppresses metastatic potential of cancer cells.* Cancer research, 2005. **65**(1): p. 113-120.
83. De Bacco, F., et al., *Induction of MET by ionizing radiation and its role in radioresistance and invasive growth of cancer.* Journal of the National Cancer Institute, 2011. **103**(8): p. 645-661.
84. Boyden, S., *The chemotactic effect of mixtures of antibody and antigen on polymorphonuclear leucocytes.* The Journal of experimental medicine, 1962. **115**(3): p. 453-466.
85. Paquette, B., et al., *Radiation-enhancement of MDA-MB-231 breast cancer cell invasion prevented by a cyclooxygenase-2 inhibitor.* British journal of cancer, 2011. **105**(4): p. 534-541.
86. Paquette, B., et al., *In vitro irradiation of basement membrane enhances the invasiveness of breast cancer cells.* British journal of cancer, 2007. **97**(11): p. 1505-1512.
87. Vilalta, M., et al., *Recruitment of circulating breast cancer cells is stimulated by radiotherapy.* Cell reports, 2014. **8**(2): p. 402-409.
88. Liang, C.-C., A.Y. Park, and J.-L. Guan, *In vitro scratch assay: a convenient and inexpensive method for analysis of cell migration in vitro.* Nature protocols, 2007. **2**(2): p. 329-333.
89. Hilsenbeck, O., et al., *Software tools for single-cell tracking and quantification of cellular and molecular properties.* Nature biotechnology, 2016. **34**(7): p. 703-706.
90. Tester, A.M., et al., *MMP-9 secretion and MMP-2 activation distinguish invasive and metastatic sublines of a mouse mammary carcinoma system showing epithelial-*

mesenchymal transition traits. Clinical & experimental metastasis, 2000. **18**(7): p. 553-560.
91. Lou, Y., et al., *Epithelial–mesenchymal transition (EMT) is not sufficient for spontaneous murine breast cancer metastasis.* Developmental Dynamics, 2008. **237**(10): p. 2755-2768.
92. Lee, H.W., et al., *Alpha-smooth muscle actin (ACTA2) is required for metastatic potential of human lung adenocarcinoma.* Clinical Cancer Research, 2013. **19**(21): p. 5879-5889.
93. Hinz, B., et al., *Alpha-smooth muscle actin expression upregulates fibroblast contractile activity.* Molecular biology of the cell, 2001. **12**(9): p. 2730-2741.
94. Chao, Y.L., C.R. Shepard, and A. Wells, *Breast carcinoma cells re-express E-cadherin during mesenchymal to epithelial reverting transition.* Molecular cancer, 2010. **9**(1): p. 179.
95. Polyak, K. and R.A. Weinberg, *Transitions between epithelial and mesenchymal states: acquisition of malignant and stem cell traits.* Nature Reviews Cancer, 2009. **9**(4): p. 265-273.
96. Hartsock, A. and W.J. Nelson, *Adherens and tight junctions: structure, function and connections to the actin cytoskeleton.* Biochimica et Biophysica Acta (BBA)-Biomembranes, 2008. **1778**(3): p. 660-669.
97. Shan, Y.-X., et al., *Ionizing radiation stimulates secretion of pro-inflammatory cytokines: dose–response relationship, mechanisms and implications.* Radiation and environmental biophysics, 2007. **46**(1): p. 21-29.
98. Barcellos-Hoff, M., *Radiation-induced transforming growth factor β and subsequent extracellular matrix reorganization in murine mammary gland.* Cancer Research, 1993. **53**(17): p. 3880-3886.
99. Carl, C., et al., *Ionizing radiation induces a motile phenotype in human carcinoma cells in vitro through hyperactivation of the TGF-beta signaling pathway.* Cellular and Molecular Life Sciences, 2016. **73**(2): p. 427-443.
100. Satoh, E., et al., *Effect of irradiation on transforming growth factor-β secretion by malignant glioma cells.* Journal of neuro-oncology, 1997. **33**(3): p. 195-200.
101. Jobling, M.F., et al., *Isoform-specific activation of latent transforming growth factor β (LTGF-β) by reactive oxygen species.* Radiation research, 2006. **166**(6): p. 839-848.
102. Giampieri, S., et al., *Localized and reversible TGFβ signalling switches breast cancer cells from cohesive to single cell motility.* Nature cell biology, 2009. **11**(11): p. 1287-1296.
103. Gorsch, S.M., et al., *Immunohistochemical staining for transforming growth factor β1 associates with disease progression in human breast cancer.* Cancer research, 1992. **52**(24): p. 6949-6952.
104. Walker, R.A. and S.J. Dearing, *Transforming growth factor beta 1 in ductal carcinoma in situ and invasive carcinomas of the breast.* European journal of cancer, 1992. **28**(2): p. 641-644.
105. Kong, F.-M., et al., *Elevated plasma transforming growth factor-beta 1 levels in breast cancer patients decrease after surgical removal of the tumor.* Annals of surgery, 1995. **222**(2): p. 155.

106. Masszi, A., et al., *Central role for Rho in TGF-β₁-induced α-smooth muscle actin expression during epithelial-mesenchymal transition.* American Journal of Physiology - Renal Physiology, 2003. **284**(5): p. F911-F924.
107. Hautmann, M.B., P.J. Adam, and G.K. Owens, *Similarities and differences in smooth muscle α-actin induction by TGF-β in smooth muscle versus non–smooth muscle cells.* Arteriosclerosis, Thrombosis, and Vascular Biology, 1999. **19**(9): p. 2049-2058.
108. Uttamsingh, S., et al., *Synergistic effect between EGF and TGF-β1 in inducing oncogenic properties of intestinal epithelial cells.* Oncogene, 2008. **27**(18): p. 2626-2634.
109. Wang, J.M., et al., *Induction of haptotactic migration of melanoma cells by neutrophil activating protein/interleukin-8.* Biochemical and biophysical research communications, 1990. **169**(1): p. 165-170.
110. Araki, S., et al., *Interleukin-8 is a molecular determinant of androgen independence and progression in prostate cancer.* Cancer research, 2007. **67**(14): p. 6854-6862.
111. Ning, Y., et al., *Interleukin-8 is associated with proliferation, migration, angiogenesis and chemosensitivity in vitro and in vivo in colon cancer cell line models.* International Journal of Cancer, 2011. **128**(9): p. 2038-2049.
112. Xie, K., *Interleukin-8 and human cancer biology.* Cytokine & growth factor reviews, 2001. **12**(4): p. 375-391.
113. Yao, C., et al., *Interleukin-8 modulates growth and invasiveness of estrogen receptor-negative breast cancer cells.* International Journal of Cancer, 2007. **121**(9): p. 1949-1957.
114. Lin, Y., et al., *Identification of interleukin-8 as estrogen receptor-regulated factor involved in breast cancer invasion and angiogenesis by protein arrays.* International Journal of Cancer, 2004. **109**(4): p. 507-515.
115. Wang, Y., et al., *Autocrine production of interleukin-8 confers cisplatin and paclitaxel resistance in ovarian cancer cells.* Cytokine, 2011. **56**(2): p. 365-375.
116. Meeren, A., et al., *Ionizing radiation enhances IL-6 and IL-8 production by human endothelial cells.* Mediators of inflammation, 1997. **6**(3): p. 185-193.
117. Pasi, F., A. Facoetti, and R. Nano, *IL-8 and IL-6 bystander signalling in human glioblastoma cells exposed to gamma radiation.* Anticancer research, 2010. **30**(7): p. 2769-2772.
118. Freund, A., et al., *IL-8 expression and its possible relationship with estrogen-receptor-negative status of breast cancer cells.* Oncogene, 2003. **22**(2): p. 256-265.
119. Lu, S. and Z. Dong, *Characterization of TGF-β-regulated interleukin-8 expression in human prostate cancer cells.* The Prostate, 2006. **66**(9): p. 996-1004.
120. Camphausen, K., et al., *Radiation therapy to a primary tumor accelerates metastatic growth in mice.* Cancer research, 2001. **61**(5): p. 2207-2211.
121. Sheldon, P. and J. Fowler, *The effect of low-dose pre-operative X-irradiation of implanted mouse mammary carcinomas on local recurrence and metastasis.* British journal of cancer, 1976. **34**(4): p. 401.
122. Bouchard, G., et al., *Pre-irradiation of mouse mammary gland stimulates cancer cell migration and development of lung metastases.* British journal of cancer, 2013. **109**(7): p. 1829-1838.

123. Freeman, S.A., et al., *Preventing the activation or cycling of the Rap1 GTPase alters adhesion and cytoskeletal dynamics and blocks metastatic melanoma cell extravasation into the lungs.* Cancer research, 2010. **70**(11): p. 4590-4601.
124. Kim, Y., et al., *Quantification of cancer cell extravasation in vivo.* Nature protocols, 2016. **11**(5): p. 937-948.